FEDERAL UNIVERSITY OF TECHNOLOGY - PARANÁ

DEPARTMENT OF ELECTRONICS

GRADUATE PROGRAM IN ELECTRICAL ENGINEERING

JOSÉ ADENILSON GONÇALVES LUZ JUNIOR

OPTIMAL CONTROL AND STATE OBSERVER FOR A ROBOTIC MANIPULATOR WITH THREE DEGREES OF FREEDOM

MASTER'S THESIS

PONTA GROSSA

2018

JOSÉ ADENILSON GONÇALVES LUZ JUNIOR

OPTIMAL CONTROL AND STATE OBSERVER FOR A ROBOTIC MANIPULATOR WITH THREE DEGREES OF FREEDOM

Document presented as partial requirement for obtaining a Master's Degree in Electrical Engineering from Department of Electronic Engineering at Federal University of Technology - Paraná

Advisor: Prof. Dr. Angelo Marcelo Tusset

Co-Advisor: Prof. Dr. Jose Manoel Balthazar

PONTA GROSSA

2018

Ficha catalográfica elaborada pelo Departamento de Biblioteca
da Universidade Tecnológica Federal do Paraná, Câmpus Ponta Grossa
n.53/18

L979 Luz Junior, José Adenilson Gonçalves

Optimal control and state observer for a robotic manipulator with three degrees of freedom. / José Adenilson Gonçalves Luz Junior. 2018.
120 f.; il. 30 cm

Orientador: Prof. Dr. Angelo Marcelo Tusset
Coorientador: Prof. Dr. Jose Manoel Balthazar

Dissertação (Mestrado em Engenharia Elétrica) - Programa de Pós-Graduação em Engenharia Elétrica. Universidade Tecnológica Federal do Paraná, Ponta Grossa, 2018.

1. Robótica. 2. Robôs - Dinâmica. 3. Controle eletrônico. I. Tusset, Angelo Marcelo. II. Balthazar, Jose Manoel. III. Universidade Tecnológica Federal do Paraná. IV. Título.

CDD 620.1

Elson Heraldo Ribeiro Junior. CRB-9/1413. 01/11/2018.

Universidade Tecnológica Federal do Paraná
Campus de Ponta Grossa

Diretoria de Pesquisa e Pós-Graduação

PROGRAMA DE PÓS-GRADUAÇÃO EM ENGENHARIA ELÉTRICA

UNIVERSIDADE TECNOLÓGICA FEDERAL DO PARANÁ

FOLHA DE APROVAÇÃO

Título de Dissetação Nº **42/2018**

OPTIMAL CONTROL AND STATE OBSERVER FOR ROBOTIC MANIPULATOR WITH THREE DEGREES OF FREEDOM

por

José Adenilson Gonçalves Luz Junior

Esta dissertação foi apresentada às **9 horas** do dia **05 de junho de 2018** como requisito parcial para a obtenção do título de MESTRE EM ENGENHARIA ELÉTRICA, com área de concentração em Controle e Processamento de Energia, Programa de Pós-Graduação em Engenharia Elétrica. O candidato foi argüido pela Banca Examinadora composta pelos professores abaixo assinados. Após deliberação, a Banca Examinadora considerou o trabalho aprovado.

Prof. Dr Frederico Martins Alves da Silva (UFG)

Prof. Dr. Max Mauro Dias Santos (UTFPR)

Prof. Dr. Federic Conrad Janzen (UTFPR)

Prof. Dr. Angelo Marcelo Tusset (UTFPR)
- Orientador

Prof. Dr. Angelo Marcelo Tusset (UTFPR)
Coordenador do PPGEE

To my mother, Roseli, and brother, Bruno.

ABSTRACT

GONÇALVES, José Adenilson Luz Junior. **Optimal control and state observer for a robotic manipulator with three degrees of freedom**. 2018. 119 p. Master's Thesis. (Master Degree in Eletrical Engineering) Federal University of Technology - Paraná, Ponta Grossa, 2018.

This work presents the modeling and simulation of a robotic manipulator robot with three degrees of freedom by considering its structures with rigid behavior. The concepts of kinematics for the mathematical deduction and the Lagrangian mechanics were applyed to obtain the dynamic models of the manipulator and the DC actuators with are considered as permanent magnet motors. Due to the nonlinearities and dynamics characteristics, both the states observer and the controler used were based on State Dependet Ricatti Equation (SDRE). The simulations made for constant performance parameters demonstrated the effectiveness of the optimal control applied to the manipulator and to the chosen DC actuator models. The applications of trajectories to the manipulator enrich the applicability of the project and the results obtained with the techniques chosen show his efficiency.

Keywords: Robotics. Robots - Dynamics. Electronic control

RESUMO

GONÇALVES, José Adenilson Luz Junior. **Controle ótimo e observador de estados em manipulador robótico com três graus de liberdade**. 2018. 119 p. Dissertação (Mestrado em Engenharia Elétrica) - Universidade Tecnológica Federal do Paraná, Ponta Grossa, 2018.

Este trabalho apresenta a modelagem e simulação de um robô manipulador com três graus de liberdade e considerando suas estruturas com comportamento rígido. Os conceitos de cinemática para a dedução matemática e a mecânica de Lagrange foram usados para obter os modelos dinâmicos do manipulador e os atuadores DC com ímã permanente. Devido às características de não-linearidade e dinâmica, tanto o observador dos estados quanto o controle utilizado foram baseados na State Dependet Ricatti Equation (SDRE). As simulações feitas para parâmetros de desempenho constantes demonstraram a eficácia do controle ótimo aplicado ao manipulador e aos modelos de atuadores DC escolhidos. As aplicações das trajetórias ao manipulador enriquecem a aplicabilidade do projeto e os resultados obtidos com as técnicas escolhidas mostram sua eficiência.

Palavras-chave: Robótica. Robôs - Dinâmica. Controle eletrônico.

LIST OF FIGURES

LIST OF TABLES

LIST OF ABBREVIATIONS

DC	Direct Current
DOF	Degrees of freedom
DH	Denavit-Hartenberg
EMF	Electro-Motive Force
LQR	Linear Quadratic Regulator
MIMO	Multiple Inputs and Multiple Outputs
SDC	State Dependent Coefficients
SDRE	State Dependent Riccati Equation
UTFPR	Universidade Tecnologocia Federal do Paraná

LIST OF SYMBOLS

$\theta_{path\ i}$	Initial position for the Path Planning
$\theta_{path\ f}$	Final position for the Path Planning
θ_1	First link position
θ_2	Second link position
θ_3	Third link position
θ_4	End-effector position
$\dot{\theta}_1$	First link speed
$\dot{\theta}_2$	Second link speed
$\dot{\theta}_3$	Third link speed
$\ddot{\theta}_1$	First link acceleration
$\ddot{\theta}_2$	Second link acceleration
$\ddot{\theta}_3$	Third link acceleration
$\hat{\theta}_1$	State Observer position for the first link
$\hat{\theta}_2$	State Observer position for the second link
$\hat{\theta}_3$	State Observer position for the third link
$\dot{\hat{\theta}}_1$	State Observer speed for the first link
$\dot{\hat{\theta}}_2$	State Observer speed for the second link
$\dot{\hat{\theta}}_3$	State Observer speed for the third link
θ_d	Position set point for the SDRE control
$\dot{\theta}_d$	Speed set point for the SDRE control
τ_1	First link external force
τ_2	Second link external force
τ_3	Third link external force
μ_k	Dissipation constant
γ_i	Generic parametric uncertainties
α	Parametric variation
$A(x)$	State Matrix
$A(x)_{Ob}$	State Matrix of the State Observer
$B(x)$	Input Matrix
$B(x)_{Ob}$	Input Matrix of the State Observer
b_v	DC actuator Viscous damping

$C(x)$	Output Matrix
$c_{n\,x\,n}$	Coefficients of the matrix $C(x)$
cm_1	First link Center of mass
cm_2	Second link Center of mass
cm_3	Third link Center of mass
$D(t)_1$	First link non-conservative forces
$D(t)_2$	Second link non-conservative forces
$D(t)_3$	Third link non-conservative forces
$E_{kin.\ 1}$	First link kinetic energy
$E_{kin.\ 2}$	Second link kinetic energy
$E_{kin.\ 3}$	Third link kinetic energy
g	Gravity constant
G	Additional control matrix
i_{ap}	Peak current of the DC actuators
$\bar{I}_1$	First link Inertial Moment
$\bar{I}_2$	Second link Inertial Moment
$\bar{I}_3$	Third link Inertial Moment
J	Performance Index
J_m	Rotor Inertia
K_m	Torque constant
K_g	Back-EMF constant
k_c	System control action matrix
$k_{c\,Ob}$	State Observer control action matrix
$k_{L\,Ob}$	State Observer gain
k	Link index
k_c	Control Matrix
l_1	First Link Lenght
l_2	Second Link Lenght
l_3	Third Link Lenght
L	Lagrangian
L_c	State Observer matrix gain
L_a	Armature Inductance
m_1	First link mass
m_2	Second link mass

m_3	Third link mass
M	Cotrolabillity matrix
O	Observabillity matrix
$p_{x\,1}$	First link position on axe x coordinates frame
$p_{y\,1}$	First link position on axe y coordinates frame
$p_{x\,2}$	Second link position on axe x coordinates frame
$p_{y\,2}$	Second link position on axe y coordinates frame
$p_{x\,3}$	Third link position on axe x coordinates frame
$p_{y\,3}$	Third link position on axe y coordinates frame
p_k	Position on the coordinate frame used for the Kinematic and Dynamics
$P_{0\,1}$	First link initial potential energy
$P_{0\,2}$	Second link initial potential energy
$P_{0\,3}$	Third link initial potential energy
P	Matrix solution of the Riccati equation
$Q(x)$	Weight matrix relative to the system states
$Q(x)_{Ob}$	Weight matrix relative to the State Observer states
$Q(x)_{L\,Ob}$	Weight matrix relative to the State Observer gain
Q_k	Non-concervative forces
q_k	Position on the coordinate frame
$\dot{q}_k$	Speed on the coordinate frame
$q_{path\,i}$	Path Planning polynomial for position
$\dot{q}_{path\,i}$	Path Planning polynomial for speed
$\ddot{q}_{path\,i}$	Path Planning polynomial for acceleration
$R(x)$	Weight matrix relative to the system inputs
$R(x)_{Ob}$	Weight matrix relative to the State Observer inputs
$R(x)_{L\,Ob}$	Weight matrix relative to the gain of the State Observer inputs
R_a	Armature resistor of the DC actuators
u_c	System control action
$u(t)_{c\,Ob}$	State Observer control action
$u_{c\,1}$	Control action for the first link
$u_{c\,2}$	Control action for the second link
$u_{c\,3}$	Control action for the third link
$u_{c\,Ob\,1}$	State Observer control action for the first link
$u_{c\,Ob\,2}$	State Observer control action for the second link

$u_{c\,Ob\,3}$	State Observer control action for the third link
V_{in}	Voltage input on the DC actuators
v_1	First link speed
v_2	Second link speed
v_3	Third link speed
$x(t)$	System states
$\hat{x}(t)$	State Observer states
$\hat{y}(t)$	State Observer outputs
ω_1	First link acceleration
ω_2	Second link acceleration
ω_3	Third link acceleration
$\omega_{path\,0}$	Initial speed for the Path Planning
$\omega_{path\,f}$	Final speed for the Path Planning
$\dot{\omega}_{path\,0}$	Initial acceleration for the Path Planning
$\dot{\omega}_{path\,f}$	Final acceleration for the Path Planning

CONTENTS

1 INTRODUCTION

The research on robotics is one of the most important areas on modern engineering. A lot of this interest and excitement is because the robotics has been seen as a tool and fundamental for another advance. Many recent medical advances are based on the incorporation of robots or robotics concepts into medical procedures because the robotics bring precision, efficiency and scalability (ITIK, SALAMCI, BANKS, 2010). Using a robot is possible to make more medical operation on the same time, with more precision and reducing the physical work of the professionals (ZARGAR, 2014; WINDER et al, 2016; ROH et al, 2018).

Even beaning a research that gain more scale and representation in the 1980, robotics represents one of the most prolific areas that can guide the science and humanity to the next level of knowledge. In a general sense, the evolution of the use of robots in several areas means a real improvement on effectiveness, productivity and risk reduction of execution of human activities (KACZMAR et al, 2016; CATHPOLE et al, 2016).

The revolution that robots bring is comparable to the revolution made in the 60’s with the semiconductors. As the word is no longer the same since the semiconductors consolidation, the word won’t be the same after the robotics consolidation.

1.1 MANIPULATORS AND MODERN ENGINEENRING

Even if the manipulators are one category of the whole robotics area, they have so many particularities in relation to function, application and design that they can be considered a complete individual section of research.

Robotic manipulators are autonomous structures characterized by the composition of links and joints, a fixed spatial reference and a great concern on the end-effect, referred as tool in some cases. The “end-effector” is the term use to describe the tool used by the manipulator and is the interface between the robot arm and the application. Grippers, pincers, welders and pick and place structures are examples of tools use as “end-effector” by robotic manipulators (LEWIS et al, 1978; MURRAY et al, 1994; BOTTEGA, PERGHER, 2009).

Another point of distinctiveness is the interest on the flexibility of the structure and how this can be controlled. There is a direct relation between the size, weight and hardness and needed of power torque (KORAYEN, 1994).

With this demands and characteristics, the application of the manipulators is only possible associated with a control technique. Both on manipulators and mobile robots, the structure of the manipulators does not have the capacity to make useful movements without the actuators and without control over the actuators there is no way to apply the robots (LEWIS et al, 2004).

The major objective of this control applied on the robots is force the variables, as position and speed, to the desired point or follow the defined path (SPONG et al, 2005; NIKU, 2011). The natural nonlinearity of the system makes the control a puzzling task and a number of techniques and strategies are commonly use depending on the specification, hardware and structural characteristics.

The interaction between robotics and some classical and new engineering areas become more and more common and one good example is the usage of neural networks. This has been seen as one of the most prodigious branches of those interactions. Solutions provided by the combination of these two fields have presented excellent results at points where robotics began to see its theoretical and conceptual limit (OGAWA, KANADA, 2010). Express the direct and inverse kinematic equations using Fuzzy, Neuro Fuzzy is a prove and funded approach to structure with kinematical redundancy and impossible algebraic solution (DUKA, 2014). Dealing with parametric error on the robotic variables using neural networks represent a great improvement on projects optimization (GUO, CHEN, 2008).

So, one of the main goals for the technological engineering is to set the conditions for the robotics being a key tool for all another scientific and social areas.

1.2 OUTLINE OF THE WORK

The work starts with the presentation on the chapter 2 the theory used to represent the kinematic and dynamical description for robotic manipulators.

On the chapter 3, the optimal control using the LQR theory as the basis for the SDRE control is presented. The possible approaches to define the weight matrices on the SDRE control is discussed to on this chapter. The state space representation is

discussed to explain who they will be used as the basis for the optimal control and the state observer, presented to on the chapter 3.

The actuators are presented on chapter 4 and how the state space representation is used to express the equations of DC motors to use on the dynamical system.

In chapter 5 the trajectory planning is deduced and explained how it was used to test the manipulator behavior under a point-to-point path.

The chapter 6 close the work shown the simulation, results and discussions using all the concepts explained on the previous chapters. The conclusion and future steps on this work are shown on the Conclusion.

2 EQUANTIONS OF MOTION

The equations of motion are one stage on the mathematical description of the robotic system, as structural and work space analysis, for example. The focus on this part of the mathematical description is specify the robotic variable on space. The manipulator description can be done using a lot of methodologies, which defines the best one is the structural characteristics of the robot, the application and in some cases what kind of actuators will be use (NIKU, 2011; CRAIG,1989)

All the motion made by the robot in a certain coordinates frame can be express using the kinematic, both informing the links position and speed based on the special localization and the special localization based on the links position and speed (MURRAY et al, 1994). Using the dynamic description is possible to relate the kinematic information with the cause of the motion, as the actuators for example. So, uniting the kinematic and the dynamic analysis all the motion variables of the robot are covered and is possible to apply additional components, as the mechanical dissipation and control strategy.

Figure 1 - Robot Manipulator Structure.

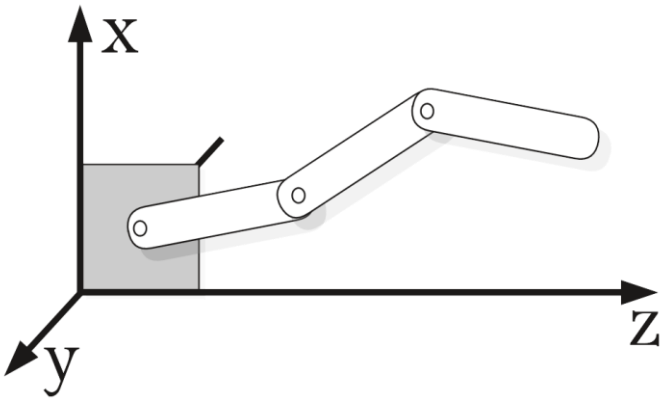

Source: Self Authorship

2.1 KNEMATICS

The Kinematics is the branch of mechanical sciences of motion which describe the system without concern with the source or cause of this motion (HIBBELER, 2006). On robots, the kinematics for a robot relate the robotic manipulator variables with the special variables of the coordinate frame chose to describe the system (CRAIG, 1994; ANGELIS, 2013). This means present a mathematical association between the links

positions and the special location in the chosen coordinate system. To do this mathematical deduction there are a lot of methods, but the robotic manipulator characteristics already commented and some additional analysis can provide a guideline to define best method.

These guidelines basically take into account the physical structure and how the robot can make movements and the best approach can be defined by considering those characteristics and the advantages that which method brings (NIKU, 2011). For example, there are methods that discard description on some axes of the coordinate frame where there is no possibility of movement and this make the kinematic analysis simpler.

On the physical structure, the actuators and the joints define two important concepts: work volume and the chain type. Based on the layout and movements allowed by the joints and links, the work volume is mapped and the chain type classification is based on the links and joints connections.

The figure 2 shown the two more common joints type, Prismatic and Revolute. Analyzing the possible movements of those joints, the conclusion is that for Revolute joints use coordinates system based on angles to express positions is a clear advantage. But using coordinates systems based on angles with Prismatic joints can make the project more complex than necessary. In a general sense Revolute joints take advantage on polar or spherical coordinates (cylindrical, for example) and Prismatic on cartesian frames (SPONG et al, 2005).

Figure 2 - Joints classification for robots.

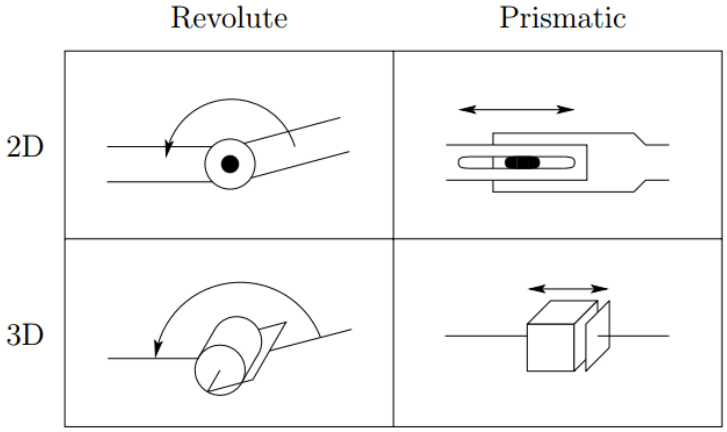

Source: Adapted from Spong *et al.*, 2005.

The Work Volume is the whole space within which the robotic manipulator end-effector can swept out (SPONG et al, 2005). Knowing this workspace covered by the end-effector brings a notion to how to relate the possible movements with a coordinate system. Taking as an example the structures shown on figure 2 is possible to have an initial idea to each coordinate system is more applicable to each robotic manipulator just based on the work volume. The figure 3 presents a wok volume basically composed by right angles and this leads to, at least, try a cartesian coordinates to describe this structure. However, on the figure 4 most of the work volume presents a spherical area and this indicates the use of coordinates that takes angles for expressed positions can be an advantage. The more coordinate systems and description of robotic systems are known to the researcher the more possibilities can be raised for how to describe the system mathematically.

Figure 3 - 3D printer and an example of robot with cartesian work space.

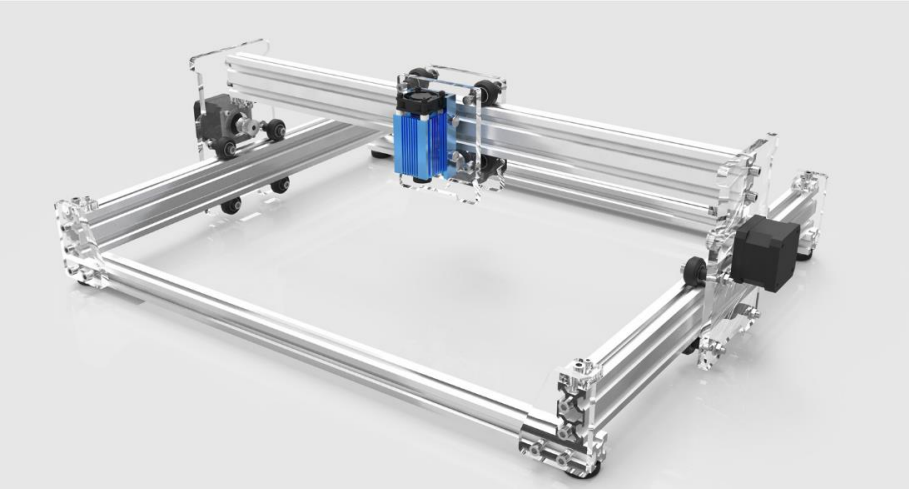

Source: Internet image

The robotic kinematic can be close or open, as illustrated in the figure 5. The chain is called open if the number of joints and degrees of freedom are the same and the chain is close if the number of degrees of freedom is the same that passive and active joints. Another way to classify the chain is if the joints and links are connected in more than two links or joints. If they are, the chain in close and if they aren't, the chain is open (CRAIG, 1994; YOU, 1994).

Figure 4 - Industrial Robotic as an example of spherical work volume.

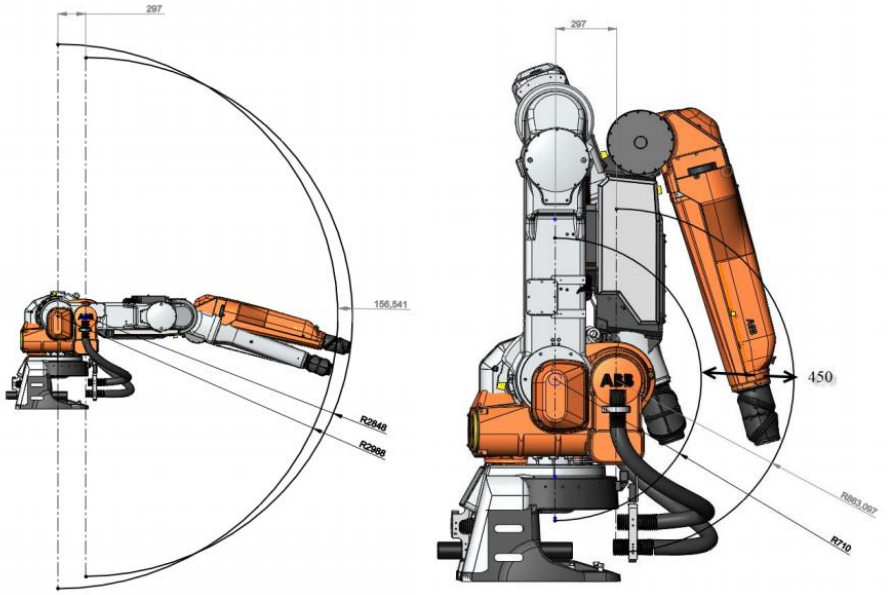

Source: Internet Image

Figure 5 - Kinematic Chain: Close and Open

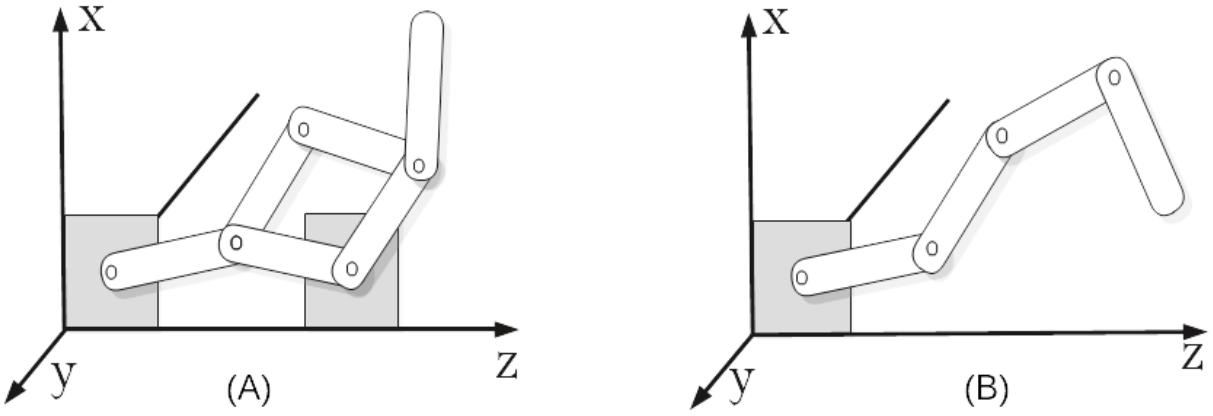

Source: Self Authorship

Based on these information, the equations of position were deducted using a cartesian coordinates frames. As the manipulator was a planar structure, there is no movement in one of the three axes on the cartesian frame. On which axis there will be no movement depends on the position of the origin of the coordinate system. The robotic system was described by defining that the axis y would not move and the axis x and z will be the axis with movement as shown in figure 6. The position presented

on the figure 4 is the initial condition of the manipulator for the mathematical deduction, but the robot can operate in any position when the control strategy is working.

Figure 6 - Coordinates frame.

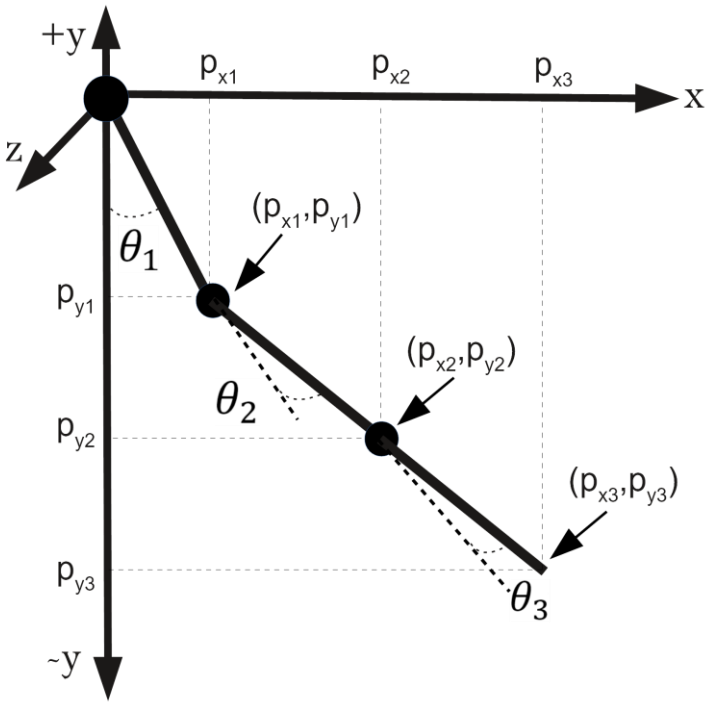

Source: Self Authorship

The kinematic is divided into two parts, the Forwards kinematics and the Inverse Kinematics. The next section goes into the deduction and application of the robotic kinematics for the manipulator.

2.1.1 Forward Kinematics

The Forward Kinematics is a mathematical deduction that provides the frame position based on the position and speed of the robot (LEWIS et al, 2004). This means that knowing the position and speed of the links is possible to determine the special location of each link.

Using the initial position presented on the figure 6, the points for the Forward deduction were chosen as the same points where the actuators were placed, since the control action always will be applied on those points. Using another point for the

position description only will turn the deduction more complicated without any advantaged or needed.

The length of the links is represented by l_1 to l_3, the center of mass by cm_1 to cm_3 and the position by θ_1 to θ_3. The equations of the points are given by:

$$p_{x1} = l_1 cm_1 sin(\theta_1) \tag{2.1}$$

$$p_{y1} = -l_1\, cm_1\, cos(\theta_1) \tag{2.2}$$

$$p_{x2} = l_1\, sin(\theta_1) + l_2 cm_2 sin(\theta_1 + \theta_2) \tag{2.3}$$

$$p_{y2} = -l_1 \cos(\theta_1) - l_2 cm_2 \cos(\theta_1 + \theta_2) \tag{2.4}$$

$$p_{x3} = l_1 \sin(\theta_1) + l_2 \sin(\theta_1 + \theta_2) + l_3 cm_3 \sin(\theta_1 + \theta_2 + \theta_3) \tag{2.5}$$

$$p_{y3} = -l_1 \cos(\theta_1) - l_2 \cos(\theta_1 + \theta_2) - l_3 cm_3 \cos(\theta_1 + \theta_2 + \theta_3) \tag{2.6}$$

2.1.2 Kinematics Redundancy

In the manipulator, the redundancy occurs when there are more degrees-of-freedom than the minimum necessary to define a position and orientation (CHANG, 1989; MOHAMMED, LI, 2016). For example, for the end-effector to go to a certain spatial position, (x_n, z_n), is necessary just move θ_3. So, θ_1 and θ_2 can assume a wide variety of values and the desired special positions are still attended. The redundancy doesn't necessarily mean a problem on the structure, in fact there is a lot of advantages if the robot has more than one way to achieve a certain point (FROM, GRAVDAHL, 2007).

The major problem with redundancy lies on the Inverse Kinematics solution and is pretty simples to understand why (GROETSCH, 1993). If it is possible to achieve a special point using more than one joint position, there will be more than one joint position that express the same special localization. Mathematically this means that the Inverse Kinematics have more than one solution (OGAWA, KANADA, 2010).

The robotic manipulator of this work has three degrees-of-freedom and analyzing the figure 5 there are a lot of possible spatial position that need just two DOF to achieve. The figure 6 gives an example of two joints configurations that provide the same special localization with complete different position.

Figure 7 - Example of redundancy of the manipulator.

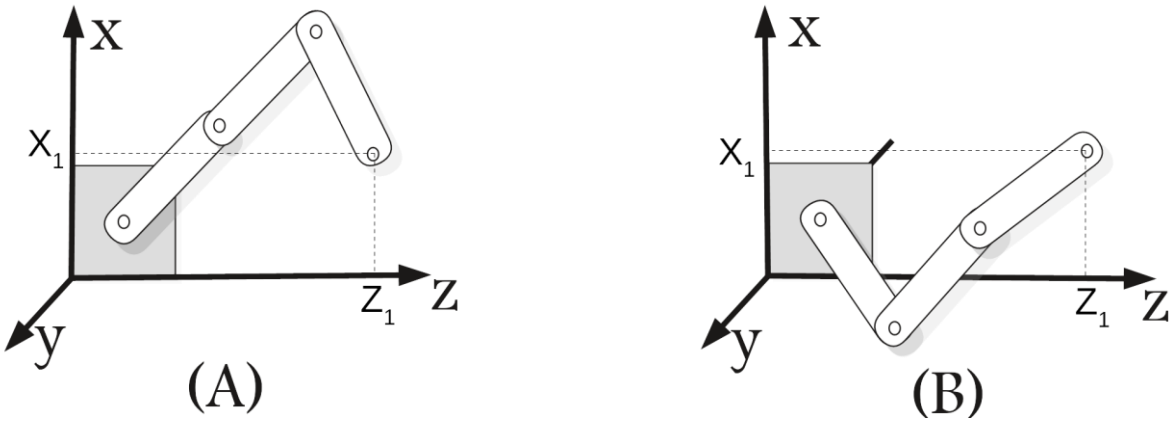

Source: Self Authorship

2.1.3 Inverse Kinematics

The Inverse Kinematics, as the name suggest, is the inverse process provide by the Forward Kinematics. So, this time the position of the links or joints of the robot can be determined by knowing the spatial position of the links. In most cases the simplest way to find the Inverse Kinematics is a mathematical manipulation of the Forward equations (NIKU, 2011; CRAIG, 1998).

As discussed on the Redundancy Kinematics, the analytical solution is not always possible. Structures with closed chain or high degrees-of-freedom are example where the analytical solution it is generally not possible to solve using mathematical manipulations (GROESTSCH, 1989; OGAWA, KANADA, 2010; DUKA, 2014). In Such cases another approach is needed to solve the problem, as Parameter Estimation, Regularization, Discretization and so on (MOHAMMED, LI, 2016).

The three DOF manipulator is one example of manipulators with kinematic redundancy and this means that the solution for the joints position is not unique. There is a lot of approaches to find the Inverse Kinematic solution and one of them is add an

additional position concerning the end-effector. The figure 8 shows this new variable on the robotic coordinates to solve the problem analytically.

Figure 8 - Position and variables for the Inverse Kinematics.

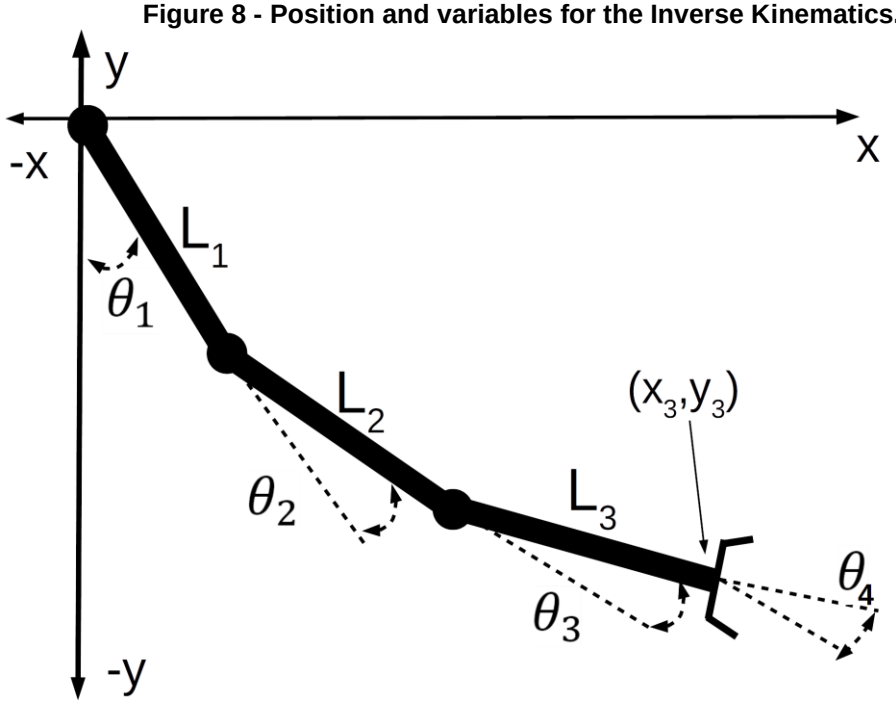

Source: Self Authorship.

The end-effector position is given by

$$\theta_4 = \theta_1 + \theta_2 + \theta_3 \tag{2.7}$$

The position equations of the second link 2.2 and 2.3 was be expressed using a trigonometric identity to expand the term $\cos(\theta_1 + \theta_2)$

$$p_{x2} = l_1 \cos(\theta_1) + l_2 cm_2(\cos(\theta_1)\sin(\theta_2) - \cos(\theta_1)\sin(\theta_2)) \tag{2.8}$$

$$p_{y2} = -l_1 \sin(\theta_1) - l_2 cm_2(\sin(\theta_1)\cos(\theta_2) - \sin(\theta_2)\cos(\theta_1)) \tag{2.9}$$

Adding the two positions, squaring both sides and solving for θ_2

$$p_{x2}^2 + p_{y2}^2 = L_1^2 + L_2^2 + 2L_1L_2\cos(\theta_2) \tag{2.10}$$

$$\theta_2 = \pm arccos\left(\frac{p_{x2}^2+p_{y2}^2- L_1^2-L_2^2}{2L_1L_2}\right) \quad (2.11)$$

The position θ_2 is express with $\pm$ because the angle can be for the left or the right of the y axis on the figure 8. To find θ_1 the equation 2.8 and 2.9 was solved to emphasize the component $\cos(\theta_1)$ in 2.8 and $\sin(\theta_1)$ in 2.9

$$\cos(\theta_1) = \frac{p_{x2}+L_2\sin(\theta_1)\sin(\theta_2)}{L_1+L_2\cos(\theta_2)} \quad (2.12)$$

$$\sin(\theta_1) = \frac{p_{xy}-L_2\sin(\theta_2)\cos(\theta_1)}{L_1+L_2\cos(\theta_2)} \quad (2.13)$$

Replacing $\sin(\theta_1)$ given by 2.13 on 2.12

$$\cos(\theta_1)\,(L_1^2 + L_2^2\cos(\theta_2)^2 + 2L_1L_2\cos(\theta_2) + L_2^2\sin(\theta_2)^2) = p_{x2}(L_1 + L_2\cos(\theta_2)) + p_{y2}L_2\sin(\theta_2) \quad (2.14)$$

Solving the equation 2.14 for $\cos(\theta_1)$ and $\sin(\theta_1)$

$$\cos(\theta_1) = \frac{p_{x2}(L_1+L_2\cos(\theta_2))+p_{y2}L_2\sin(\theta_2)}{p_{x2}^2+p_{y2}^2} \quad (2.15)$$

$$\sin(\theta_1) = \frac{p_{y2}(L_1+L_2\cos(\theta_2))-p_{x2}L_2\sin(\theta_2)}{p_{x2}^2+p_{y2}^2} \quad (2.16)$$

Using a trigonometry identity, θ_1 is given by

$$\theta_1 = \arctan\left(\frac{p_{y2}(L_1+L_2\cos(\theta_2))-p_{x2}L_2\sin(\theta_2)}{p_{x2}(L_1+L_2\cos(\theta_2))+p_{y2}L_2\sin(\theta_2)}\right) \quad (2.17)$$

To find θ_3 the joints position θ_2, θ_1, calculated in this order, and the end-effector position θ_4 was needed. The equation 2.7 was rewritten to emphasize θ_3

$$\theta_3 = \theta_4 - \theta_1 - \theta_2 \quad (2.18)$$

The equations 2.11, 2.17 and 2.18 can be used to define the kinematic behavior of the manipulator concerning the end-effector.

2.2 DYNAMICS

Still within the definitions by the mechanical science, the dynamic, as in kinematics, describes the equation o movement but this time consider the cause of motion (HIBBELER, 2006; ANGELES, 2013). In robotic system, this means that the natural movement is not able to satisfy the desired performance and is necessary apply external forces to guide and control the system (KORAYEM, 1994). This behavior control is made by the system control and is from the dynamic description that is possible to introduce the variables that are used to apply the control on the system.

Regardless of which type of actuator will be used in the system, the dynamic deduction is made to correlate the movements of the robot with the additions made by these external forces of movement. Dynamic deduction does not require specifying the type of actuator even if it adds new variables to the system, this will be done by substitution at the appropriate time of deduction of the actuators (MURRAY et al, 1994; You, 1994).

With the equations of position using the cartesian coordinates as shown in 2.1 to 2.6, the Lagrangian Mechanics is one of the best combinations to describe the dynamics (NIKU, 2011). Using the energy of the system as the basis to calculate de dynamic instead to analyses the forces, the kinetic and potential energy of the system are analyses to define how is the body behavior. In the following dynamic equations of motion, the link index is express by k and the upper bound of the links formulation by n, where both in this work goes from the first link to third link.

$$L = \sum_{k=1}^{n} E_{Kinetic} - \sum_{k=1}^{n} E_{Potential} \quad (2.19)$$

The kinetic energy for the k links was given by

$$E_{Kinetic\ k} = \sum_{k=1}^{n} \left(\frac{1}{2} [m_k v_k^2 + \bar{I}_k\ \omega_k^2] \right) \tag{2.20}$$

where $\bar{I}_k$ is the Inertial Moment, m_k is the link mass, ω_k is the acceleration and v_k is the link speed.

The speed component used on the equations of motion, v_k^2 in 2.20 for example, are dependent of the special coordinates given by 2.1 to 2.6, $p_{x\,1}$ to $p_{x\,3}$ and $p_{y\,1}$ to $p_{y\,3}$. To define the link speed v_k for the first link, $k = 1$, the position used were the first link position $p_{x\,1}$ and $p_{y\,1}$, 2.1 and 2.2, and so on for the second and third link. The position p_k relative to v_k can be express as

$$p_k = \sqrt{p_{x\,k}^2 + p_{y\,k}^2} \tag{2.21}$$

and the speed derivative was taken with respect to those positions express by p_k

$$v_k = \frac{d}{dt} \left(\frac{dp_k}{d\theta_k} \right) \tag{2.22}$$

Based on that and taking advantage of kinematic equation, 2.20, the speed was expressed following the needs of this equation. That means, express the speed component as v_k^2. The position equation, 2.21, were expressed getting rid of the square root and the speed used

$$v_k^2 = \frac{d}{dt} \left(\frac{d(p_{x\,k} + p_{y\,k})}{d\theta_k} \right) \tag{2.23}$$

The equations for the speed component of the kinetic energy can be expressed as:

$$v_1^2 = {cm_1}^2\ {l_1}^2\ \dot{\theta}_1^2 \tag{2.24}$$

$$v_2^2 = cm_2{}^2 l_2{}^2 \dot{\theta}_2^2 + \dot{\theta}_1^2\left(cm_2{}^2 l_2{}^2 + 2l_1 l_2 cm_2 cos(\theta_2) + l_1{}^2\right) + \dot{\theta}_1\dot{\theta}_2(2cm_2{}^2 l_2{}^2 + 2l_1 l_2 cm_2 cos(\theta_2)) \quad (2.25)$$

$$v_3^2 = -2l_1 l_3 cm_3 sin(\theta_2) sin(\theta_3)(\dot{\theta}_1^2 + \dot{\theta}_1\dot{\theta}_2 + \dot{\theta}_1\dot{\theta}_3) + 2l_1 l_3 cm_3 cos(\theta_2) cos(\theta_3)(\dot{\theta}_1^2 + \dot{\theta}_1\dot{\theta}_2 + \dot{\theta}_1\dot{\theta}_3) + l_1{}^2\dot{\theta}_1^2 + \dot{\theta}_1^2 l_2{}^2 + 2\dot{\theta}_1\dot{\theta}_2 l_2{}^2 + l_2{}^2\dot{\theta}_2^2 + 2l_2 l_3 cm_3 cos(\theta_3)(\dot{\theta}_1^2 + \dot{\theta}_1\dot{\theta}_3 + \dot{\theta}_2^2) + 2l_2 l_3 cm_3 cos(\theta_3)(\dot{\theta}_2\dot{\theta}_3 + 2\dot{\theta}_1\dot{\theta}_2) + 2cm3^2 l_3{}^2(\dot{\theta}_1^2 + \dot{\theta}_1\dot{\theta}_2 + \dot{\theta}_1\dot{\theta}_3) + 2\dot{\theta}_1\dot{\theta}_2 cos(\theta_2) l_1 l_2 + cm3^2 l_3{}^2\dot{\theta}_2^2 + 2cm3^2 l_3{}^2\dot{\theta}_2\dot{\theta}_3 + cm3^2 l_3{}^2\dot{\theta}_3^2 + 2\dot{\theta}_1^2 cos(\theta_2) l_1 l_2 \quad (2.26)$$

The kinetic energy of the three links are

$$E_{kin.\ 1} = \frac{1}{2} I_1\dot{\theta}_1^2 + \frac{1}{2} m_1 cm_1{}^2 I_1{}^2\dot{\theta}_1^2 \quad (2.27)$$

$$E_{kin.\ 2} = \frac{1}{2} m_2(cm_2{}^2 I_2{}^2\dot{\theta}_2^2 + \dot{\theta}_1^2(cm_2{}^2 I_2{}^2 + 2l_1 l_2 cm_2\cos(\theta_2) + l_2{}^2) + \dot{\theta}_1\dot{\theta}_2(cm_2{}^2 I_2{}^2 + +2l_1 l_2 cm_2 cos(\theta_2))) + \frac{1}{2} I_2\left(\dot{\theta}_1 + \dot{\theta}_2\right)^2 \quad (2.28)$$

$$E_{kin.\ 3} = \frac{1}{2} m3(\dot{\theta}_1^2(2l_1 l_3 cm_3\cos(\theta_2 + \theta_3) + 2\cos(\theta_3)\, l_2 l_3 cm_3 + cm_3{}^2 l_3{}^2 + l_1{}^2 + + 2\cos(\theta_2) l_1 l_2 + l_2{}^2) + \dot{\theta}_2^2(2\cos(\theta_3) l_2 l_3 cm_3 + cm3^2 l3^2 + l2^2) + cm_3{}^2 l_3{}^2\dot{\theta}_3^2 + +2\dot{\theta}_1\dot{\theta}_2\left(l_1 l_3 cm_3\cos(\theta_2 + \theta_3) + 2\cos(\theta_3)\, l_1 l_3 cm_3 + \cos(\theta_2)\, l_1 l_2 + l_2{}^2\right) + +2l_3 cm_3\dot{\theta}_1\dot{\theta}_3(l_1\cos(\theta_2 + \theta_3) + \cos(\theta_3) l_2 + l_3 cm_3) + 2l_3 cm_3\dot{\theta}_2\dot{\theta}_3(cos(\theta_3) l_2 + +cm_3{}^2 l_3{}^2 + l_3 cm_3)) + \frac{1}{2} I_3\left(\dot{\theta}_1 + \dot{\theta}_2 + \dot{\theta}_3\right)^2 \quad (2.29)$$

The final kinematic energy for the whole system is the sum of the three components

$$E_{kin.} = E_{kin.\ 1} + E_{kin.\ 2} + E_{kin.\ 3} \quad (2.30)$$

The potential energy is given by

$$E_{potential} = p_k\, m_k\, g \tag{2.31}$$

$$E_{pot\ 1} = -cm_1 l_1 m_1 \cos(\theta_1)\, g + P_{01} \tag{2.32}$$

$$E_{pot\ 2} = -g\, m_2 (l_1 \cos(\theta_1) + cm_2 l_2 \cos(\theta_2)) + P_{02} \tag{2.33}$$

$$E_{pot\ 3} = -g\, m_3 (l_1 \cos(\theta_1) + l_2 \cos(\theta_2) + cm_3 l_3 \cos(\theta_3)) + P_{03} \tag{2.34}$$

The potential energy of the three links is given by:

$$E_{pot} = +P_{01} + P_{02} + P_{03} - g(\cos(\theta_1)\,(cm_1 l_1 m_1 + l_1 m_2 + l_1 m_3) + \\ + cos(\theta_2)\,(cm_2 l_2 m_2 + l_2 m_3) + cos(\theta_3)\,(cm_3 l_3 m_3) \tag{2.35}$$

where P_{03}, P_{02} and P_{01} are possible initial potential energy based on the initial position of the links. Even in the position chosen as the initial condition on this work these components are null, this component can have values during the manipulator operations.

Adding all the energy components using the Lagrangian equation 2.19, the final result is:

$$L = +\dot{\theta}_2^2 \Omega_1 + \dot{\theta}_2^2 \Omega_2 + \dot{\theta}_2^2 \Omega_3 + \dot{\theta}_1(\dot{\theta}_2 \Omega_4 + \dot{\theta}_3 \Omega_5) + \dot{\theta}_2 \dot{\theta}_3 \Omega_6 - g(cos(\theta_2)(l_2 m_3 + \\ + cm_2 l_2 m_2) + cos(\theta_3)\,(cm_3 l_3 m_3) + \cos(\theta_1)\,(cm_1 l_1 m_1 + l_1 m_2 + l_1 m_3)) \tag{2.36}$$

with the variables that resume some common terms

$$\Omega_1 = {l_1}^2 (m_2 + m_3 + m_1 {cm_1}^2) + I_1 + I_2 + I_3 + {l_2}^2 (m_2 {cm_2}^2 + m_3 {cm_3}^2 {l_3}^2) + \\ + 2\big(m_3 cos(\theta_3) cm_3 l_2 l_3 + cos(\theta_2) l_1 l_2 (cm_2 m_2 + m_3) + m_3 cm_3 l_1 l_3 cos(\theta_2 + \theta_3)\big)$$

$$\Omega_2 = 2 m_3 cos(\theta_3) cm_3 l_2 l_3 + m_2 {cm_3}^2 {l_2}^2 + m_3 {cm_3}^2 {l_3}^2 + m_3 {l_2}^2 + I_2 + I_3$$

$$\Omega_3 = cm_3{}^2 l_3{}^2 m_3 + I_3$$

$$\Omega_4 = 2m_3 cos(\theta_3) cm_3 l_2 l_3 + cos(\theta_2)(cm_2 l_2 l_1 m_2 + l_2 l_1 m_3) + m_3 cm_3 l_2 l_1 cos(\theta_2 + + \theta_3) + m_2 cm_2{}^2 l_2{}^2 + m_3 cm_3{}^2 l_2{}^2 + m_3 l_2{}^2 + I_2 + I_3$$

$$\Omega_5 = m_3 cos(\theta_3) cm_3 l_2 l_3 + m_3 cm_3 l_1 l_3 cos(\theta_2 + \theta_3) + m_3{}^2 l_3{}^2 + I_3$$

$$\Omega_6 = m_3 cos(\theta_3) cm_3 l_2 l_3 + m_3 cm_3{}^2 l_3{}^2 + I_3$$

The Lagrangian, 2.36, can be used to express the dynamical behavior of a body and evidencing the input forces starting from the Newton's second law of motion for linear and rotational movements.

$$\sum F = m_k a_k \qquad \sum T = I_k \omega_k \tag{2.37}$$

Considering the body with movement on y axis the second law is

$$f - m_k g = m_k \ddot{y} \tag{2.38}$$

The component provides from the acceleration, right hand side of equation 2.38, can be express as

$$m_k \ddot{y} = \frac{d}{dt}(m_k \dot{y}) = \frac{\partial}{\partial t}\frac{\partial}{\partial \dot{y}}(1/2\, m_k \dot{y}^2) \tag{2.39}$$

Looking at the kinematic energy equation 2.39, the acceleration of the particle can be express in function of the kinematic energy

$$\frac{d}{dt}\frac{\partial}{\partial \dot{y}}\left(\frac{m\dot{y}^2}{2}\right) = \frac{d}{dt}\frac{\partial E_{Kin.}}{\partial \dot{y}} \tag{2.40}$$

The gravitational acceleration, left hand side of equation 2.38, can be rewritten to express the potential energy of the particle

$$mg = \frac{\delta}{\delta y}(mgy) = \frac{\delta E_{Pot}}{\delta y} \tag{2.41}$$

Compering the Lagrangian, 2.19, the kinematic and potential energy, 2.30, and 2.35 with the derivation of these two energy components is proved that those equation are equal

$$\frac{\delta L}{\delta \dot{y}} = \frac{\delta E_{Kin}}{\delta \dot{y}} \tag{2.42}$$

$$\frac{\delta L}{\delta y} = -\frac{\delta E_{Pot}}{\delta y} \tag{2.43}$$

Replacing these two proofs on the Lagrangian equation, the final motion equation is

$$\frac{d}{dt}\left(\frac{\partial L}{\partial \dot{q_k}}\right) - \frac{\partial L}{\partial k q_k} = Q_k \tag{2.44}$$

The variable y is replaced for q as the special coordinates arising from the generalized coordinates and Q_k, f on the equation 2.38, is the generalized force resulting from the k particle of the body (SPONG et al, 2005; NIKU, 2011).

In the robot used in this work, three angles were defined for which position of the three links, corresponding to each of the three parts of the whole manipulator body. This leads to three equations, 2.45 to 2.47. Derivating the Lagrangian equation, 2.36, with respect to θ_k and $\dot{\theta_k}$, the Torque equation are given by the equations 2.48 to 2.50.

$$\frac{d}{dt}\left(\frac{\partial L}{\partial \dot{\theta}_1}\right) - \frac{\partial L}{\partial_{\theta_1}} = \tau_1 \tag{2.45}$$

$$\frac{d}{dt}\left(\frac{\partial L}{\partial \dot{\theta}_2}\right) - \frac{\partial L}{\partial_{\theta_2}} = \tau_2 \tag{2.46}$$

$$\frac{d}{dt}\left(\frac{\partial L}{\partial \dot{\theta}_3}\right) - \frac{\partial L}{\partial_{\theta_3}} = \tau_3 \tag{2.47}$$

$$\tau_1 = \Omega_1\ddot{\theta}_1 + \Omega_4\ddot{\theta}_2 + \Omega_6\ddot{\theta}_3 - \dot{\theta}_2^2(sin(\theta_2)(cm_2l_1l_2m_2 + l_1l_2m_3) - 2\dot{\theta}_1\dot{\theta}_3cm_3l_3m_3(sin(\theta_3)l_2 + sin(\theta_2 + \theta_3)l_1) - \dot{\theta}_3^2cm_3l_3m_3(sin(\theta_3)l_2 - sin(\theta_2 + \theta_3)l_1) - \dot{\theta}_1\dot{\theta}_2(sin(\theta_2)2l_1l_2(cm_2m_2 - m_3) + 2sin(\theta_2 + \theta_3)cm_3l_3l_1m_3) - -\dot{\theta}_2\dot{\theta}_3cm_3l_3l_2m_3(2sin(\theta_3)l_1 + 2sin(\theta_2 + \theta_3)l_2 + sin(\theta_2 + \theta_3)l_1) + g(sin(\theta_1)(cm_1l_1m_1 + l_1m_2 + l_1m_3) + g(\sin(\theta_1 + \theta_2)l_2\,(cm_2m_2 + m_3) + sin(\theta_1 + \theta_3 + \theta_2)cm_3l_3m_3) \quad (2.48)$$

$$\tau_2 = \ddot{\theta}_1\Omega_4 + \ddot{\theta}_2\Omega_2 + \ddot{\theta}_3\Omega_6 - \dot{\theta}_1\dot{\theta}_3(2\sin(\theta_3)\,cm_3l_2l_3m_3 + \sin(\theta_2 + \theta_3)\,cm_3l_3l_1m_3) - -cm_3l_2l_3m_3(2\dot{\theta}_2\dot{\theta}_3\sin(\theta_3) + \dot{\theta}_3^2\sin(\theta_3)) - \dot{\theta}_1\dot{\theta}_2(\sin(\theta_2 + \theta_3)\,cm_3l_3l_1m_3 + -\dot{\theta}_1\dot{\theta}_2(\sin(\theta_2 + \theta_3)\,cm_3l_3l_1m_3 + \sin(\theta_2)\,(cm_2l_2l_1m_2 + l_2l_1m_3) + +g(\sin(\theta_1 + \theta_2)l_2\,(cm_2m_2 + m_3) + \sin(\theta_1 + \theta_2 + \theta_3)cm_3l_3m_3) \quad (2.49)$$

$$\tau_3 = \ddot{\theta}_1\Omega_5 + \ddot{\theta}_2\Omega_6 + \ddot{\theta}_3\Omega_3 - \sin(\theta_2 + \theta_3)\,cm_3l_3l_1m_3\left(\dot{\theta}_1\dot{\theta}_2 + \dot{\theta}_1\dot{\theta}_3\right) - -\dot{\theta}_1\dot{\theta}_3\sin(\theta_3)\,cm_3l_3l_1m_3 - \dot{\theta}_2\dot{\theta}_3sin(\theta_3)cm_3l_2l_3m_3 + gsin(\theta_1 + \theta_2 + \theta_3)cm_3l_3m_3 \quad (2.50)$$

The final dynamic equations 2.48 to 2.50 still had two problems for their use in simulations. At first, due to the Euler-Lagrange formulation those equations are written in terms of the inputs τ_k, but for the simulation and dynamic analysis is necessary that the equations be written in terms of the system states. And the second problem is that there was a coupling relation of the acceleration components in all three equations, that is, on the first torque τ_1, equation 2.48, is an occurrence of $\ddot{\theta}_2$ and $\ddot{\theta}_3$ and so on.

This occurrence makes impossible solve and simulate the dynamic equation. Even if it is known the initial condition for all three accelerations, the problem still remains because there will always be an acceleration $\ddot{\theta}_{n+i}$ on an equation $\ddot{\theta}_n$ on the same time calculation range. That means at an instant t_n on the simulation, $\ddot{\theta}_n$ is being calculated but on the same equation is an $\ddot{\theta}_{n+2}$ which will only be determined after $\ddot{\theta}_n$ and $\ddot{\theta}_{n+1}$. On that instant t_n the acceleration of the first link is being calculated and the acceleration of the third link is dependent of that value, so even if $\ddot{\theta}_3$ is known, this value is known for at least t_{n-1} and never for t_n.

To solve these two problems, the dynamic system needed to be rewritten to solve the coupling and emphasize the system states. So, the three dynamic equations, 2.48 to 2.50, were treated as a linear system with the acceleration $\ddot{\theta}_1$, $\ddot{\theta}_2$ and $\ddot{\theta}_3$ as the unknow variables and all other components resumed on λ_1 to λ_{12}

$$\tau_1 = \ddot{\theta}_1\lambda_1 + \ddot{\theta}_2\lambda_2 + \ddot{\theta}_3\lambda_3 + \lambda_4 \tag{2.51}$$

$$\tau_2 = \ddot{\theta}_1\lambda_5 + \ddot{\theta}_2\lambda_6 + \ddot{\theta}_3\lambda_7 + \lambda_8 \tag{2.52}$$

$$\tau_3 = \ddot{\theta}_1\lambda_9 + \ddot{\theta}_2\lambda_{10} + \ddot{\theta}_3\lambda_{11} + \lambda_{12} \tag{2.53}$$

The solution was presented in function of the variables resumed on λ_1 to λ_{12} on the equations 2.48 to 2.50 and the inputs τ_k.

$$\ddot{\theta}_1 = \left(\frac{\tau_1(\lambda_{10}\lambda_7-\lambda_{11}\lambda_6)+\tau_2(\lambda_{11}\lambda_2-\lambda_{10}\lambda_3)+\tau_3(\lambda_3\lambda_6-\lambda_2\lambda_7)}{\lambda_1\lambda_{10}\lambda_7-\lambda_1\lambda_{11}\lambda_6-\lambda_{10}\lambda_3\lambda_5+\lambda_{11}\lambda_2\lambda_5-\lambda_2\lambda_7\lambda_9+\lambda_3\lambda_6\lambda_9}\right) + \left(\frac{\lambda_{10}(\lambda_3\lambda_8-\lambda_4\lambda_7)+\lambda_{11}(\lambda_4\lambda_6-\lambda_2\lambda_8)+\lambda_{12}(\lambda_2\lambda_7-\lambda_3\lambda_6)}{\lambda_1\lambda_{10}\lambda_7-\lambda_1\lambda_{11}\lambda_6-\lambda_{10}\lambda_3\lambda_5+\lambda_{11}\lambda_2\lambda_5-\lambda_2\lambda_7\lambda_9+\lambda_3\lambda_6\lambda_9}\right) \tag{2.54}$$

$$\ddot{\theta}_2 = \left(\frac{\tau_1(\lambda_{11}\lambda_5-\lambda_7\lambda_9)+\tau_2(\lambda_3\lambda_9-\lambda_1\lambda_{11})+\tau_3(\lambda_1\lambda_7-\lambda_3\lambda_5)}{\lambda_1\lambda_{10}\lambda_7-\lambda_1\lambda_{11}\lambda_6-\lambda_{10}\lambda_3\lambda_5+\lambda_{11}\lambda_2\lambda_5-\lambda_2\lambda_7\lambda_9+\lambda_3\lambda_6\lambda_9}\right) + \left(\frac{+\lambda_1(\lambda_8\lambda_{11}-\lambda_{12}\lambda_7)+\lambda_5(\lambda_{12}\lambda_3-\lambda_{11}\lambda_4)+\lambda_9(\lambda_3\lambda_8-\lambda_4\lambda_7)}{\lambda_1\lambda_{10}\lambda_7-\lambda_1\lambda_{11}\lambda_6-\lambda_{10}\lambda_3\lambda_5+\lambda_{11}\lambda_2\lambda_5-\lambda_2\lambda_7\lambda_9+\lambda_3\lambda_6\lambda_9}\right) \tag{2.55}$$

$$\ddot{\theta}_3 = -\left(\frac{\tau_1(\lambda_{10}\lambda_5-\lambda_6\lambda_9)+\tau_2(\lambda_2\lambda_9-\lambda_1\lambda_{10})+\tau_3(\lambda_1\lambda_6-\lambda_2\lambda_5)}{\lambda_1\lambda_{10}\lambda_7-\lambda_1\lambda_{11}\lambda_6-\lambda_{10}\lambda_3\lambda_5+\lambda_{11}\lambda_2\lambda_5-\lambda_2\lambda_7\lambda_9+\lambda_3\lambda_6\lambda_9}\right) + \left(\frac{\lambda_1(\lambda_{10}\lambda_8-\lambda_{12}\lambda_6)+\lambda_5(\lambda_{12}\lambda_2-\lambda_{10}\lambda_4)+\lambda_9(\lambda_4\lambda_6-\lambda_2\lambda_8)}{\lambda_1\lambda_{10}\lambda_7-\lambda_1\lambda_{11}\lambda_6-\lambda_{10}\lambda_3\lambda_5+\lambda_{11}\lambda_2\lambda_5-\lambda_2\lambda_7\lambda_9+\lambda_3\lambda_6\lambda_9}\right) \tag{2.56}$$

2.3 MECHANICAL DISSIPATION

All the mechanical dissipation, provides from vibration and friction for example, were resumed on one equation (NEUMAN, TOURASSIS, 1985)

$$D(t)_n = \frac{1}{2}\sum_{i=1}^{n}\sum_{j=1}^{n}\mu_{ij}\,\dot{q}_j\dot{q}_i \tag{2.57}$$

That can be express as

$$D(t) = \frac{1}{2}\mu_1\dot{\theta}_1^2 + \frac{1}{2}\mu_2\left(\dot{\theta}_1 + \dot{\theta}_2\right)^2 + \frac{1}{2}\mu_3\left(\dot{\theta}_1 + \dot{\theta}_2 + \dot{\theta}_3\right)^2 \tag{2.58}$$

The equation 2.58 leads to three equations for witch degree-of-freedom and joint. The dissipation coefficient is μ_k and $\dot{\theta}_k$ is the joint speed.

$$D(t)_1 = \mu_1\dot{\theta}_1 + \mu_2\dot{\theta}_1 + \mu_2\dot{\theta}_2 + \mu_3\dot{\theta}_1 + \mu_3\dot{\theta}_2 + \mu_3\dot{\theta}_3 \tag{2.59}$$

$$D(t)_2 = \mu_2\dot{\theta}_1 + \mu_2\dot{\theta}_2 + \mu_3\dot{\theta}_1 + \mu_3\dot{\theta}_2 + \mu_3\dot{\theta}_3 \tag{2.60}$$

$$D(t)_3 = \mu_3\dot{\theta}_1 + \mu_3\dot{\theta}_2 + \mu_3\dot{\theta}_3 \tag{2.61}$$

2.4 DYNAMICAL MODEL UNDER PARAMETRIC UNCERTAINTIES

Even if the model considered all the dynamical components, as dissipations forces and influences on the model, all the physical parameters can have a minimal change on their values (TUSSET et al, 2013; GUO, LI, 2008).

This can be provided from error on sensing measurement, error on experimental parameters determination and even natural model variations provide from the movement, such as small increase or decrease on link size given by heat or friction. This variation was made using the equation 2.62.

$$\gamma_i = \left[0.8 \times \gamma_i + 0.4 \times \gamma_i \times \alpha\right] \qquad \alpha \in (0,1) \tag{2.62}$$

The parametrical variation of the i variable is given by γ_i. If α have the maximum value, 1, the variable γ_i increase in 20%. If α have the minimum value, 0, the variable γ_i decrease in 20%. The equations 2.63 to 2.65 shown the equation for the physical variables.

$$m_i = [0.8 \times m_i + 0.4 \times m_i \times \alpha] \qquad \alpha \in (0,1) \qquad (2.63)$$

$$l_i = [0.8 \times l_i + 0.4 \times l_i \times \alpha] \qquad \alpha \in (0,1) \qquad (2.64)$$

$$cm_i = [0.8 \times cm_i + 0.4 \times cm_i \times \alpha] \qquad \alpha \in (0,1) \qquad (2.65)$$

This approach can be on any system variable and the random value α can be increase or decrease as the project needs. For this work, the link mass m_i, the link length l_i and center of mass cm_i were the variables for the parametric uncertainty.

3 SYSTEM CONTROL USING STATE VARIABLE

The focus of the control is guide the system to a define behavior. This objective can be achieved using a vast majority of control approaches, all fully depending on the system and aim characteristics. In robotic manipulators is common don't know the control technique that is more efficient for the robotic struct used but have the performance specification in terms of what the robot need to be capable to do (LEWIS, 2004; NIKU, 2011). Knowing what the performance specification define to the system response is viable suppose and list different control techniques and strategies to achieve the best performance.

Even so, robotic manipulators have characteristics that provide some guidelines for witch control technique control can be use or witch control technique is more appropriate for certain systems (BELLON, 2008). Even if control is applied on the individually in the links, the system is a chain with inseparable relations between the links. That means that the variations on the control action and therefore on the variables on any link change these same values on the other links. Looking at the general spatial location and not at the individual positions of the links, ranging 10% on the position of the first link, increases also 10% the position of the others links if none action control is used to discount this grip applied on the first link.

The general characteristics of robotic system leads to the approach that has to be made for the mathematical representation and control strategy. Except very simple robotic system, such as one degree-of-freedom, robotic system tends to be a MIMO system (multiple-input and multiple-output). Being a MIMO system with non-linear and chaotic behavior point to the usage of state dependent representation, hence s time-domain approach (NAIDU, 2003).

The control using a state dependent approach can be divided in three parts. First of all, the system is considered a full-state feedback, that is, all the system states are available to measure. This assumption is not practical and, in most cases, there is states that can be monitored by sensors or use another approach different than measure all states can be a big financial and practical advantage for the project. The second step is solving the problem of how knowing all the system states. The third and final step is to connect to the control and the solution to define all the states of the system (DORF, BISHOP, 2010; OGATA, 2010).

When considering a full-state feedback system is possible to assume that exist an action control u_c with is a gain k_c multiplied by the states $x(t)$ that is capable to guide the system from an initial condition to any other condition in a finite time interval.

$$u_c = -k_c x(t) \tag{3.1}$$

Replacing this on the state space representation, 2.61 and 2.62

$$\dot{x} = (A - Bk_c)x(t) \tag{3.2}$$

The solution for the equation 3.2 informs that the answer is provide by the eigenvalues of the exponent $(A - Bk_c)$. As the values for A and B are already know, the control is defined by the values of the matrix k_c.

The difference between many of the control methods starts with how k_c is calculated.

3.1 STATE SPACE REPRESENTATION

The mathematical representation known as State Space is the approach made to deal with system described by differential equations and set a relation of input, output and the system variables using matrices. The need to represent the complexity of reality and the problems of modern engineering has increased the role of these mathematical models (LEWIS et al, 2004; OGATA, 2004).

One of the main characteristics of the state space representation is work with a time-domain approach, this because the time-domain is the variable used on the differential equation description. Using a representation by differential equations, this mathematical description has a more inclusive application and can be used for the vast majority of system as multivariable on input and output, nonlinear, time-variant, time-dependent and so on (DORF, BISHOP, 2010).

On the state space, the state variables are those who can determine the system behavior in time based on the differential equations description, presenting values and the input excitation. The differential equation describes the system behavior

in at least two groups of equation, the inputs and the outputs, as shown on the figure 9.

Figure 9 - Diagram for input and outputs on a MIMO system.

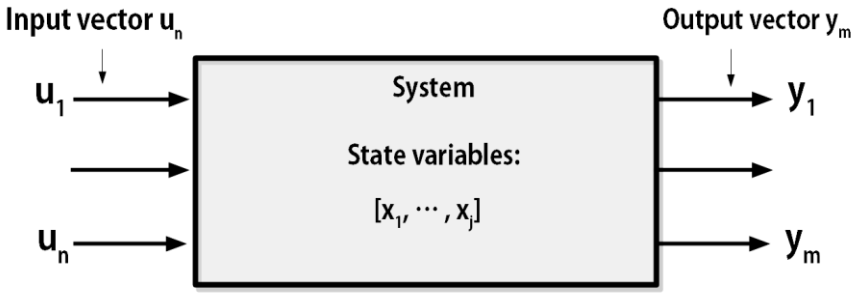

Source: Self Authorship.

The input equations are usually represented with the variables shown in the equation 3.3, where x_n are the state variables, u_n are the inputs and a_n and b_n are coefficients used for the matrix representation.

$$\begin{aligned}\dot{x}_1 &= a_{11}x_1 + a_{12}x_2 + \cdots + a_{1n}x_n + \cdots + b_{11}u_1 + \cdots b_{1m}u_m \\ \dot{x}_2 &= a_{21}x_1 + a_{22}x_2 + \cdots + a_{2n}x_n + \cdots + b_{21}u_1 + \cdots b_{2m}u_m \\ \dot{x}_n &= a_{n1}x_1 + a_{n2}x_2 + \cdots + a_{nm}x_n + \cdots + b_{n1}u_1 + \cdots b_{nm}u_m\end{aligned} \tag{3.3}$$

The state space represents the differential equation 3.3 in matrices as

$$\frac{d}{dx}\begin{bmatrix}x_1\\x_2\\...\\x_n\end{bmatrix} = \begin{bmatrix}a_{11} & a_{12} & ... & a_{1n}\\a_{21} & a_{22} & ... & a_{2n}\\... & ... & ... & ...\\a_{n1} & a_{n2} & ... & a_{nm}\end{bmatrix}\begin{bmatrix}x_1\\x_2\\...\\x_n\end{bmatrix} + \begin{bmatrix}b_{11} & ... & b_{1m}\\... & ... & ...\\b_{n1} & ... & b_{nm}\end{bmatrix}\begin{bmatrix}u_1\\...\\u_m\end{bmatrix} \tag{3.4}$$

The general representation for state space provide four matrices, where $A(x)$ is the state matrix, $B(x)$ is the input matrix, $C(x)$ is the output matrix and $D(x)$ is the direct transmission matrix (Ogata, 2010). The vector $[x_1,\ x_2, \ldots, x_n]$ are the state vector and vector $[u_1,\ u_2, \ldots, u_n]$ are the input vector.

This group of matrices is represented to in the form of

$$\dot{x} = Ax(t) + Bu(t) \tag{3.5}$$

The same principle is used to the input equation shown on 3.6 and 3.7 are used for the output equations

$$\begin{aligned} y_1 &= c_{11}x_1 + c_{12}x_2 + \cdots + c_{1n}x_n + \cdots + d_{11}u_1 + \cdots d_{1m}u_m \\ y_2 &= c_{21}x_1 + c_{22}x_2 + \cdots + c_{2n}x_n + \cdots + d_{21}u_1 + \cdots d_{2m}u_m \\ y_n &= c_{n1}x_1 + c_{n2}x_2 + \cdots + c_{nm}x_n + \cdots + d_{n1}u_1 + \cdots d_{nm}u_m \end{aligned} \tag{3.6}$$

$$\begin{bmatrix} y_1 \\ y_2 \\ \dots \\ y_n \end{bmatrix} = \begin{bmatrix} c_{11} & c_{12} & \dots & c_{1n} \\ c_{21} & c_{22} & \dots & c_{2n} \\ \dots & \dots & \dots & \dots \\ c_{n1} & c_{n2} & \dots & c_{nm} \end{bmatrix} \begin{bmatrix} x_1 \\ x_2 \\ \dots \\ x_n \end{bmatrix} + \begin{bmatrix} d_{11} & \dots & d_{1m} \\ \dots & \dots & \dots \\ d_{n1} & \dots & d_{nm} \end{bmatrix} \begin{bmatrix} u_1 \\ \dots \\ u_m \end{bmatrix} \tag{3.7}$$

$$y = Cx(t) + Du(t) \tag{3.8}$$

3.2 OPTIMAL CONTROL

The optimal control follows the same objective already presented for any control system: drive the system to the desired states. But besides driving the system to the aim, the optimal control is the control that provide the best performance for this task (ANDERSON, MOORE 1989; KASTEV, 2006).

Using the affirmation that the definition of k_c is the difference between the control techniques and lead to the equation 3.1 and 3.2, the optimal control defines this matrix using a performance indicator.

Define the best control means that in optimal control there is a performance that is defined as the “best” based on a criterion. This criterion can be a mathematical expression that provides all the achievement needed or can be a generic main goal, as minimize error, have the fastest stabilization and so on (NAIDU, 2003; BRYSON, HO, 1975). On the robotics is possible to use an example to clarify these possibilities. Part of the aim for the system is take the joint from θ_i to θ_f. Looking at this problem is possible to suppose a lot of criterion to the control achieve, as minimizing the run time, the error during the path or the actuators requirement.

Before setting the optimal control, it is necessary to express the system in one of the mathematical representations used for non-linear control and define if this

system is controllable. For non-linear system, the state space representation can be use and this was presented on the equation 2.53 to 2.55, and here is use as the basis to the optimal control and for verification of controllability, observability and many other conceptual checks about the system.

$$\dot{x} = Ax(t) + Bu(t) \tag{3.9}$$

$$y = Cx(t) + Du(t) \tag{3.10}$$

Conceptually, the system is controllable is exist a function $u_c(x,t)$ that is capable to drive the system to the origin in a finite time interval (BELLON, 2008; BRYSON, HO, 1975). Using equation 3.1, the control can be seen as the way to find matrix k using the index of performance as a guide.

The equations represented in 3.9 and 3.10 define the system description, with the matrices A and C that are state dependents and the matrix B that is related with the inputs. This can be understood as if the output of the depends on the system states and the inputs. So, to specify if is possible control the system is necessary analyze the values presented on these matrices.

$$M = [B\ AB\ A^2B\ \ldots\ A^{n-1}B] \tag{3.11}$$

Where the matrices A and B was the size defined by

$$A = n \times n \tag{3.12}$$

$$B = n \times m \tag{3.13}$$

The system is controllable calculating the rank of the matrix M. If the rank of M is n, the system is completely controllable. If the rank is lower or higher than n, the system isn't completely controllable (OGATA, 2010). The system not be completely controllable doesn't mean the control can be used but means that additional considerations and strategies are needed to apply the optimal control (DORF, BISHOP, 2010). Those particularities will be discussed forward on this work.

Control over chaotic behavior, optimization in the use of input actions and fulfillment of optimization criteria are examples of advantages of using optimal control

(TUSSET et al, 2013). For these and other reason that will be discussed, currently we see an increase on works that uses optimal control and robot manipulators.

3.3 LQR CONTROL

The LQR control is use for a lot of optimal control techniques because provides adaptive guidelines that allow a vast number of approaches, mainly because the mathematical feature know as Linear Quadratic Regulator that is the base for a lot of control techniques.

As the control is applied on the whole-time span, $t \to \infty$, the performance index for the optimal control is given by

$$J = \int (x^T Q(x)x + u^T R(x)x)dt \tag{3.14}$$

The matrices B is provide by the system deduction and the matrices Q and R are weights matrices. Those weight matrices, Q and R, are subject on the optimization of the control and will be discussed on the next section. The simplest choice is use the main diagonal with a constant value.

$$Q = \begin{bmatrix} q_1 & \dots & 0 \\ \dots & q_2 & \dots \\ 0 & \dots & q_n \end{bmatrix} \tag{3.15}$$

$$R = \begin{bmatrix} r_1 & \dots & 0 \\ \dots & r_2 & \dots \\ 0 & \dots & r_n \end{bmatrix} \tag{3.16}$$

Using the notation presented on 3.9 and assuming the dual module of that same system compose by the transpose of those matrices

$$\dot{x} = Ax(t) + Bu(t) \tag{3.17}$$

$$\dot{x}^T = \big(Ax(t) + Bu(t)\big)^T = A^T x^T(t) + B^T u^T(t) \tag{3.18}$$

This same assumption is made for the control law, 3.1, and the substitution of this control law on the system 3.2.

$$u^T = -k^T x^T(t) \tag{3.19}$$

$$\dot{x}^T = (A^T - B^T k^T) x^T(t) \tag{3.20}$$

Replacing the equations 3.19 on 3.14.

$$J = \int_0^\infty (x^T Q(x) x + x^T k^T R(x) k x) dt \tag{3.21}$$

Evidencing the states components x and x^T in 3.21.

$$J = \int_0^\infty x^T (Q(x) + k^T R(x) k)\, x\, dt \tag{3.22}$$

$$J = x^T \left(\int_0^\infty (Q(x) + k^T R(x) k)\, dt \right) x \tag{3.23}$$

Is possible to assume that the function on 3.23 can be solve using a matrix P.

$$-\frac{d}{dt}(J) = -\frac{d}{dt}\left(x^T \left(\int_0^\infty (Q(x) + k^T R(x) k)\, dt \right) x \right) = x^T (Q(x) + k^T R(x) k) x \tag{3.24}$$

$$P = \int_0^\infty (Q(x) + k^T R(x) k)\, dt \tag{3.25}$$

Using the assumption 3.25, the equation 3.24 can be express as

$$-\frac{d}{dt}(x^T P x) = -\dot{x}^T P x - x P \dot{x} \tag{3.26}$$

$$-\dot{x}^T P x - x P \dot{x} = -Px[(A - Bk)x] - Px^T[(A - Bk)^T x^T] \tag{3.27}$$

Expanding 3.27 to evidence the term $(A - Bk_c)x$ that is the solution given by the equation 3.2:

$$x^T[(A - Bk_c)^T P + P(A - Bk_c)]x \tag{3.28}$$

Comparing the solution given by 3.28 and the equation 3.24 is possible to see the relation:

$$(A - Bk_c)^T P + P(A - Bk_c) = -Q(x) + {k_c}^T R(x) k_c \tag{3.29}$$

The conclusion is that there is a matrix P that satisfies and solve this problem.

As the problem is assume an infinite-horizon, the index J can be evaluated as:

$$J = \int_0^\infty x^T (Q(x) + k^T R(x) k_c)\, x\, dt = (-x^* P x)|_0^\infty \tag{3.30}$$

$$J = -x^*(\infty) P x(\infty) + x^*(0) P x(0) \tag{3.31}$$

As the component $(A - Bk_c)$ is assume to be stable, the real parts of the eigenvalues have negative real parts, so:

$$x(\infty) \to 0$$

$$J = x^*(0) P x(0)$$

For the solution of the problem this means that the performance index depends on the initial conditions and the matrix P.

As R is defined as positive-definite Hermitian, that means a real symmetric matrix, it can be express as a generic matrix T which just cannot be a singular matrix

$$R = T^T T \tag{3.32}$$

Using that assumption on the equation 3.32:

$$(A - Bk_c)^T P + P(A - Bk_c) + Q(x) + {k_c}^T T^T T k_c = 0 \tag{3.33}$$

$$A^T P + PA + [Tk_c - (T^T)^{-1}B^T P]^T [Tk_c - (T^T)^{-1}B^T P] - PBR^{-1}B^T P + Q = 0 \quad (3.34)$$

So, the minimization of J with respect of k is provide from the component:

$$x^T [Tk_c - (T^T)^{-1}B^T P]^T [Tk_c - (T^T)^{-1}B^T P]x \quad (4.35)$$

And the minimization is found evaluating the equation 3.35 on zero or using the term Tk_c to eliminate the other component on the brackets. Using the second possibility this leads to.

$$Tk_c = (T^T)^{-1}B^T P \quad (3.36)$$

Evidencing k_c on 3.36:

$$k_c = T^{-1}(T^T)^{-1}B^T P = -R^{-1}B^T P \quad (3.37)$$

Since the control law is given in terms of $u(t)$:

$$u_c(t) = -k_c x(t) = -R^{-1}B^T P\, x(t) \quad (3.38)$$

The full-state feedback control is still given by the equation 3.1 and the matrix k_c is given by:

$$k_c = R^{-1}(B^T P + N^T) \quad (3.39)$$

$$A^T P + PA - PBR^{-1}B^T P + Q = 0 \quad (3.40)$$

As the matrices A, B, N, Q and R are known, one possibility to found the matrix P is use the Riccati Differential Equation as basis to the solution. The Riccati Differential equation can be express as presented on 3.33 and 3.35, resulting on the equation 3.40.

3.4 STATE DEPENDENT COEFFICIENTS (SDC) ON SDRE CONTROL

Before using the LQR control as the basis for a non-linear application, the SDRE control used on this work, is necessary understand how this connection between the linear and non-linear application is possible.

The SDRE control uses the state matrices to found the control law but these matrices are not necessarily used as defined for LQR control. To differentiate these two representations, for the SDRE control the input equation of the state space system, equation 3.9, can be written as:

$$\dot{x} = f(x) + g(x)u(t) \tag{3.41}$$

where $f(x)$ is analogous to the matrix $A(x)$ on 3.9 and $g(x)$ to $B(x)$ on 3.9 to. Found the values for the matrices $f(x)$ and $g(x)$ is process to define the State Dependent Coefficients (SDC) for the SDRE control. Determine the values for $f(x)$ and $g(x)$ is not a single solution problem and many methods are developed to define the best representation for these matrices (TELLEZ-ORNELAS et al, 2014).

Kastev (2006) recalls that a possible solution is use the LQR representation for $A(x)$ and $B(x)$ and calculate the values for these matrices at each instant of the solution. Based on this approach, for use the LQR principle on non-linear application is necessary define the system behavior multiple times, evaluated the system n times during the solution and considering these n system as individual linear systems. That is, finding the SDC is to rewrite the state matrices so that the nonlinearities are isolated and that part of the system can be recalculated whenever necessary to find a linear system on that instant.

For the system presented on the equation 2.47 to 2.49, all the coefficients related with the system states are resumed on the matrix $A(x)$, the coefficients related with the inputs on the matrix B and all the other components on the matrix G. The state space matrices were defined using the equation that describe the whole dynamic system, that means using the equations of motion shown in 2.47 to 2.49 and the dissipations equations 2.58 to 2.60.

$$A(x) = \begin{bmatrix} 0 & 1 & 0 & 0 & 0 & 0 \\ 0 & 0 & 0 & \varphi_{24} & 0 & \varphi_{26} \\ 0 & 0 & 0 & 1 & 0 & 0 \\ 0 & 0 & 0 & \varphi_{42} & 0 & \varphi_{36} \\ 0 & 0 & 0 & 0 & 0 & 1 \\ 0 & 0 & 0 & \varphi_{62} & 0 & \varphi_{66} \end{bmatrix} \tag{3.42}$$

Where non-null elements of $A(x)$ are:

$$\varphi_{24} = \dot{\theta}_1 \left(\frac{-\Omega_6^2 c_1 - \Omega_4 \Omega_3 c_7 + \Omega_6 \Omega_5 c_7 + \Omega_2 \Omega_6 c_{12} + \Omega_2 \Omega_3 c_1 - \Omega_4 \Omega_6 c_{12}}{\Omega_3 {\Omega_4}^2 - 2\Omega_4 \Omega_5 \Omega_6 + \Omega_2 {\Omega_5}^2 + \Omega_1 {\Omega_6}^2 - \Omega_1 \Omega_2 \Omega_3} \right)$$
$$+\dot{\theta}_2 \left(\frac{-{\Omega_6}^2 {c_4}^2 + \Omega_2 \Omega_3 c_4}{(\Omega_3 {\Omega_4}^2 - 2\Omega_4 \Omega_5 \Omega_6 + \Omega_2 {\Omega_5}^2 + \Omega_1 {\Omega_6}^2 - \Omega_1 \Omega_2 \Omega_3)} \right)$$
$$+\dot{\theta}_3 \left(\frac{-\Omega_6^2 c_3 + \Omega_4 \Omega_3 c_9 - \Omega_6 \Omega_5 c_9 + \Omega_2 \Omega_6 n + \Omega_2 \Omega_3 c_{14} - \Omega_4 \Omega_6 c_{14}}{(\Omega_3 {\Omega_4}^2 - 2\Omega_4 \Omega_5 \Omega_6 + \Omega_2 {\Omega_5}^2 + \Omega_1 {\Omega_6}^2 - \Omega_1 \Omega_2 \Omega_3)} \right)$$

$$\varphi_{26} = +\dot{\theta}_1 \left(\frac{\Omega_6 \Omega_5 c_8 - \Omega_6^2 c_2 - \Omega_4 \Omega_3 c_8 - \Omega_2 \Omega_6 c_{13} + \Omega_2 \Omega_3 c_2 + \Omega_4 \Omega_6 c_{13}}{\Omega_3 {\Omega_4}^2 - 2\Omega_4 \Omega_5 \Omega_6 + \Omega_2 {\Omega_5}^2 + \Omega_1 {\Omega_6}^2 - \Omega_1 \Omega_2 \Omega_3} \right)$$
$$+\dot{\theta}_3 \left(\frac{\Omega_4 \Omega_3 c_j - \Omega_6^2 c_5 + \Omega_6 \Omega_5 c_{10} + \Omega_2 \Omega_3 c_5}{\Omega_3 {\Omega_4}^2 - 2\Omega_4 \Omega_5 \Omega_6 + \Omega_2 {\Omega_5}^2 + \Omega_1 {\Omega_6}^2 - \Omega_1 \Omega_2 \Omega_3} \right)$$

$$\varphi_{42} = \dot{\theta}_1 \left(\frac{-{\Omega_5}^2 c_7 + \Omega_1 \Omega_3 c_7 + \Omega_1 \Omega_6 c_{11} - \Omega_4 \Omega_5 c_{11} - \Omega_4 \Omega_3 c_1 + \Omega_5 \Omega_6 c_1}{\Omega_3 {\Omega_4}^2 - 2\Omega_4 \Omega_5 \Omega_6 + \Omega_2 {\Omega_5}^2 + \Omega_1 {\Omega_6}^2 - \Omega_1 \Omega_2 \Omega_3} \right)$$
$$+\dot{\theta}_2 \left(\frac{c_4 (\Omega_5 \Omega_6 - \Omega_4 \Omega_3)}{\Omega_3 {\Omega_4}^2 - 2\Omega_4 \Omega_5 \Omega_6 + \Omega_2 {\Omega_5}^2 + \Omega_1 {\Omega_6}^2 - \Omega_1 \Omega_2 \Omega_3} \right)$$
$$+\dot{\theta}_3 \left(\frac{c_9 ({\Omega_5}^2 - \Omega_1 \Omega_3) + c_{14} (\Omega_1 \Omega_6 - \Omega_4 \Omega_5) + c_3 (\Omega_5 \Omega_6 - \Omega_4 \Omega_3)}{\Omega_3 {\Omega_4}^2 - 2\Omega_4 \Omega_5 \Omega_6 + \Omega_2 {\Omega_5}^2 + \Omega_1 {\Omega_6}^2 - \Omega_1 \Omega_2 \Omega_3} \right)$$

$$\varphi_{46} = \dot{\theta}_1 \left(\frac{-\Omega_5^2 c_8 + \Omega_1 \Omega_3 c_8 - \Omega_1 \Omega_6 c_{13} + \Omega_4 \Omega_5 c_{13} - \Omega_4 \Omega_3 c_2 + \Omega_5 \Omega_6 c_2}{\Omega_3 {\Omega_4}^2 - 2\Omega_4 \Omega_5 \Omega_6 + \Omega_2 {\Omega_5}^2 + \Omega_1 {\Omega_6}^2 - \Omega_1 \Omega_2 \Omega_3} \right)$$
$$+\dot{\theta}_3{}^2 \left(\frac{\Omega_5^2 c_{10} - \Omega_1 \Omega_3 c_{10} - \Omega_3 \Omega_4 c_5 + \Omega_5 \Omega_6 c_5}{\Omega_3 {\Omega_4}^2 - 2\Omega_4 \Omega_5 \Omega_6 + \Omega_2 {\Omega_5}^2 + \Omega_1 {\Omega_6}^2 - \Omega_1 \Omega_2 \Omega_3} \right)$$

(3.43)

$$\varphi_{62} = \dot{\theta}_2 \left(\frac{\Omega_4^2 c_{12} - \Omega_1 \Omega_6 c_7 + \Omega_4 \Omega_5 c_7 - \Omega_1 \Omega_2 c_{12} - \Omega_2 \Omega_5 c_1 + \Omega_4 \Omega_6 c_1}{\Omega_3 {\Omega_4}^2 - 2\Omega_4 \Omega_5 \Omega_6 + \Omega_2 {\Omega_5}^2 + \Omega_1 {\Omega_6}^2 - \Omega_1 \Omega_2 \Omega_3} \right)$$
$$+\dot{\theta}_3 \left(\frac{(-\Omega_4^2 c_{14} - \Omega_1 \Omega_6 c_8 + \Omega_4 \Omega_5 c_8 + \Omega_1 \Omega_2 c_{14} - \Omega_2 \Omega_5 c_2 + \Omega_4 \Omega_6 c_2)}{\Omega_3 {\Omega_4}^2 - 2\Omega_4 \Omega_5 \Omega_6 + \Omega_2 {\Omega_5}^2 + \Omega_1 {\Omega_6}^2 - \Omega_1 \Omega_2 \Omega_3} \right)$$

$$\varphi_{64} = +\dot{\theta}_2 \left(\frac{-\Omega_2 \Omega_5 c_4 + \Omega_4 \Omega_6 c_4}{\Omega_3 {\Omega_4}^2 - 2\Omega_4 \Omega_5 \Omega_6 + \Omega_2 {\Omega_5}^2 + \Omega_1 {\Omega_6}^2 - \Omega_1 \Omega_2 \Omega_3} \right)$$
$$+\dot{\theta}_3 \left(\frac{{\Omega_4}^2 c_{13} + \Omega_1 \Omega_6 c_8 - \Omega_4 \Omega_6 c_8 - \Omega_1 \Omega_2 c_{13} - \Omega_2 \Omega_5 c_3 + \Omega_4 \Omega_6 c_3}{\Omega_3 {\Omega_4}^2 - 2\Omega_4 \Omega_5 \Omega_6 + \Omega_2 {\Omega_5}^2 + \Omega_1 {\Omega_6}^2 - \Omega_1 \Omega_2 \Omega_3} \right)$$

$$\varphi_{66} = \dot{\theta}_3 \left(\frac{(\Omega_1 \Omega_6 c_{10} - \Omega_4 \Omega_6 c_{10} - \Omega_2 \Omega_5 c_5 + \Omega_4 \Omega_6 c_5)}{\Omega_3 {\Omega_4}^2 - 2\Omega_4 \Omega_5 \Omega_6 + \Omega_2 {\Omega_5}^2 + \Omega_1 {\Omega_6}^2 - \Omega_1 \Omega_2 \Omega_3} \right)$$

With the auxiliary variables c_1 to c_{15}:

$$c_1 = (-sin(\theta_2) 2 l_1 l_2 (cm_2 m_2 + m_3) - 2sin(\theta_2 + \theta_3) m_3 cm_3 l_1 l_3)$$

$$c_2 = (-2m_3 \sin(\theta_3) cm_3 l_2 l_3 - 2\sin(\theta_2 + \theta_3) m_3 cm_3 l_1 l_3)$$

$$c_3 = (-2m_3 sin(\theta_3) cm_3 l_2 l_3 - 2sin(\theta_2 + \theta_3) m_3 cm_3 l_1 l_3)$$

$$c_4 = (-sin(\theta_2) l_2 l_1 (m_2 cm_2 + m_3) - sin(\theta_2 + \theta_3) m_3 cm_3 l_1 l_3)$$

$$c_5 = (-sin(\theta_3) m_3 cm_3 l_2 l_3 - sin(\theta_2 + \theta_3) m_3 cm_3 l_1 l_3)$$

$$c_6 = g(sin(\theta_1) l_1 (m_1 cm_1 + m_2 + m_3) + sin(\theta_1 + \theta_2) l_2 (cm_2 m_2 + m_3) + sin(\theta_1 + \theta_2 + \theta_3) m_3 cm_3 l_3)$$

$$c_7 = (-sin(\theta_2) l_1 l_2 (m_2 cm_2 + m_3) - sin(\theta_2 + \theta_3) m_3 cm_3 l_1 l_3) \qquad (3.44)$$

$$c_8 = (-2m_3 sin(\theta_3) cm_3 l_2 l_3 - sin(\theta_2 + \theta_3) m_3 cm_3 l_1 l_3)$$

$$c_9 = 2sin(\theta_3) m_3 cm_3 l_2 l_3$$

$$c_{10} = sin(\theta_3) m_3 cm_3 l_2 l_3$$

$$c_{11} = -g(-sin(\theta_1 + \theta_2) l_2 (m_2 cm_2 + m_3) - sin(\theta_1 + \theta_2 + \theta_3) m_3 cm_3 l_3)$$

$$c_{12} = sin(\theta_2 + \theta_3)m_3cm_3l_1l_3$$

$$c_{13} = (-sin(\theta_3)m_3cm_3l_2l_3 - sin(\theta_2 + \theta_3)m_3cm_3l_1l_3)$$

$$c_{14} = sin(\theta_3)m_3cm_3l_2l_3$$

$$c_{15} = gsin(\theta_1 + \theta_2 + \theta_3)m_3cm_3l_3$$

$$B(x) = \begin{bmatrix} 0 & 0 & 0 \\ \beta_{21} & \beta_{22} & \beta_{23} \\ 0 & 0 & 0 \\ \beta_{41} & \beta_{42} & \beta_{43} \\ 0 & 0 & 0 \\ \beta_{61} & \beta_{62} & \beta_{63} \end{bmatrix} \quad (3.45)$$

$$\beta_{21} = \frac{\Omega_6{}^2 - \Omega_2\Omega_3}{\Omega_3\Omega_4{}^2 - 2\Omega_4\Omega_5\Omega_6 + \Omega_2\Omega_5{}^2 + \Omega_1\Omega_6{}^2 - \Omega_1\Omega_2\Omega_3}$$

$$\beta_{22} = \frac{\Omega_3\Omega_4 - \Omega_5\Omega_6}{\Omega_3\Omega_4{}^2 - 2\Omega_4\Omega_5\Omega_6 + \Omega_2\Omega_5{}^2 + \Omega_1\Omega_6{}^2 - \Omega_1\Omega_2\Omega_3}$$

$$\beta_{23} = \frac{\Omega_2\Omega_5 - \Omega_4\Omega_6}{\Omega_3\Omega_4{}^2 - 2\Omega_4\Omega_5\Omega_6 + \Omega_2\Omega_5{}^2 + \Omega_1\Omega_6{}^2 - \Omega_1\Omega_2\Omega_3}$$

$$\beta_{41} = \frac{\Omega_3\Omega_4 - \Omega_6\Omega_5}{\Omega_3\Omega_4{}^2 - 2\Omega_4\Omega_5\Omega_6 + \Omega_2\Omega_5{}^2 + \Omega_1\Omega_6{}^2 - \Omega_1\Omega_2\Omega_3\Omega_3}$$

$$\beta_{42} = \frac{\Omega_5^2 - \Omega_1\Omega_3}{\Omega_3\Omega_4{}^2 - 2\Omega_4\Omega_5\Omega_6 + \Omega_2\Omega_5{}^2 + \Omega_1\Omega_6{}^2 - \Omega_1\Omega_2\Omega_3}$$

$$\beta_{43} = \frac{\Omega_1\Omega_6 - \Omega_4\Omega_5}{\Omega_3\Omega_4{}^2 - 2\Omega_4\Omega_5\Omega_6 + \Omega_2\Omega_5{}^2 + \Omega_1\Omega_6{}^2 - \Omega_1\Omega_2\Omega_3} \quad (3.46)$$

$$\beta_{61} = \frac{\Omega_2\Omega_6 - \Omega_2\Omega_6}{\Omega_3\Omega_4{}^2 - 2\Omega_4\Omega_5\Omega_6 + \Omega_2\Omega_5{}^2 + \Omega_1\Omega_6{}^2 - \Omega_1\Omega_2\Omega_3}$$

$$\beta_{62} = \frac{\Omega_1\Omega_6 - \Omega_2\Omega_6}{\Omega_3\Omega_4{}^2 - 2\Omega_4\Omega_5\Omega_6 + \Omega_2\Omega_5{}^2 + \Omega_1\Omega_6{}^2 - \Omega_1\Omega_2\Omega_3}$$

$$\beta_{63} = \frac{\Omega_4^2 - \Omega_1\Omega_6}{\Omega_3{\Omega_4}^2 - 2\Omega_4\Omega_5\Omega_6 + \Omega_2{\Omega_5}^2 + \Omega_1{\Omega_6}^2 - \Omega_1\Omega_2\Omega_3}$$

$$G = \begin{bmatrix} 0 \\ \psi_1 \\ 0 \\ \psi_2 \\ 0 \\ \psi_3 \end{bmatrix} \tag{3.47}$$

$$\psi_1 = \frac{-{\Omega_6}^2 c_6 - \Omega_3\Omega_4 c_{11} + \Omega_5\Omega_6 c_{11} - \Omega_5\Omega_2 c_{15} + \Omega_3\Omega_2 c_6 + \Omega_5\Omega_6 c_{15}}{\Omega_3{\Omega_4}^2 - 2\Omega_4\Omega_5\Omega_6 + \Omega_2{\Omega_5}^2 + \Omega_1{\Omega_6}^2 - \Omega_1\Omega_2\Omega_3}$$

$$\psi_2 = \frac{-{\Omega_5}^2 c_{11} + \Omega_1\Omega_3 c_{11} - \Omega_1\Omega_6 c_{15} + \Omega_4\Omega_6 c_{15} - \Omega_4\Omega_3 c_6 + \Omega_5\Omega_6 c_6}{\Omega_3{\Omega_4}^2 - 2\Omega_4\Omega_5\Omega_6 + \Omega_2{\Omega_5}^2 + \Omega_1{\Omega_6}^2 - \Omega_1\Omega_2\Omega_3} \tag{3.48}$$

$$\psi_3 = \frac{-{\Omega_4}^2 c_{15} - \Omega_1\Omega_6 c_6 + \Omega_4\Omega_6 c_6 + \Omega_1\Omega_2 c_{15} - \Omega_2\Omega_6 c_6 + \Omega_4\Omega_6 c_6}{\Omega_3{\Omega_4}^2 - 2\Omega_4\Omega_5\Omega_6 + \Omega_2{\Omega_5}^2 + \Omega_1{\Omega_6}^2 - \Omega_1\Omega_2\Omega_3}$$

$$C(x) = \begin{bmatrix} C_{11} & 0 & 0 & 0 & 0 & 0 \\ 0 & C_{22} & 0 & 0 & 0 & 0 \\ 0 & 0 & C_{33} & 0 & 0 & 0 \\ 0 & 0 & 0 & C_{44} & 0 & 0 \\ 0 & 0 & 0 & 0 & C_{55} & 0 \\ 0 & 0 & 0 & 0 & 0 & C_{66} \end{bmatrix} \tag{3.49}$$

$$\dot{x} = \begin{bmatrix} \dot{\theta}_1 \\ \ddot{\theta}_1 \\ \dot{\theta}_2 \\ \ddot{\theta}_2 \\ \dot{\theta}_3 \\ \ddot{\theta}_3 \end{bmatrix} \tag{3.50}$$

$$u(x) = \begin{bmatrix} \tau_1 \\ \tau_2 \\ \tau_3 \end{bmatrix} \tag{3.51}$$

The elements of $C(x)$ (3.49), C_{11} to C_{66} ,changes from 1 to 0 depending on with output is needed. The states $\theta_1, \dot{\theta}_1, \theta_2, \dot{\theta}_2, \theta_3$ and $\dot{\theta}_3$ are related with these elements C_{11} to C_{66}, respectively. If the state is needed on the output the element $C_{i\,j}$ is 1 and if the state in no longer needed the element $\delta_{i\,j}$ turns to 0 (OGATA, 2010; DORF, BISHOP, 2010). This variations and possibilities for the matrix $C(x)$ will be presented and discussed on the section dealing with the State Observer.

The states matrix, equation 3.50, and the input matrix, equation 3.51, complete the state space representation. On the input the elements τ_k represent a generic input force or any external element applied on the system.

3.5 SDRE CONTROL

As already discussed, the LQR control has the characteristic of treat only linear system and the constant evolution of the needs for control systems increases to the non-linear area. The main problem with non-linear systems is the computational cost, the high technology structure for operation and the low generalization for the developed solution. Most linearization methods use Local Linearization and, even though this gives good results, there are counterparts in using this approach. The need of re-linearize the model every iteration of the solution and the probable small area of operation are some of the counterparts. It is in this scenario that the SDRE control is shown as an alternative to solve these issues (KASTEV, 2006).

The fact that SDRE uses a semi-global linearization ensures a good balance between applicability and complexity. Actually, the SDRE treats the non-linear system as a linear system in a region defined by the mathematical development.

All the theory developed for the LQR control is used as the basis for the SDRE. That means, the cost functional presented in 3.8 continues to be used as the fundamental cost function and still express considering the optimization using a finite time-horizon problem, initially the matrices Q and R follow the same principals presented for LQR control, equation 3.15 and 3.16.

Using this methodology, the SDRE control can be resumed on eight steps:

- Step 1: Use or find the SDC representation on the system 3.9 and 3.10 and define the values for $A(x)_n$, $B(x)_n$ and $C(x)_n$

- Step 2: Define if the system is controllable using the criterion on the equation 3.11 for the n interaction

$$M_n = [B_n \quad A_n B_n \quad A^2{}_n B_n \quad \dots \quad A^{n-1}{}_n B_n] \tag{3.52}$$

- Step 3: Use or redefine the values for Q and R, 3.15 and 3.16
- Step 4: Solve the Riccati Equation for the interaction n

$$A(x_n)^T P(x)_{n+1} + P(x)_{n+1} A(x_n) - P(x) B(x_n) R^{-1} B(x_n)^T P(x)_{n+1} + Q = 0 \tag{3.53}$$

- Step 5: Use the value of $P(x)_n$ to find the control signal $u(t)_n$;

$$u(t)_n = R_n{}^{-1} B(x_n)^T P(x)_n x(t)_n \tag{3.54}$$

- Step 6: Use the signal control on the system 3.9 and 3.10;
- Step 7: Return to the Step 1 and define the values for $A(x)_{n+1}$, $B(x)_{n+1}$ and $C(x)_{n+1}$;
- Step 8: Redo the criterion verification on Step 2. If the system given by $A(x)_{n+1}$, $B(x)_{n+1}$ and $C(x)_{n+1}$ is controllable, continues to the Step 3. If the system given by $A(x)_{n+1}$, $B(x)_{n+1}$ and $C(x)_{n+1}$ is not controllable, use the values already calculated and given by $A(x)_n$, $B(x)_n$ and $C(x)_n$.

3.6 STATE OBSERVER

The assumption made that all the system states are available to measure by sensors is a very complex statement. This because in real application this tends to don't be true for a number of reasons. But nevertheless, the best way to approach this question it isn't on the side of the availability to measure the state but if it is necessary measure all the states. Besides the obviously growth on cost, using sensors greatly increases the complexity of the system much more compare to the costs. On solution for this kind of issue is use the State Observer to provide the values for the system states.

The system is classified as completely observable if every state $x(t)_n$ can be determined only from the observation of the outputs $y(t)_m$ over finite time interval $t_0 < t < t_f$ (DORF, BISHOP, 2010). As for check if the system can be controllable, to define if it is possible to use the State Observer for a set of states a similar verification is used. The equation 3.55 shown the Observability matrix. To the configuration tested on 3.55 be completely Observable the determinant of that matrix must be nonzero.

$$O = \begin{bmatrix} C \\ CA \\ \dots \\ CA^{n-1} \end{bmatrix} \tag{3.55}$$

The states estimated are represented as $\hat{x}(t)$ and the state space representation on 3.9 and 3.10 becomes:

$$\dot{\hat{x}} = A(x)\hat{x} + B(x)u(t) \pm L_c(y - C(x)\hat{x}) \tag{3.55}$$

$$\hat{y}(t) = C\hat{x}(t) + D(t)u(t) \tag{3.56}$$

The component $L_c(y - C(x)\hat{x})$ on 3.55 is represented with positive and negative signal because is the system configuration that will define if this component controls the state estimation adding or subtracting. These two possibilities can be found on projects and application with perfect operation.

The error on the state estimation is given by:

$$e(t) = x(t) - \hat{x}(t) \tag{3.57}$$

Using the equation 3.57 and the output equation, 3.56, the error signal progress according to the follow differential relation:

$$\dot{e}(t) = \dot{x}(t) - \dot{\hat{x}}(t) = Ax(t) + Bu(t) - (A - L_cC)\hat{x}(t) - (B - L_cD)u(t) - L_cy(t) \tag{3.58}$$

$$\dot{e}(t) = \big(A(x) - L_cC(x)\big)e(t) \tag{3.59}$$

Figure 10 - Full State Observer.

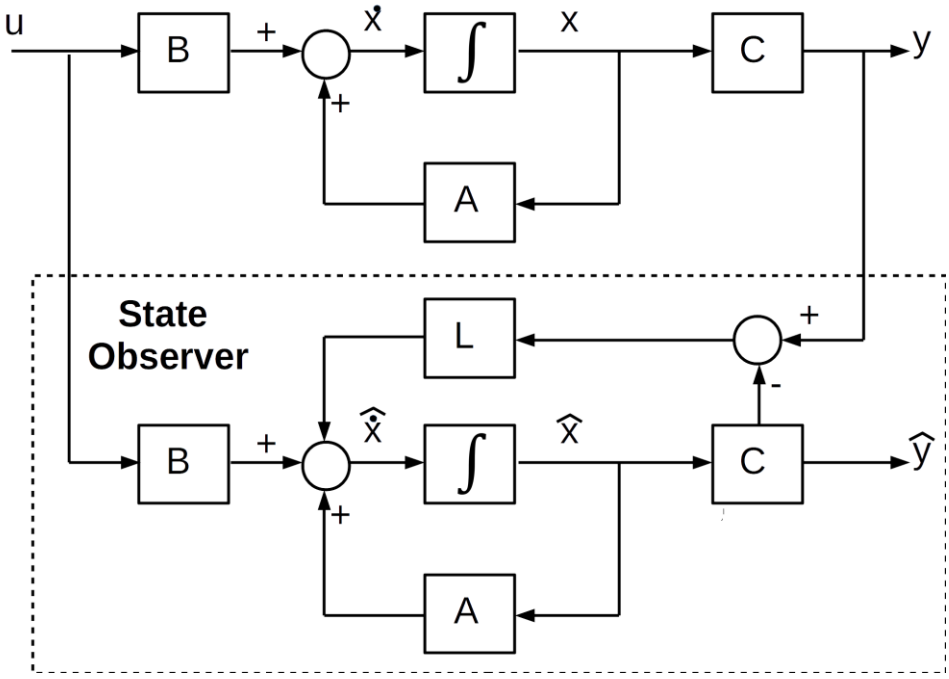

Source: Self Authorship.

The solution for 3.59 is given by the equation 3.60. This solution leads to the conclusion that the desired behavior is given by the eigenvalues of $(A - L_c C)$, a similar conclusion obtained on the equation 3.2 by the control law.

$$e(t) = e^{(A-L_c C)t} e(0) \tag{3.60}$$

$$L_c = \begin{bmatrix} L_{c_{1\,1}} & \dots & L_{c_{1\,n}} \\ \dots & \dots & \dots \\ L_{c_{n\,1}} & \dots & L_{c_{n\,n}} \end{bmatrix} \tag{3.61}$$

The gain matrix L_c can be define using a lot of methods, but this comparison is an important information to define how these eigenvalues can be found using the same approach made for the control.

3.7 OPTIMIZATION BASED ON THE WEIGHT MATRICES Q AND R

The solution of the Riccati Equations uses several matrices to define the result, and main ones are the weight matrices Q and R. Those weight matrices are responsible

to provide balance between the desired behavior and the control requirements, how expensive the action control will need to be to meet this desired behavior. This means the control response depends directly on those matrices and the values assigned to them define how effective, fast and within the desired range the answer values will be. For all the matrices Q and R used, equations 3.60 to 3.66, the same criterion was used to define the coefficients, the elements $q_{n\,m}$ and $r_{n\,m}$.

Kastev (2006) strengthens that there isn't a definition or rigorous method to define the matrices Q and R, as there is for the techniques used to linear control. This absence shouldn't be seen as a failure or gap on the control strategy, but as a characteristic. It is a methodological error compare the nonlinear and linear techniques and expect for the same approach, implementation process and performance parameters. But is possible to follow a few advisement and strategies applied on related researches.

As presented on the LQR solution, the vast majority of applications use Q and R as identity matrices with coefficients with the same value. The main reason to use a diagonal matrix for Q and R is to ensure that the supervision on each state variable can be independent and for using the same value is guaranteed the same action over the system variables (KASTEV, 2006).

On the use of diagonal matrix for Q and R, when $n = m$, elements are adjustable and when $n \neq m$ the element is null. When the coefficients present $n = m$, theis coefficient are direct related with the state of the system. So, using a diagonal matrix the supervision on the states is guaranteed individually. For example, q_{22} is related with the second state variable and so on. The same principle is transposed to the matrix R but this time the relation is with the inputs, r_{22} is connected with the second input signal, as exemplify on 3.51.

On the coefficients values, as many the elements of Q rise, more faster the system response will be but with more expensive control. R penalize the system inputs. As higher $r_{n\,m}$ is, on the main diagonal, freer the inputs are to assume larger values. If the state variables, inputs and control signals can't be large, the elements on Q and R should be adjusted.

The matrix Q is related with the states, ensuring that these states don't depart from the desired range. The dimension follows the number of states used on the

system, so the equation 3.62 shown the matrix Q used to control the robotic system states on the SDRE control.

$$Q = \begin{bmatrix} q_{11} & q_{21} & q_{31} & q_{41} & q_{51} & q_{61} \\ q_{12} & q_{22} & q_{32} & q_{42} & q_{52} & q_{62} \\ q_{13} & q_{23} & q_{33} & q_{43} & q_{53} & q_{63} \\ q_{14} & q_{24} & q_{34} & q_{44} & q_{54} & q_{64} \\ q_{15} & q_{25} & q_{35} & q_{45} & q_{55} & q_{65} \\ q_{16} & q_{26} & q_{36} & q_{46} & q_{56} & q_{66} \end{bmatrix} \tag{3.62}$$

The matrix R was used to define how the control action act on the system and their dimension followed the number of inputs used. To the robotic system, the equation 3.63 shown the matrix R used.

$$R = \begin{bmatrix} r_{11} & r_{21} & r_{31} \\ r_{12} & r_{22} & r_{32} \\ r_{13} & r_{23} & r_{33} \end{bmatrix} \tag{3.63}$$

For the SDRE applied in the State Observer to ensure the control over this second system, the same rules discussed above were used to define Q_{Ob} and R_{Ob}. The equations 3.64 and 6.65 shown those matrices, Q_{Ob} and R_{Ob}, respectively.

$$Q_{Ob} = \begin{bmatrix} q_{Ob_{11}} & q_{Ob_{21}} & q_{Ob_{31}} & q_{Ob_{41}} & q_{Ob_{51}} & q_{Ob_{61}} \\ q_{Ob_{12}} & q_{Ob_{22}} & q_{Ob_{32}} & q_{Ob_{42}} & q_{Ob_{52}} & q_{Ob_{62}} \\ q_{Ob_{13}} & q_{Ob_{23}} & q_{Ob_{33}} & q_{Ob_{43}} & q_{Ob_{53}} & q_{Ob_{63}} \\ q_{Ob_{14}} & q_{Ob_{24}} & q_{Ob_{34}} & q_{Ob_{44}} & q_{Ob_{54}} & q_{Ob_{64}} \\ q_{Ob_{15}} & q_{Ob_{25}} & q_{Ob_{35}} & q_{Ob_{45}} & q_{Ob_{55}} & q_{Ob_{65}} \\ q_{Ob_{16}} & q_{Ob_{26}} & q_{Ob_{36}} & q_{Ob_{46}} & q_{Ob_{56}} & q_{Ob_{66}} \end{bmatrix} \tag{3.64}$$

$$R_{Ob} = \begin{bmatrix} r_{Ob_{11}} & r_{Ob_{21}} & r_{Ob_{31}} \\ r_{Ob_{12}} & r_{Ob_{22}} & r_{Ob_{32}} \\ r_{Ob_{13}} & r_{Ob_{23}} & r_{Ob_{33}} \end{bmatrix} \tag{3.65}$$

To define the matrix L_c responsible for regulate the State Observer gain the matrix $Q_{L\,Ob}$ remains the same in dimension as shown in 3.62 and 3.64. But $R_{L\,Ob}$ changed to follow the inputs on this third control system, since their inputs are the outputs of the State Observer, that is, six inputs since the State Observer has the same number of state as the system. The equation 3.66 shown the matrix used for $R_{L\,Ob}$.

$$R_{L\,Ob} = \begin{bmatrix} r_{L\,Ob_{11}} & r_{L\,Ob_{21}} & r_{L\,Ob_{31}} & r_{L\,Ob_{41}} & r_{L\,Ob_{51}} & r_{L\,Ob_{61}} \\ r_{L\,Ob_{12}} & r_{L\,Ob_{22}} & r_{L\,Ob_{32}} & r_{L\,Ob_{42}} & r_{L\,Ob_{52}} & r_{L\,Ob_{62}} \\ r_{L\,Ob_{13}} & r_{L\,Ob_{23}} & r_{L\,Ob_{33}} & r_{L\,Ob_{43}} & r_{L\,Ob_{53}} & r_{L\,Ob_{63}} \\ r_{L\,Ob_{14}} & r_{L\,Ob_{24}} & r_{L\,Ob_{34}} & r_{L\,Ob_{44}} & r_{L\,Ob_{54}} & r_{L\,Ob_{64}} \\ r_{L\,Ob_{15}} & r_{L\,Ob_{25}} & r_{L\,Ob_{35}} & r_{L\,Ob_{45}} & r_{L\,Ob_{55}} & r_{L\,Ob_{65}} \\ r_{L\,Ob_{16}} & r_{L\,Ob_{26}} & r_{L\,Ob_{36}} & r_{L\,Ob_{46}} & r_{L\,Ob_{56}} & r_{L\,Ob_{66}} \end{bmatrix} \quad (3.66)$$

The tests to define the value and weights applied on all Q and R were made following three main criterions:

- The control needs; as overshoot, stabilization time and error;
- Limitation based on the actuators used;
- Response variation with increasing or decreasing in the coefficients values in R and Q.

The first two, control criterion and speed limitation will be discussed in the chapter 6 when the different control strategies are presented. But the coefficients variations were used as criterion in all strategies and controls in the same way.

As presented, the higher the coefficients are more expensive the control is and this is an important information to limit the values assumed by the coefficients. Even if the response can improve increasing or decreasing the coefficients, this wasn't done freely. One example of this is presented in the figure 11.

Using the matrix Q shown in 3.67 for two different control strategies, called Control 1 and Control 2, and for the Control 1 the matrix R shown in 3.68 and for the Control 2 the matrix R shown 3.69.

$$Q = \begin{bmatrix} 150 & 0 & 0 & 0 & 0 & 0 \\ 0 & 1 & 0 & 0 & 0 & 0 \\ 0 & 0 & 150 & 0 & 0 & 0 \\ 0 & 0 & 0 & 1 & 0 & 0 \\ 0 & 0 & 0 & 0 & 100 & 0 \\ 0 & 0 & 0 & 0 & 0 & 1 \end{bmatrix} \quad (3.67)$$

$$R_{Control\,1} = \begin{bmatrix} 0.1 & 0 & 0 \\ 0 & 0.1 & 0 \\ 0 & 0 & 0.1 \end{bmatrix} \quad (3.68)$$

$$R_{Control\ 2} = \begin{bmatrix} 1 \times 10^{-3} & 0 & 0 \\ 0 & 1 \times 10^{-3} & 0 \\ 0 & 0 & 1 \times 10^{-3} \end{bmatrix} \quad (3.69)$$

Figure 11 - Standard answer for position and speed without any concern in the coefficients values.

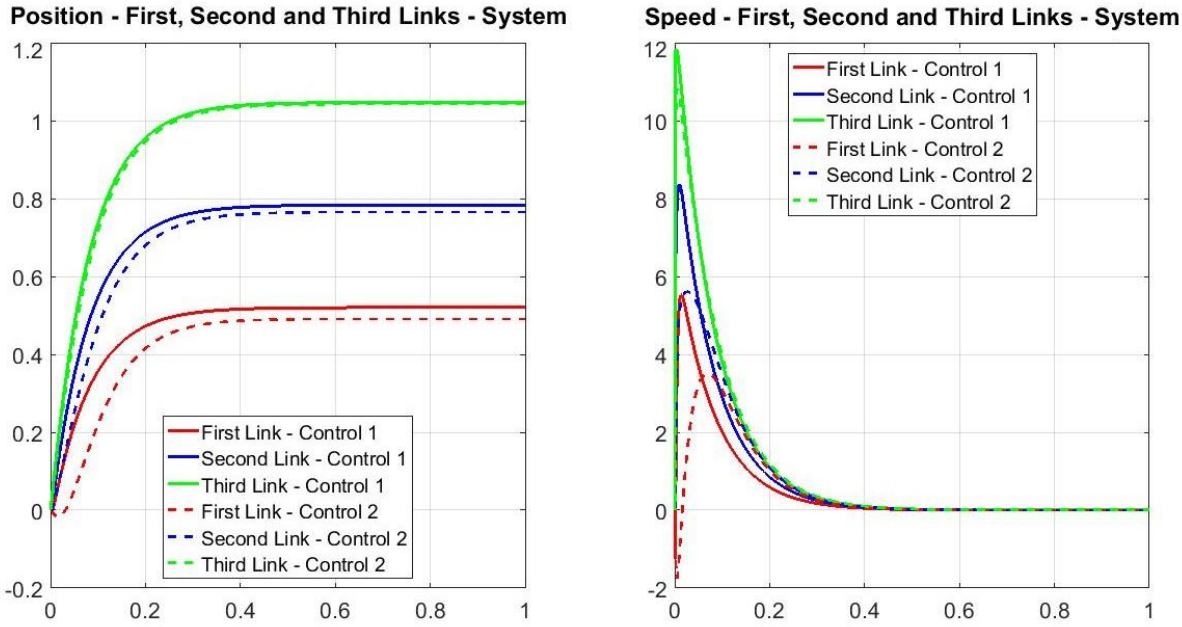

Source: Self Authorship

Comparing the results shown for the first and second link, position and speed, in the figure 11 is possible to see that changing the coefficients for R improve the control efficiency. But looking at the position and speed of the third link, the conclusion is that it is indifferent to use the matrix R presented on 3.68 or 3.69.

Knowing that the variations in those matrices influences on the control cost, as discussed on the SDRE deduction, in situations where were responses such as the third link control the matrix that minimize the control cost was the chosen one, $R_{Control\ 1}$ in this example. The criterion adopted was that when the coefficients $q_{n\,m}$ and $r_{n\,m}$ increasing or decreasing doesn't improve the desired answer in, at least, 10%, those original values before increasing or decreasing used on $q_{n\,m}$ and $r_{n\,m}$ were chosen as the ideal values.

4 ACTUATORS

Actuators are the mechanical component responsible to change the joint position, speed and acceleration. The most known and disseminated actuators are the hydraulic, pneumatic and electrical (CRAIG, 1989; NIKU, 2011). Hydraulic and Pneumatic are examples of popular and widespread actuators used on application which require strength but do not necessarily precision. Most of the robotic system use electric actuators for a lot of reasons, as price, applicability, possibility of control using electronical components directly and the combination with drive system.

For that and some reasons that will be presented and disused, on this work DC actuators was used on the project development.

4.1 DC MOTORS

In this work, the actuators used on the manipulator project was the DC motors type. The figure 12 shown the electrical and mechanical schema used for the mathematical deduction.

Figure 12 - Actuator CC circuit

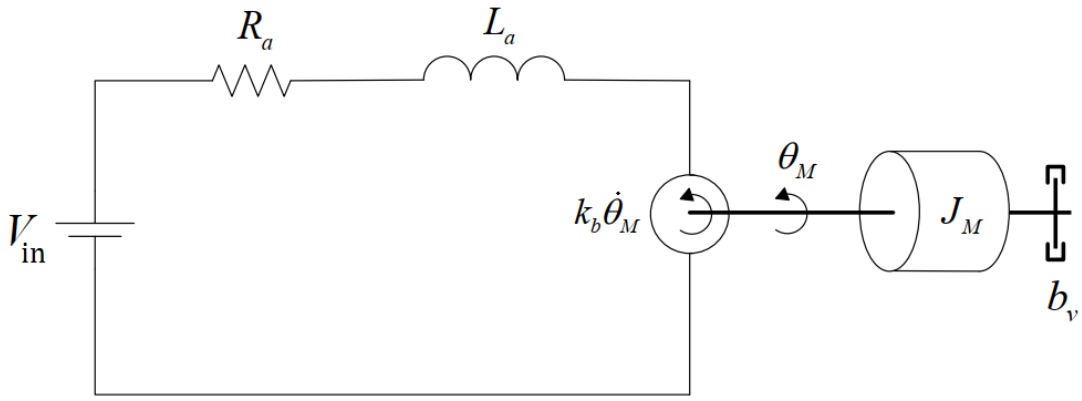

Source: Adapted from Lima, 2014.

The physical parameters of the DC motor, viscous damping (b_v), rotor inertia (J_m), torque constant (K_m), back-EMF constant (k_b), armature resistance (R_a), armature inductance (L_a), reference voltage (V_{in}) are obtained on the documentation available from Pitman. The model used was the DC motor CC GM9413-3. These motor

data can be seen on the table 1. The graphs for the Torque, Speed and Output power are shown on the figure 13.

Table 1 - Data and constants of the actuators CC GM9413-3 - 2001

Data	Symbol	Unit	Value
Viscous damping	b_v	N-m-s	$7{,}6 \times 10^{-7}$
Rotor inertia	J_m	Kg-m^2	$2{,}8 \times 10^{-6}$
Torque constant	K_m	N-m/A	$3{,}95 \times 10^{-2}$
Back-EMF constant	K_g	V/rad/s	$3{,}95 \times 10^{-2}$
Armature resistance	R_a	Ω	8,33
Armature inductance	L_a	mH	6,17
Reference voltage	v_{in}	V	12
Peak Current	i_{ap}	A	1,44
Peak Toque	τ_p	N-m	2,3

Source: Self Authorship.

Figure 13 - Operation of the actuator

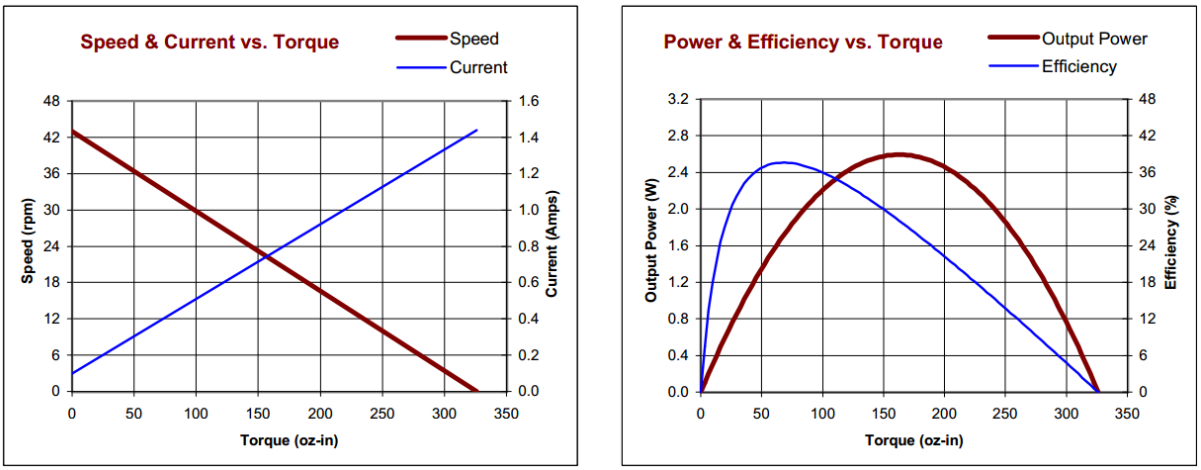

Source: Adapted from Pittman (2001).

The electrical and mechanical differential equation that represents que system are:

$$\dot{\theta}_{m\,i} = \frac{d}{dx}(\theta_{m\,i}) = \omega_{m\,i} \tag{4.1}$$

$$\dot{\omega}_{m\,i} = \omega_{m\,i}\left(\frac{-b_v}{J_m}\right) + i_a\left(\frac{K_m}{J_m}\right) \tag{4.2}$$

$$\frac{\delta i_a}{\delta t} = \omega_{m\,i}\left(\frac{-K_g}{L_a}\right) + i_a\left(\frac{-R_a}{L_a}\right) + V_{in}\left(\frac{1}{L_a}\right) \tag{4.3}$$

$$\frac{dy}{dx}\begin{bmatrix}\theta_m\\ \omega_m\\ i_a\end{bmatrix} = \begin{bmatrix}0 & 1 & 0\\ 0 & -\frac{b_v}{J_m} & \frac{K_m}{J_m}\\ 0 & -\frac{K_g}{L_a} & -\frac{R_a}{L_a}\end{bmatrix}\begin{bmatrix}\theta_m\\ \omega_m\\ i_a\end{bmatrix} + \begin{bmatrix}0\\ 0\\ \frac{1}{L_a}\end{bmatrix}[V_{in}] \tag{4.4}$$

$$\frac{dy}{dx}\begin{bmatrix}\theta_m\\ \omega_m\\ i_a\end{bmatrix} = \begin{bmatrix}1 & 0 & 0\\ 0 & 0 & 0\\ 0 & 0 & 0\end{bmatrix}\begin{bmatrix}\theta_m\\ \omega_m\\ i_a\end{bmatrix} + [0][V_{in}] \tag{4.5}$$

The output of the state space system was considered the position, θ_m, and the input voltage supply, V_{in}. The equations 4.4 and 4.5 shown the state space representation.

4.2 PARAMETRIC VARIANTION IN DC ACTUATORS

The same principle presented on the Equation of Motion chapter, most precisely on the equation 2.61, is used to the parametric uncertainty on the DC motors. In motors this kind consideration is more realistic than in the other robotic variables.

The physical variables given by the fabricant documentation are the most important variables when the subject is variations on their values. A lot of works are entirely based on define those values on the most precisely way (GUO, CHEN, 2008). The main objective of this work is analyzing the robotic system under a usage of a control law, so using the values given by the fabricant is sufficient to this objective. Assume that there are variations on those constants is highly recommended.

On the physical contents, these parametric variations are given by

$$b_v = [0.8 \times b_v + 0.4 \times b_v \times \alpha] \qquad \alpha \in (0,1) \tag{4.7}$$

$$J_m = [0.8 \times J_m + 0.4 \times J_m \times \alpha] \qquad \alpha \in (0,1) \tag{4.8}$$

$$K_m = [0.8 \times K_m + 0.4 \times K_m \times \alpha] \qquad \alpha \in (0,1) \tag{4.9}$$

$$K_g = \left[0.8 \times K_g + 0.4 \times K_g \times \alpha\right] \qquad \alpha \in (0,1) \qquad (4.10)$$

$$R_a = \left[0.8 \times R_a + 0.4 \times R_a \times \alpha\right] \qquad \alpha \in (0,1) \qquad (4.11)$$

$$L_a = \left[0.8 \times L_a + 0.4 \times L_a \times \alpha\right] \qquad \alpha \in (0,1) \qquad (4.12)$$

The variables related with inputs, like input voltage V_{in}, and the operating parameters i_{ap} and τ_p can also present parametric variations, even if they aren't used on the dynamical simulation directly:

$$V_{in} = \left[0.8 \times V_{in} + 0.4 \times V_{in} \times \alpha\right] \qquad \alpha \in (0,1) \qquad (4.13)$$

$$i_{ap} = \left[0.8 \times i_{ap} + 0.4 \times i_{ap} \times \alpha\right] \qquad \alpha \in (0,1) \qquad (4.14)$$

$$\tau_p = \left[0.8 \times \tau_p + 0.4 \times \tau_p \times \alpha\right] \qquad \alpha \in (0,1) \qquad (4.15)$$

These parametric variations can be seeing as a tool to analyses the capability of the system control to act over not ideal circumstances, as noise on the sensing components or calculation approximation.

5 PERFORMANCE ANALYSIS ON TRAJECTORY PLANNING

The robotic dynamical description gives the equation to control the behavior of position, speed, acceleration and so on. The next step in making the robotic system useful is to define how it will move on the coordinate frame and which mathematical and technical mechanisms can provide that. Besides application using the control law to guide the links and joints to a desired point, it is necessary a more robust tool to control the robot positions, speed and any another system variable. This robustness can be provided if the robotic system is under a trajectory control.

On robotics, the trajectory control is provided by the branch known as Trajectory Planning (SPONG et al, 2004; FAHIMI, 2009). Trajectory Planning is guide the structure from an initial to a final point avoiding obstacles or following a path during the trajectory. Most of the trajectory planning are interested on the tool, or end-effector, position. Craig (1994) makes the distinction between having an initial and final point for the trajectory and define a sequence of points to describe in more details that trajectory. This detailed approach is known as Via Points trajectory description and the path points describe all the points to the initial to the final point. So, provide the path points solve a lot of problems, as the kinematics redundancy already discussed and illustrated on the figure 14.

One of the most used methods for Trajectory Planning is use an interpolation of a set n^{th} order functions and found the desired path, either directly by the complete polynomial application or sum of i polynomials that compose a particular path (PORAWAGAMA, MUNASINGHE, 2014; GUO, CHEN, 2008).

Figure 14 - Example of kinematic redundancy on the trajectory possibilities from θ_i and θ_f. Source: Adapted from Craig, 1989.

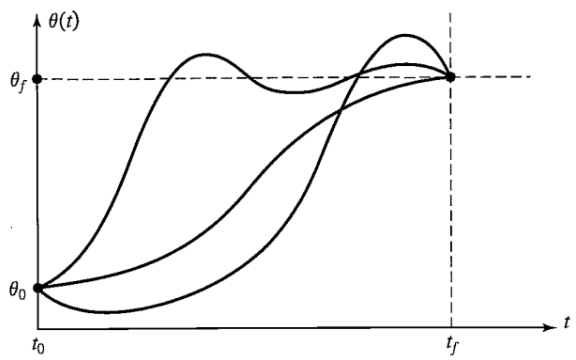

Source: Craig, 1988

5.1 TRAJECTORY PLANNING USIGN 5TH ORDER POLYNOMIAL

The usage of 5th order polynomial allows to have a point-to-point trajectory for the three dynamical variables used on robotic systems: position, speed and acceleration.

Using a 5th order polynomial

$$q_{path\,i}(t) = a_{i5}t^5 + a_{i4}t^4 + a_{i3}t^3 + a_{i2}t^2 + a_{i1}t + a_{i0} \tag{5.1}$$

is possible to find the first and second derivatives

$$\dot{q}_{path\,i}(t) = 5a_{i5}t^4 + 4a_{i4}t^3 + 3a_{i3}t^2 + 2a_{i2}t + a_{i1} \tag{5.2}$$

$$\ddot{q}_{path\,i}(t) = 20a_{i5}t^3 + 12a_{i4}t^2 + 6a_{i3}t + 2a_{i2} \tag{5.3}$$

The variables $q_{path\,i}$ and their respective derivatives, $\dot{q}_{path\,i}$ and $\ddot{q}_{path\,i}$, can be seen as the generalized coordinates used on the dynamic deduction, shown on the equation 2.43 for example.

The trajectory planning calculates the values for the coefficients $a_{i\,j}$ on 5.1 to 5.3. These coefficients are defined based on the initial points for position $q_{path\,i}(t_0)$, speed $\dot{q}_{path\,i}(t_0)$ and acceleration $\ddot{q}_{path\,i}(t_0)$ to the final points $q_{path\,i}(t_f)$, $\dot{q}_{path\,i}(t_f)$ and $\ddot{q}_{path\,i}(t_f)$ within the time range t_0 and t_f. These coefficients are found solving 5.1 to 5.3 considering this set of equations a linear system with the coefficients $a_{i\,j}$ being the unknow variables, a similar process used to solve the dynamic redundancy on 2.50 to 2.52.

After defining the values for $a_{i\,j}$, the polynomials $q_{path\,i}$, $\dot{q}_{path\,i}$ and $\ddot{q}_{path\,i}$ are found and then composes a vector with all the values for position, speed and acceleration, respectively.

$$a_{i5} = \frac{t_f[(\ddot{q}_{path\,if} - \ddot{q}_{path\,i0})t_f - 6(\dot{q}_{path\,if} + \dot{q}_{path\,i0}) + 12(q_{path\,if} - q_{path\,i0})]}{2t_f^5} \tag{6.4}$$

$$a_{i4} = \frac{t_f[16\dot{q}_{path\,i0}+14\ddot{q}_{path\,if}+(3\ddot{q}_{path\,i0}-2\ddot{q}_{path\,if})t_f+30(q_{path\,i0}-q_{path\,if})]}{2t_f^4} \quad (6.5)$$

$$a_{i3} = \frac{t_f[(\ddot{q}_{path\,if}-3\ddot{q}_{path\,i0})t_f-4(2\dot{q}_{path\,if}+3\dot{q}_{path\,i0})+20(q_{path\,if}-q_{path\,i0})]}{2t_f^3} \quad (6.6)$$

$$a_{i2} = \frac{\ddot{q}_{path\,i0}}{2} \quad (6.7)$$

$$a_{i1} = \dot{q}_{path\,i0} \quad (6.8)$$

$$a_{i0} = q_{path\,i0} \quad (6.9)$$

One important concept in using polynomial path planning is how the graph and values change based on the parameters used to calculate $q_{path\,i}$, $\dot{q}_{path\,i}$ and $\ddot{q}_{path\,i}$. Even if the values presented on the table 2 were changed the overall graphic or path for position, speed and acceleration doesn't change. What will change are values such as maximums and minimums but keeping the same graph. In situations where the graph or shape doesn't meet the robotic system needs, it will be necessary to change the polynomial used or use trajectory by function composition or sum. For example, the figure 15 show the trajectory using the data from table 2.

Table 2 - Data for Trajectory planning

Data	Simble	Unit	Value
Initial time	$t_{path\,0}$	s	0
Final time	$t_{path\,f}$	s	2
Initial position	$\theta_{path\,0}$	rad	0
Final position	$\theta_{path\,f}$	rad	$\pi/6$
Initial speed	$\omega_{path\,0}$	rad/s	0
Final speed	$\omega_{path\,f}$	rad/s	0
Initial acceleration	$\dot{\omega}_{path\,0}$	rad/s²	0
Final acceleration	$\dot{\omega}_{path\,f}$	rad/s²	0

Soruce: Self Authorship

Figure 15 - Trajectory Planning for Position, Speed and Acceleration.

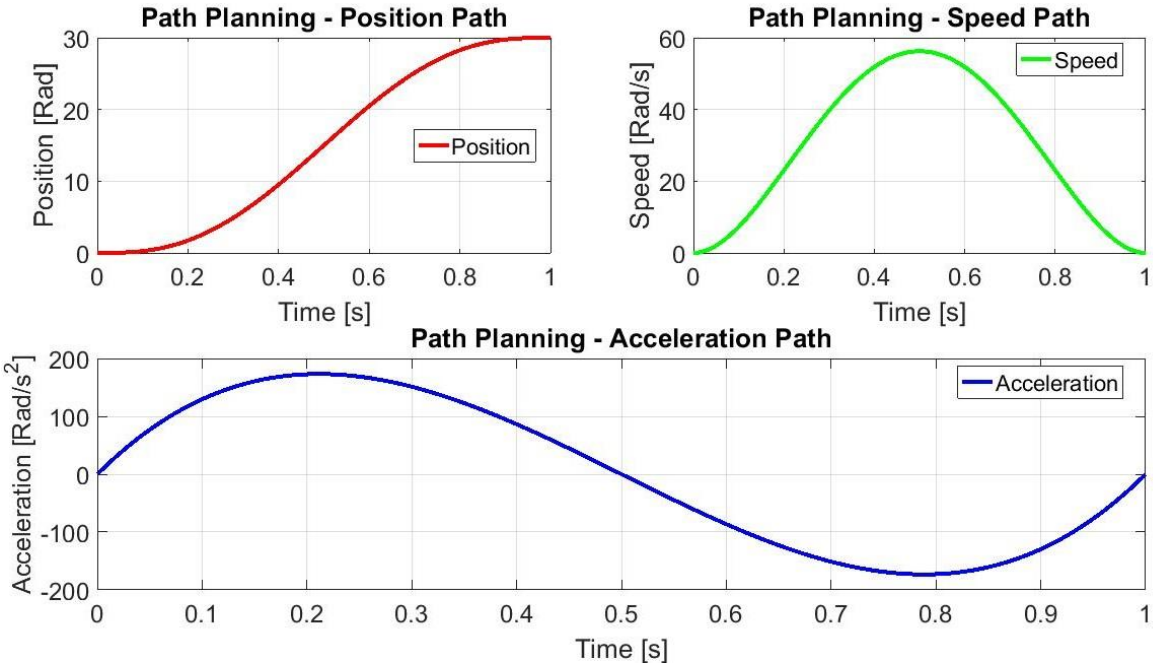

Source: Self Authorship

6 SIMULATION AND RESULTS

The efficiency of the project was proved using numerical simulation under a several approaches. The software MATLAB® made and market by Mathworks® was the main tool to solve and simulate the results for this work. Some algebraical solution, the acceleration redundancy for example, were found using the software Maple® made and market by Maplesoft®.

The system was tested in five stages for prove step by step that all the solutions and deductions was successful:

- Stage 1: Kinematic and dynamical behavior;
- Stage 2: SDRE control to a fixed final position θ_f without any concern with how the path was made;
- Stage 3: State Observer for estimate some system states and use those states with the SDRE control;
- Stage 4: Using the State Observer, simulate the dynamic system with a trajectory planning;
- Stage 5: Parametric uncertainty on the physical variables, measurement and constants.

6.1 KINEMATICS AND DYNAMICS

The dynamical model was simulated to confirm the model efficiency and tune the dissipation forces in the model. Simulate the system only concerned with the dynamical without any external force or control was to verify if the open loop behavior match with the expectation. Analysis and simulation to tune the dissipation forces, length and mass variations of the links are some tests made to verify the dynamical system on open loop. The final values for mass and length were defined using the links projects build for this work. This project makes use of the links available in the UTFPR - Ponta Grossa Robotics Laboratory. The table 3 shows the data links used for all the simulation. The figure 16 shown the project for the links and structure for the manipulator.

Table 3 - Links Data

Data	Simble	Unit	Value
Links mass	m_k	kg	0,275
Links lenght	l_k	cm	0,157
Dissipation constant	c_k	-	0,15

Soruce: Self Authorship

Figure 16 - Project for the links and structure of the manipulator.

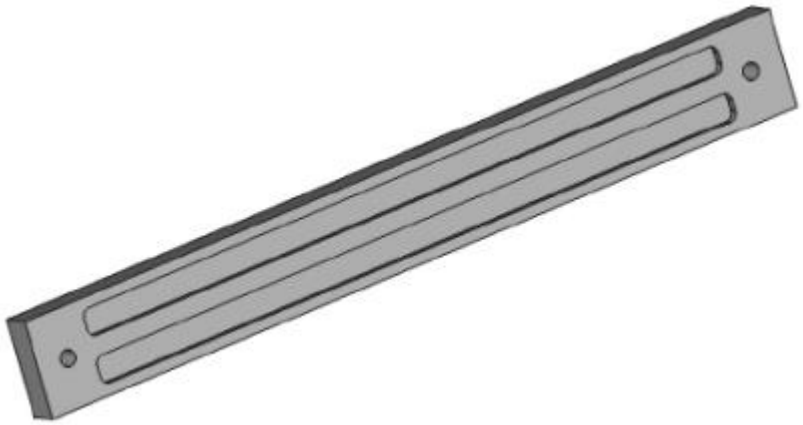

Source: Adapted from Lima, 2014.

The simulation model was defined using the state space representation given by the equation 2.53 to 2.55 and the matrix 3.50.

$$\dot{x(1)} = x(2) \tag{6.1}$$

$$\dot{x(2)} = \left(\frac{(m3\ cm3^2\ l3^2+I3)(gsin(x(1)(l1\ m2+l1\ m3+cm1\ l1\ m1\ldots}{(l1^2\ l2^2\cos(x(1)-x(3))^2(m3\ cm3^2\ l3^2+I3)\ldots}\right) \tag{6.2}$$

$$\dot{x(3)} = x(4) \tag{6.3}$$

$$\dot{x(4)} = \left(\frac{(m3\ cm3^2 l3^2+I3)(g\ l2\sin(x(3))(m3+cm2\ m2)+l1\ l2x(2)\sin(x(1)-x(3))\ldots}{(l1^2\ l2^2\cos(x(1)-x(3))^2(m3\ cm3^2 l3^2\ +I3)\ldots}\right) \tag{6.4}$$

$$\dot{x(5)} = x(6) \tag{6.5}$$

$$\dot{x(6)} = \left(\frac{(u_3(m2\ cm2^2\ l2^2+m3\ l2^2+I2)(m1\ cm1^2\ l1^2+m3l1^3\ m2\ l2^2+I1)\ldots}{(l1^2\ l2^2\ \cos(x(1)-x(3))^2(m3\ cm3^2\ l3^2+\ I3)\ldots}\right) \quad (6.6)$$

The interval of integration was defined according to the desired time range, from t_0 to t_f but always keeping the same number of calculations made. So, even the final point t_f was changed according to the needs, the same number of points for integration was generated using the equation 6.7.

$$Interval\ of\ Integration = \frac{t_f - t_0}{n-1} \quad (6.7)$$

Except in exceptional situations, that are discussed when they happen, the simulation was made using 2000 interpolations, the initial time range t_0 starts on 0 and the n was 2000.

$$Interval\ of\ Integration = \frac{t_f - 0}{2000-1} \quad (6.8)$$

The figure 17 shows the dynamical response for the all system variables, position, speed, acceleration and dissipation, without any external force applied.

The initial condition used has changed depending on the analysis, but on the major part of the simulation was made using the following initial conditions:

$$x(t)_0 = \begin{bmatrix} 0 & 0 & 0 & 0 & \pi/6 & 0 \end{bmatrix}$$

6.2 CONTROL SDRE

With the dynamical response tuned and confirmed, the next step was test the system with a fixed set point for the joints positions. The matrix $k_{c\,i}$ on the SDRE control, equation 3.39, was set with the same rows as the number of inputs, hence the same columns as $B(x)$, and the same number of columns as the system states, hence the same rows as $A(x)$.

Figure 17 - Position, speed, acceleration and dissipation of the dynamical system without any external force.

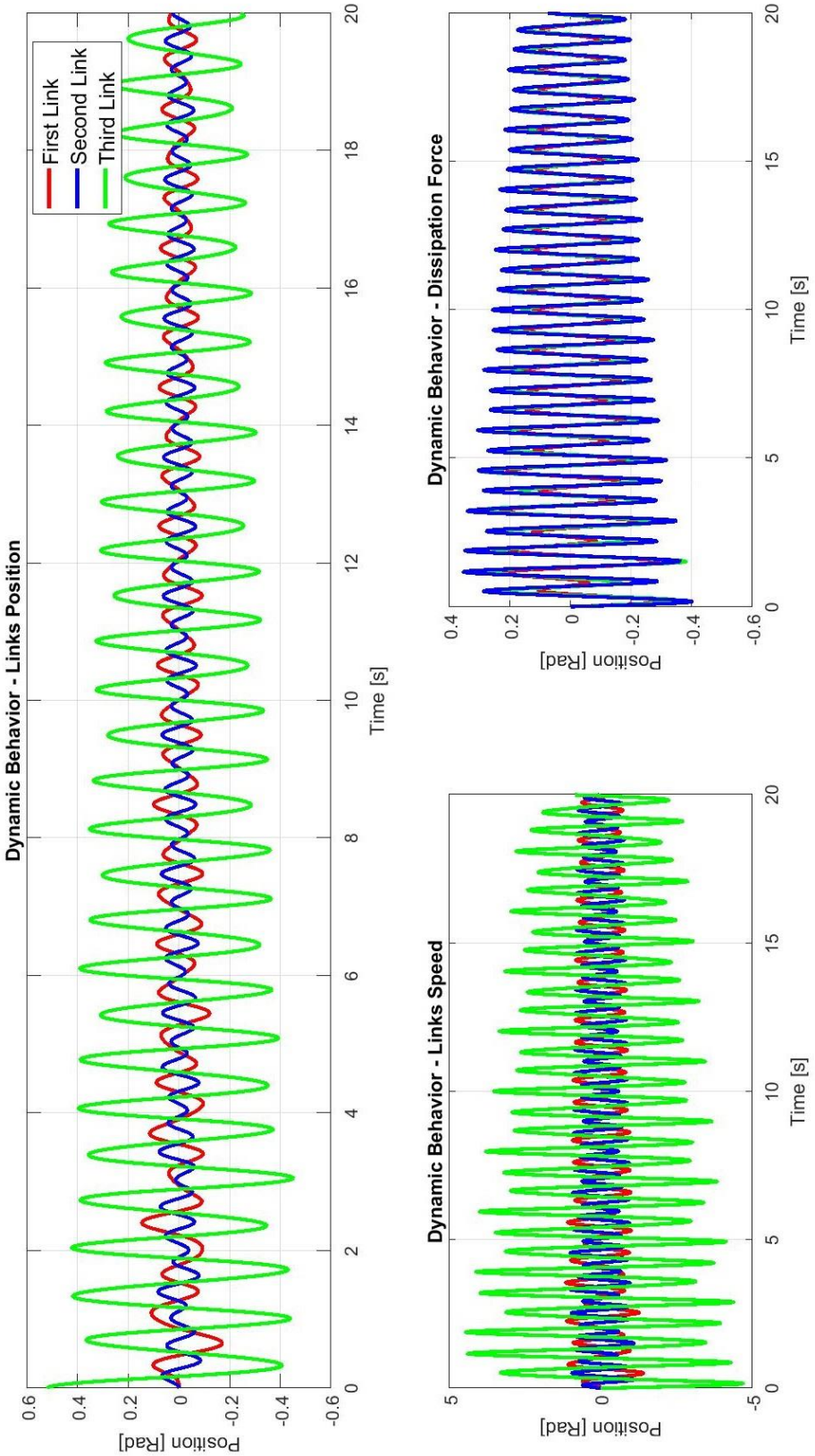

Source: Self Authorship.

Every i integration of the n presented on 6.7 and 6.8 a matrix $k_{c\,i}$ was set to be used as the basis for control the system

$$k_{c\,i} = \begin{bmatrix} k_{c\,11} & k_{c\,21} & k_{c\,31} & k_{c\,41} & k_{c\,51} & k_{c\,61} \\ k_{c\,12} & k_{c\,22} & k_{c\,32} & k_{c\,42} & k_{c\,52} & k_{c\,62} \\ k_{c\,13} & k_{c\,23} & k_{c\,33} & k_{c\,43} & k_{c\,53} & k_{c\,63} \end{bmatrix} \tag{6.9}$$

The elements of $k_{c\,i}$, equation 6.9, was used to define the action control u_n. Those action controls were based on the error for each state, defined by the difference between the actual state, $x(n)$, and the desired value for that state, $x(n)_d$.

$$e_{x(n)} = x(n) - x(n)_d \qquad n = 1, 2\ ou\ 3 \tag{6.10}$$

The error for the n, in 6.10, state was the values adjusted by the coefficient $k_{c\,i\,(n)}$

$$u_{c\,1} = -k_c(1,1)(x(1) - x(1)_d) - k_c(2,1)(x(2) - x(2)_d) - k_c(3,1)(x(3) - x(3)_d) \\ -k_c(4,1)(x(4) - x(4)_d) - k_c(5,1)(x(5 - x(5)_d) - k_c(6,1)(x(6) - x(6)_d) \tag{6.11}$$

$$u_{c\,2} = -k_c(2,1)(x(1) - x(1)_d) - k_c(2,2)(x(2) - x(2)_d) - k_c(3,2)(x(3) - x(3)_d) \\ - k_c(2,2)(x(4) - x(4)_d) - k_c(5,2)(x(5) - x(5)_d) - k_c(6,2)(x(6) - x(6)_d) \tag{6.12}$$

$$u_{c\,3} = -k_c(1,3)(x(1) - x(1)_d) - k_c(2,3)(x(2) - x(2)_d) - k_c(3,3)(x(3) - x(3)_d) \\ -k_c(4,3)(x(4) - x(4)_d) - k_c(5,3)(x(5) - x(5)_d) - k_c(6,3)(x(6) - x(6)_d) \tag{6.13}$$

For the SDRE control was defined the initial and final values for the system variables and the time range for the control. The table 4 show those parameters and data.

The figures 18 and 19 shown the position and speed using the SDRE control without any concern over the values. The control simulations shown that is possible control the system for any position for all three links.

Table 4 - Data and parameters for the SDRE control

Data	Simble	Unit	Value
Time - Initial	t_0	s	0
Time - Final	t_f	s	0.1
Initial Position - Link 1	θ_{01}	rad	0
Final Position - Link 1	θ_{f1}	rad	$\pi/6$
Initial Position - Link 2	θ_{02}	rad	0
Final Position - Link 2	θ_{f2}	rad	$\pi/4$
Initial Position - Link 3	θ_{03}	rad	0
Final Position - Link 3	θ_{f3}	rad	$\pi/3$
Initial Speed - Links 1, 2 e 3	ω_0	rad/s	0
Final Speed - Links 1, 2 e 3	ω_f	rad/s	0
Initial Acceleration - Links 1, 2 e 3	$\dot{\omega}_0$	rad/s^2	0
Final Speed - Links 1, 2 e 3	$\dot{\omega}_f$	rad/s^2	0

Source: Self Authorship.

Figure 18 - Position response using SDRE control for a fixed point.

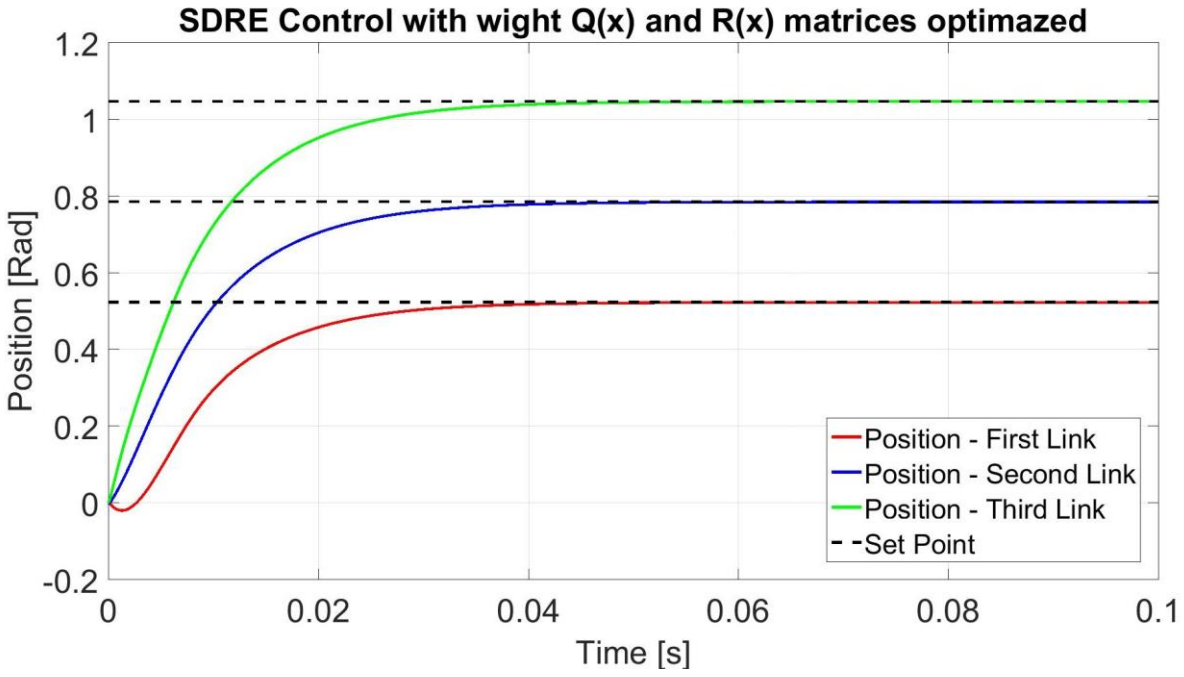

Source: Self Authorship.

Figure 19 - Speed response using SDRE control for a fixed point.

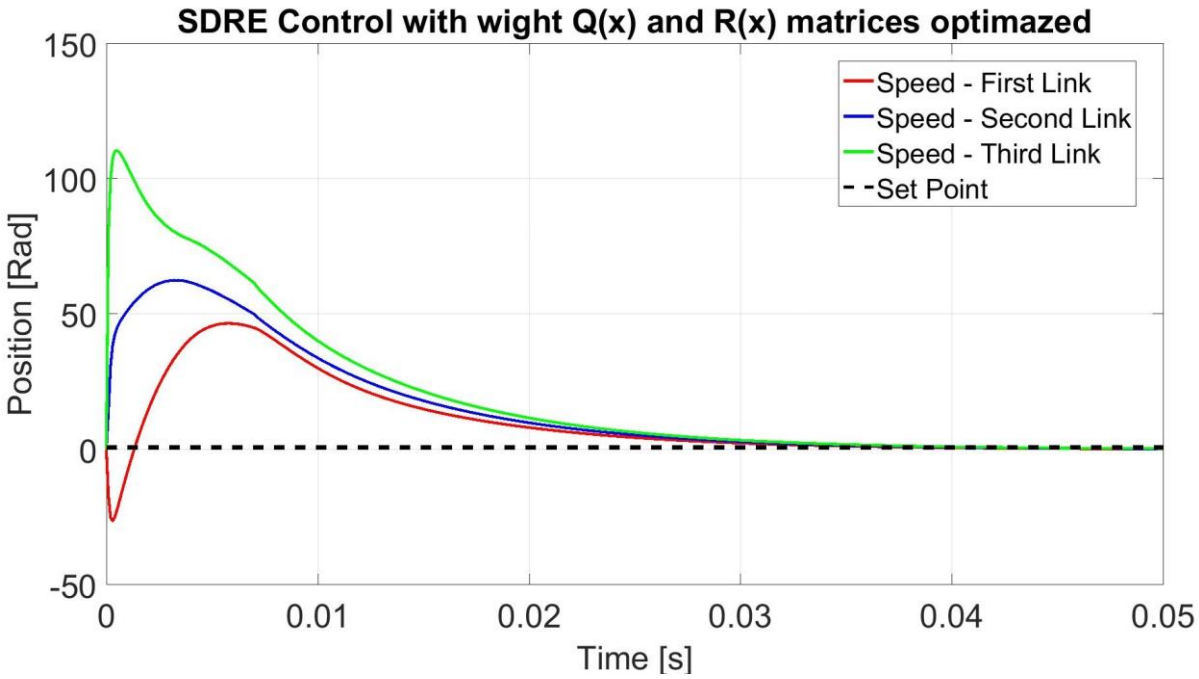

Source: Self Authorship.

6.3 STATE OBSERVER

The state observer was used to eliminate or supply the need of measuring the system states. Based on the equations 3.55 to 3.57, the state observer was rewritten using the state space representation of the dynamical system as the basis.

The first step for implement the state observer is guarantee that the state observer answers the same wat as the dynamical system when subjected to the same conditions. This was done by rewriting the dynamical equation and state space matrices presented on 3.42 to 3.48 but using the original $x(t)$ now as $\hat{x}(t)$.

That means, the system states $x(1)$ to $x(6)$, representing $\theta_1, \theta_2, \theta_3, \dot{\theta}_1, \dot{\theta}_2$ and $\dot{\theta}_3$, becomes $x(7)$ to $x(12)$ on the state observer representing the states variables $\hat{\theta}_1, \hat{\theta}_2, \hat{\theta}_3, \dot{\hat{\theta}}_1, \dot{\hat{\theta}}_2$ and $\dot{\hat{\theta}}_3$. The matrices used to the system, state observer and state observer gain was defined as presented and on the figure 20.

- System matrices: $A(x), B(x), R, Q,\ k_c(t)$ and $u(t)$;
- State Observer: $A(x)_{Ob}, B(x)_{Ob}, R_{Ob}, Q_{Ob}, k_c(x)_{Ob}$ and $u(t)_{Ob}$;
- State Observer Gain: $R_{L\,Ob}, Q_{L\,Ob}, k_c(x)_{L\,Ob}$ and $L_{Ob}(t)$.

Figure 20 - Block diagram for the control: dynamical system and state observer.

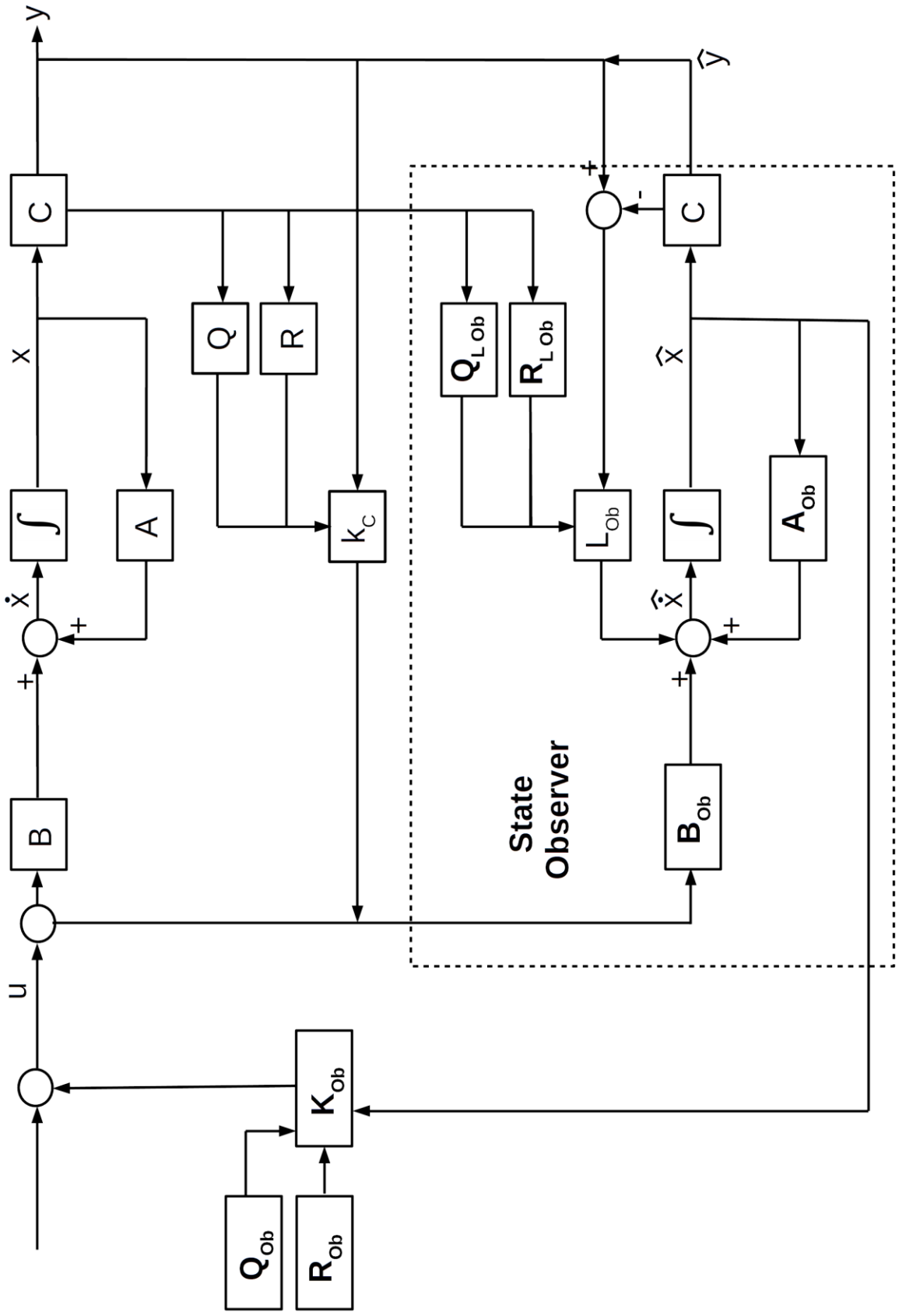

Source: Self Authorship

For the SDRE control law applied on the state observer this led to the n inputs $u_{Ob\,n}$ as shown on 6.14 to 6.16.

$$u_{c\,ob\,1} = -k_{c\,ob}(1,1)(\hat{x}(1) - x(1)_d) - k_{c\,ob}(2,1)(\hat{x}(2) - x(2)_d) - k_{c\,ob}(3,1)(\hat{x}(3) - x(3)_d - \\ - k_{c\,ob}(4,1)(\hat{x}(4) - x(4)_d) - k_{c\,ob}(5,1)(\hat{x}(5 - x(5)_d) - k_{c\,ob}(6,1)(\hat{x}(6) - x(6)_d) \quad (6.14)$$

$$u_{c\,ob\,2} = -k_{c\,ob}(1,2)(\hat{x}(1) - x(1)_d) - k_{c\,ob}(2,2)(\hat{x}(2) - x(2)_d) - k_{c\,ob}(3,2)(\hat{x}(3) - x(3)_d) - \\ - k_{c\,ob}(4,2)(\hat{x}(4) - x(4)_d) - k_{c\,ob}(5,2)(\hat{x}(5) - x(5)_d) - k_{c\,ob}(6,2)(\hat{x}(6) - x(6)_d) \quad (6.15)$$

$$u_{c\,ob\,3} = -k_{c\,ob}(1,2)(\hat{x}(1) - x(1)_d) - k_{c\,ob}(2,3)(\hat{x}(2) - x(2)_d) - k_{c\,ob}(3,3)(\hat{x}(3) - x(3)_d) \\ -k_{c\,ob}(4,3)(\hat{x}(4) - x(4)_d) - k_{c\,ob}(5,3)(\hat{x}(5) - x(5)_d) - k_{c\,ob}(6,3)(\hat{x}(6) - x(6)_d) \quad (6.16)$$

where $\hat{x}(1) = x(7)$, $\hat{x}(2) = x(8)$, $\hat{x}(3) = x(9)$, $\hat{x}(4) = x(10)$, $\hat{x}(5) = x(11)$ and $\hat{x}(6) = x(12)$ on the overall system representation.

To certify that the system and the state observer can become in tune over a finite time t, the tests were done applying different initial conditions on the system and the state observer and checking if the error between $x(n)$ and $\hat{x}(t)$ would go to zero. The initial conditions used to the system and the state observer was defined with an additional of 10% on the positions and 5% on the speeds

$$x(t)_0 = [0 \quad 0 \quad 0 \quad 0 \quad 0 \quad 0] \quad (6.17)$$

$$\hat{x}(t)_0 = [0.1 \quad 0.05 \quad 0.1 \quad 0.05 \quad 0.1 \quad 0.05] \quad (6.18)$$

The answers presented on the figures 21 to 24 shown that state observer was capable to minimize the error on the estimation even with different initial conditions.

But this result only took in consideration the controllability criterion, equation 3.11, and even if all the states observer was capable to minimize the error estimation for all the states, this doesn't mean that all the states can be used on the state observer. To define the usage of the state observer on the system were made tests with all the possible system states combination. Those tests were made changing the values of the matrix $C(x)$ and checking if the matrix $C(x)$ and $A(x)$ can make the system completely observable.

Figure 21 - Positions of the first, second and third joints for the system and state observer with different initial condition positions.

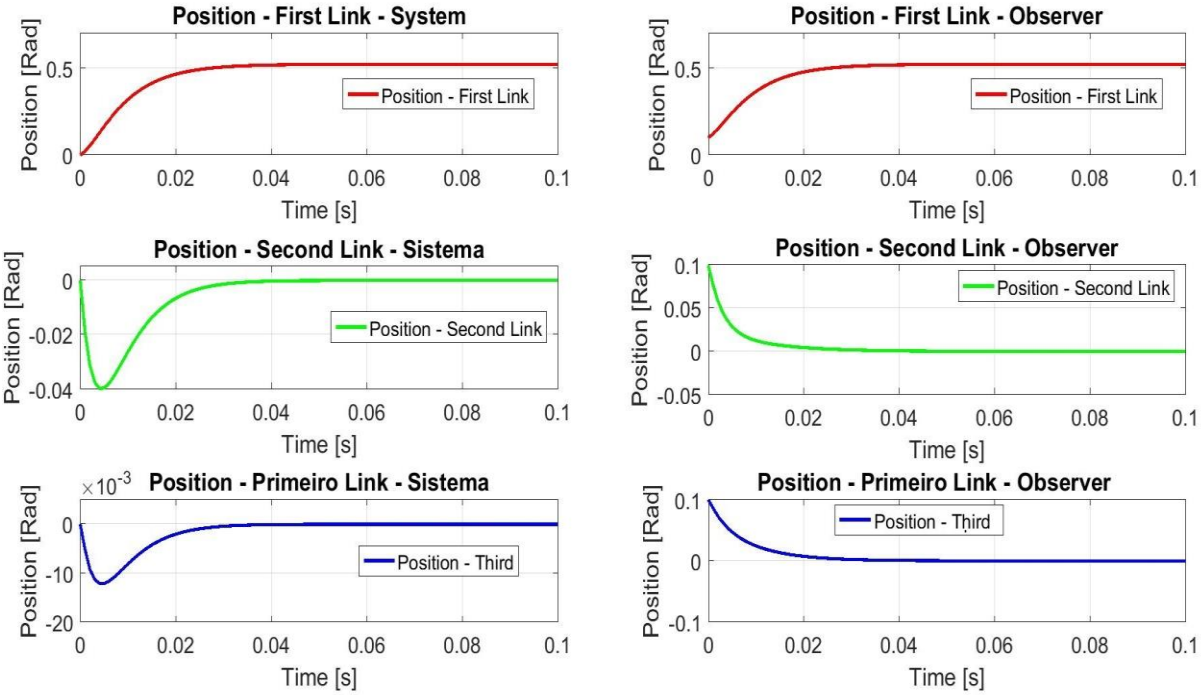

Source: Self Authorship.

Figure 22 - Error on the estimation of the first, second and third joints position.

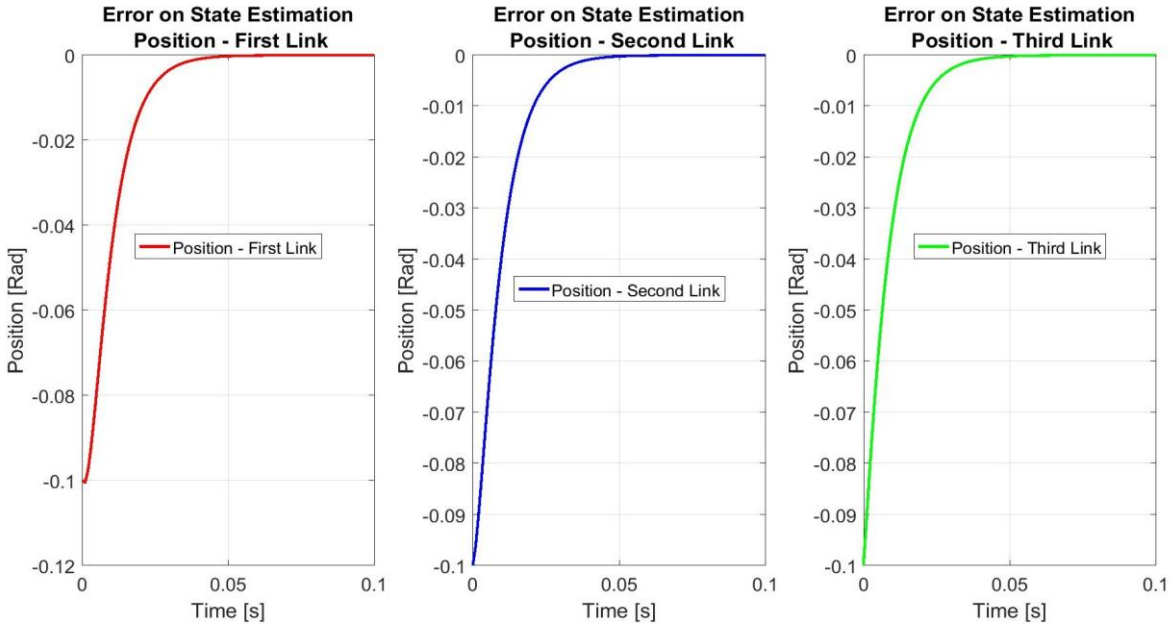

Source: Self Authorship.

Figure 23 - Speeds of the first, second and third joints for the system and state observer with different initial condition positions.

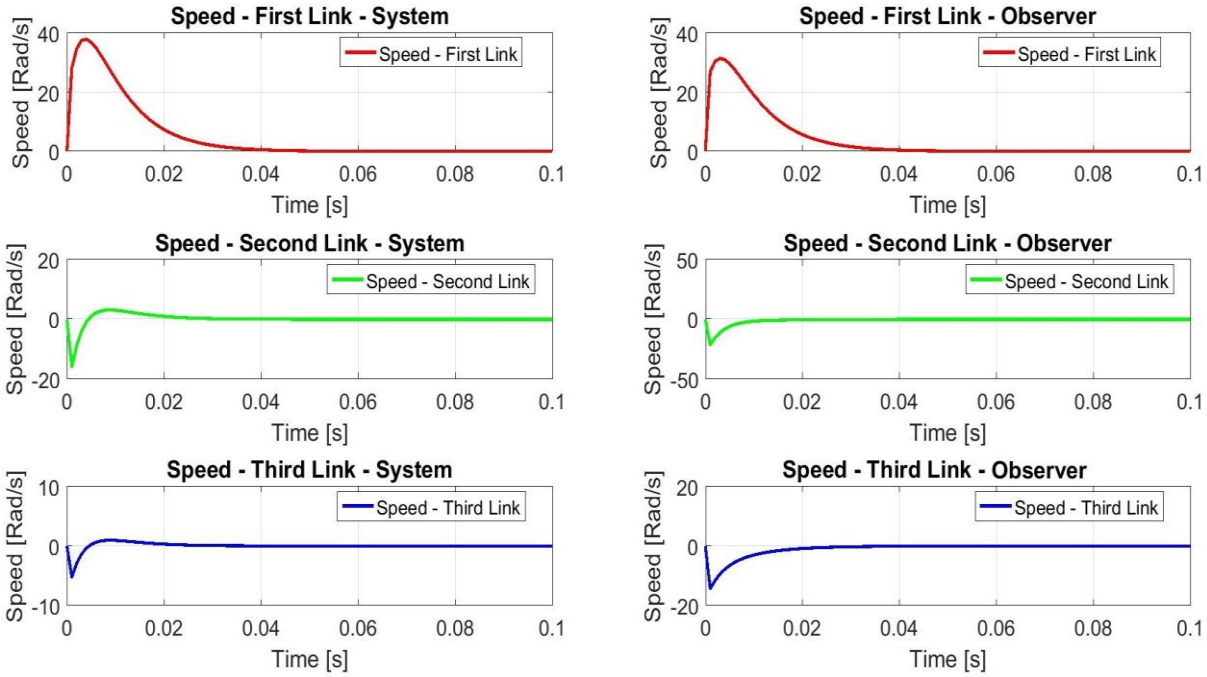

Source: Self Authorship.

Figure 24 - Error on the estimation of the first, second and third joints speed.

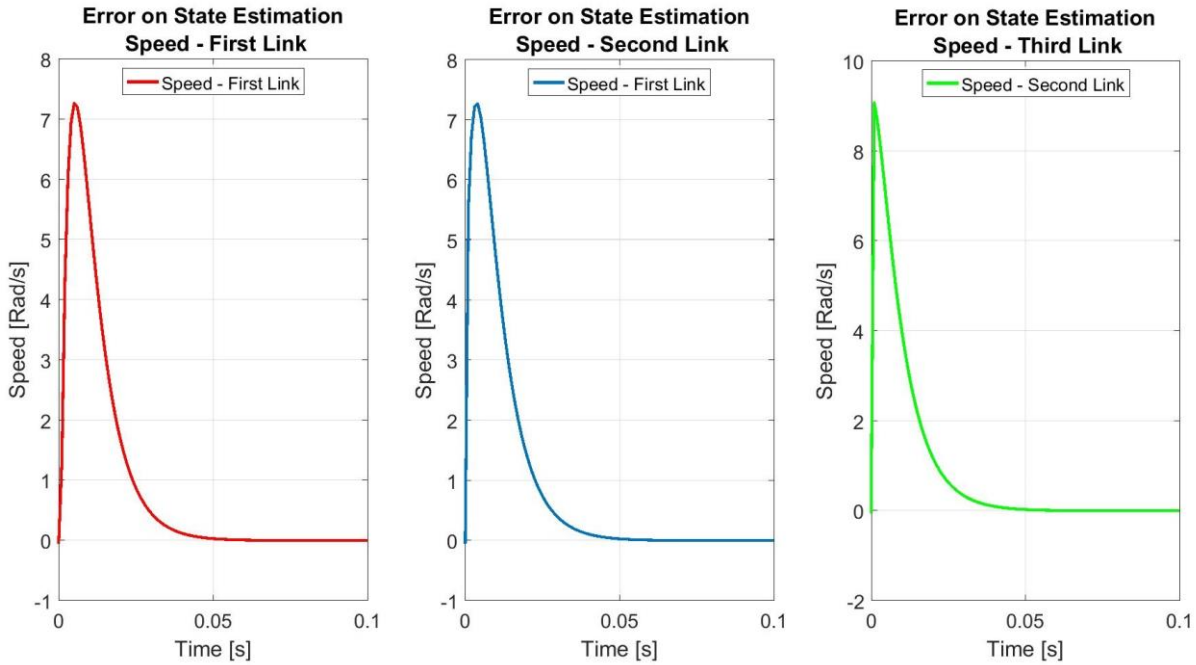

Source: Self Authorship.

The elements c_{11} to c_{66} of the matrix $C(x)$ can assume values 0 or 1 depending if the output is available or not, respectively. Those possibilities can be express as dependent of those variations:

$$C(x) = \begin{bmatrix} c_{11} & 0 & 0 & 0 & 0 & 0 \\ 0 & c_{22} & 0 & 0 & 0 & 0 \\ 0 & 0 & c_{33} & 0 & 0 & 0 \\ 0 & 0 & 0 & c_{44} & 0 & 0 \\ 0 & 0 & 0 & 0 & c_{55} & 0 \\ 0 & 0 & 0 & 0 & 0 & c_{66} \end{bmatrix} \tag{6.19}$$

The eigenvalue positions and the stabilization on close-loop was used as a criterion to verify the controllability of the system given by the selection of $C(x)$ and $A(x)$ for each possible combination.

After all the tests, the three combinations passed the Observer criterion presented on 3.55.

- State Observer on the first link speed, $x(2)$;
- State Observer on the second link speed, $x(4)$;
- State Observer on the first and second links speed, $x(2)$ and $x(4)$.

Paying attention to equation 3.55, the matrix $L_{Ob}(t)$ is responsible to eliminate the error on the state estimation and as already discussed, this can be made using a lot of methods. On this work, the LQR/SDRE control method was used to find the gain matrix $L_{Ob}(t)$ and minimize the error on the approximation $x(t)$ to $\hat{x}(t)$.

Even if the state observer follows the same guidelines used to the dynamical system, the matrix $L_{Ob}(t)$ isn't directly composed by the elements defined by the matrix $k(t)_{L\,Ob}$ calculated using the LQR solution, equation 3.39.

The gain matrix using the LQR control was calculated setting the value for four matrices, M_1 and M_2 that are the state space matrices, that was chosen based on being the system or the state observer calculating, and the weight matrices Q and R

$$Gain\ matrix = lqr(M_1, M_2, Q, R) \tag{6.20}$$

To use the SDRE control the weight matrix R must have the same number of columns as the matrix use on M_2, this leads to change the matrix R from a 3×3 to a 6×6 since the matrix $C(x)$ was used on M_2 and $C(x)$ always was 6×6.

So, $R(x)_{L\,Ob}$ for the state observer gain continued to be an identity matrix but with the following disposition

$$R(x)_{L\,Ob} = \begin{bmatrix} R_{L\,Ob_{11}} & 0 & 0 & 0 & 0 & 0 \\ 0 & R_{L\,Ob_{22}} & 0 & 0 & 0 & 0 \\ 0 & 0 & R_{L\,Ob_{33}} & 0 & 0 & 0 \\ 0 & 0 & 0 & R_{L\,Ob_{44}} & 0 & 0 \\ 0 & 0 & 0 & 0 & R_{L\,Ob_{55}} & 0 \\ 0 & 0 & 0 & 0 & 0 & R_{L\,Ob_{66}} \end{bmatrix} \tag{6.21}$$

Due to the characteristics of the matrices $A(x)$ transpose, $C(x)$ transpose, $R_{L\,Ob}$ and $Q_{L\,Ob}$, the gain matrix $K_{L\,Ob}$ present the following form

$$K_{L\,Ob} = \begin{bmatrix} K_{L\,Ob\,11} & K_{L\,Ob\,12} & K_{L\,Ob\,13} & K_{L\,Ob\,14} & K_{L\,Ob\,15} & K_{L\,Ob\,16} \\ K_{L\,Ob\,21} & K_{L\,Ob\,22} & K_{L\,Ob\,23} & K_{L\,Ob\,24} & K_{L\,Ob\,25} & K_{L\,Ob\,26} \\ K_{L\,Ob\,31} & K_{L\,Ob\,32} & K_{L\,Ob\,33} & K_{L\,Ob\,34} & K_{L\,Ob\,35} & K_{L\,Ob\,36} \\ K_{L\,Ob\,41} & K_{L\,Ob\,42} & K_{L\,Ob\,43} & K_{L\,Ob\,44} & K_{L\,Ob\,45} & K_{L\,Ob\,46} \\ K_{L\,Ob\,51} & K_{L\,Ob\,52} & K_{L\,Ob\,45} & K_{L\,Ob\,54} & K_{L\,Ob\,55} & K_{L\,Ob\,56} \\ K_{L\,Ob\,61} & K_{L\,Ob\,62} & K_{L\,Ob\,46} & K_{L\,Ob\,64} & K_{L\,Ob\,65} & K_{L\,Ob\,66} \end{bmatrix} \tag{6.22}$$

The matrix $K_{L\,ob}$ is transpose, so the coefficients of the columns and rows switch position. So, the transpose matrix K_{ob} is call $K_{ob\,trans}$ on the following equation. The error on estimation was still given by the equation 3.57 and these was expanded to all the system states:

$$e(t) = x_n - \hat{x}_n \cong x(n) - x(n+6) \qquad n = 1, 2 \ldots 6 \tag{6.23}$$

The final State Observer Gain matrix was given by the sum of the components provide by $K_{L\,Ob\,trans}$, the error estimation $e(t)_n$ and the input configuration given by $C(x)$:

$$L_{Ob} = \begin{bmatrix} \sum_{n=1}^{6} C_{nn} e(t)_n \, K_{on\ trans\ 1n} \\ \sum_{n=1}^{6} C_{nn} e(t)_n \, K_{on\ trans\ 2n} \\ \sum_{n=1}^{6} C_{nn} e(t)_n \, K_{on\ trans\ 3n} \\ \sum_{n=1}^{6} C_{nn} e(t)_n \, K_{on\ trans\ 4n} \\ \sum_{n=1}^{6} C_{nn} e(t)_n \, K_{on\ trans\ 5n} \\ \sum_{n=1}^{6} C_{nn} e(t)_n \; K_{on\ trans\ 6n} \end{bmatrix} \qquad n = 1, 2 \dots 6 \tag{6.24}$$

Following the representation on 6.1 to 6.6, the state observer was written to continue the state space representation. The final gain was added to the state observer state space representation as shown:

$$\dot{\hat{x}}(7) = \; L_{Ob\ 11} + \hat{x}(2) \tag{6.25}$$

$$\dot{\hat{x}}(8) = \; L_{Ob\ 22} + \left(\frac{(m3\ cm3^2\ l3^2 + I3)(g sin(x(7)(l1\ m2 + l1\ m3 + cm1\ l1\ m1 \dots}{(l1^2\ l2^2 \cos(x(7) - x(9))^2 (m3\ cm3^2\ l3^2 + I3) \dots} \right) \tag{6.26}$$

$$\dot{\hat{x}}(9) = \; L_{Ob\ 33} + \hat{x}(10) \tag{6.27}$$

$$\dot{\hat{x}}(10) = \; L_{Ob\ 44} + \left(\frac{(m3\ cm3^2 l3^2 + I3)(g\ l2 \sin(\hat{x}(9))(m3 + cm2\ m2) + \cdots}{(l1^2\ l2^2 \cos(\hat{x}(7) - \hat{x}(9))^2 (m3\ cm3^2 l3^2 + I3) \dots} \right) \tag{6.28}$$

$$\dot{\hat{x}}(11) = \; L_{Ob\ 55} + \hat{x}(12) \tag{6.29}$$

$$\dot{\hat{x}}(12) = \; L_{Ob\ 66} + \left(\frac{(u_{Ob\ 3} (m2\ cm2^2\ l2^2 + m3\ l2^2 + I2)(m1\ cm1^2\ l1^2 + m3 l1^3\ m2\ l2^2 + I1) \dots}{(l1^2\ l2^2 \cos(\hat{x}(7) - \hat{x}(9))^2 (m3\ cm3^2\ l3^2 + I3) \dots} \right) \tag{6.30}$$

When using the state observer, the weight matrices, Q_{Ob} and R_{Ob}, are defined to provide the best control action without considering the dimension of the inputs or the systems variables, like speed and acceleration.

What was noticed during the control tests and simulations was that the values of the weight matrices become to a point where increasing their values does not provide any substantial, or even any, improvement on the optimal control. So, the main criterion for defining the final values of Q_{Ob} and R_{Ob}, was to find this optimal control point. When increasing his values did not alter the answers, his final values had been found.

As discussed, the state observer equations were used to estimate the values for $x(2), x(4)$ and $x(2)$ and $x(4)$ at the same time. Those simulations and discussion are presented as follows.

6.3.1 State Observer in the first link speed, $\dot{\theta}_1$

To use the state observer in $\dot{\theta}_1$ the matrix $C(x)$, $R_{L\,Ob}$ and $Q_{L\,Ob}$ assumed the following values and the figures 25 and 26 show the simulation answer.

$$C(x) = \begin{bmatrix} 1 & 0 & 0 & 0 & 0 & 0 \\ 0 & 0 & 0 & 0 & 0 & 0 \\ 0 & 0 & 1 & 0 & 0 & 0 \\ 0 & 0 & 0 & 1 & 0 & 0 \\ 0 & 0 & 0 & 0 & 1 & 0 \\ 0 & 0 & 0 & 0 & 0 & 1 \end{bmatrix} \tag{6.32}$$

$$Q = \begin{bmatrix} 35 \times 10^3 & 0 & 0 & 0 & 0 & 0 \\ 0 & 1 & 0 & 0 & 0 & 0 \\ 0 & 0 & 35 \times 10^3 & 0 & 0 & 0 \\ 0 & 0 & 0 & 1 & 0 & 0 \\ 0 & 0 & 0 & 0 & 35 \times 10^3 & 0 \\ 0 & 0 & 0 & 0 & 0 & 1 \end{bmatrix} \tag{6.33}$$

$$R = \begin{bmatrix} 1 \times 10^{-4} & 0 & 0 \\ 0 & 1 \times 10^{-4} & 0 \\ 0 & 0 & 1 \times 10^{-4} \end{bmatrix} \tag{6.34}$$

$$Q_{Ob} = \begin{bmatrix} 10 \times 10^1 & 0 & 0 & 0 & 0 & 0 \\ 0 & 1 & 0 & 0 & 0 & 0 \\ 0 & 0 & 10 \times 10^1 & 0 & 0 & 0 \\ 0 & 0 & 0 & 1 & 0 & 0 \\ 0 & 0 & 0 & 0 & 10 \times 10^1 & 0 \\ 0 & 0 & 0 & 0 & 0 & 1 \end{bmatrix} \tag{6.35}$$

$$R_{Ob} = \begin{bmatrix} 1 \times 10^{-2} & 0 & 0 \\ 0 & 1 \times 10^{-2} & 0 \\ 0 & 0 & 1 \times 10^{-2} \end{bmatrix} \tag{6.36}$$

Figure 25 - Position and speed of the system and state observer on $\dot{\theta}_1$ with fixed point without concern about the path to this point.

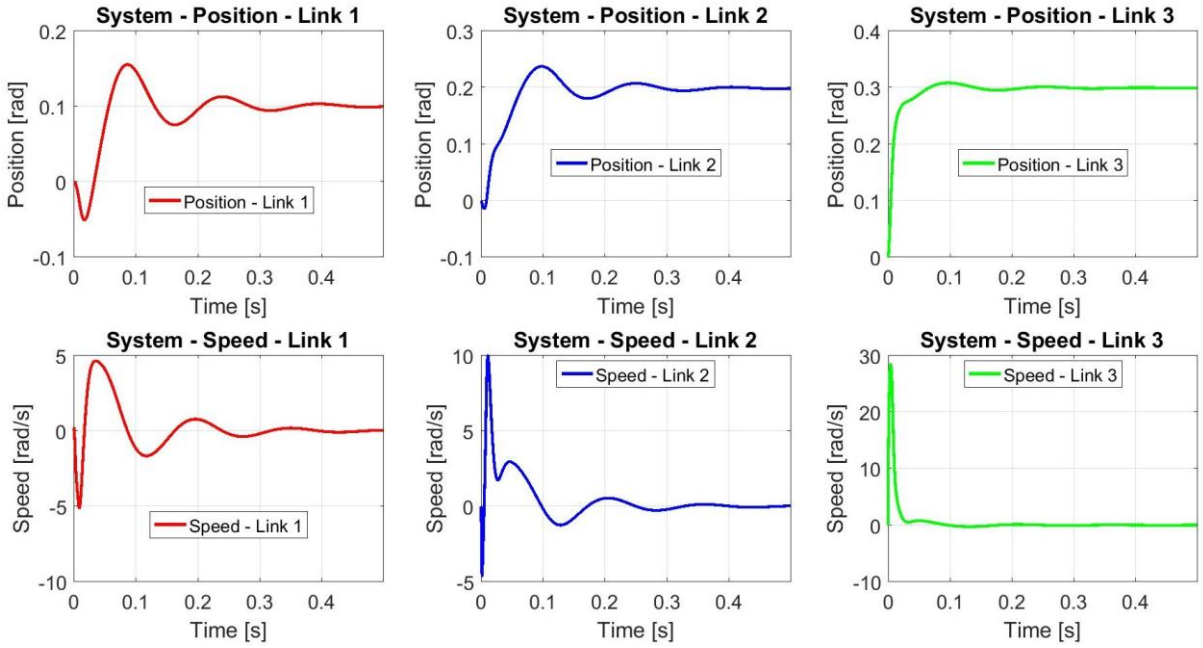

Source: Self Authorship.

Figure 26 - Position and speed of the State Observer.

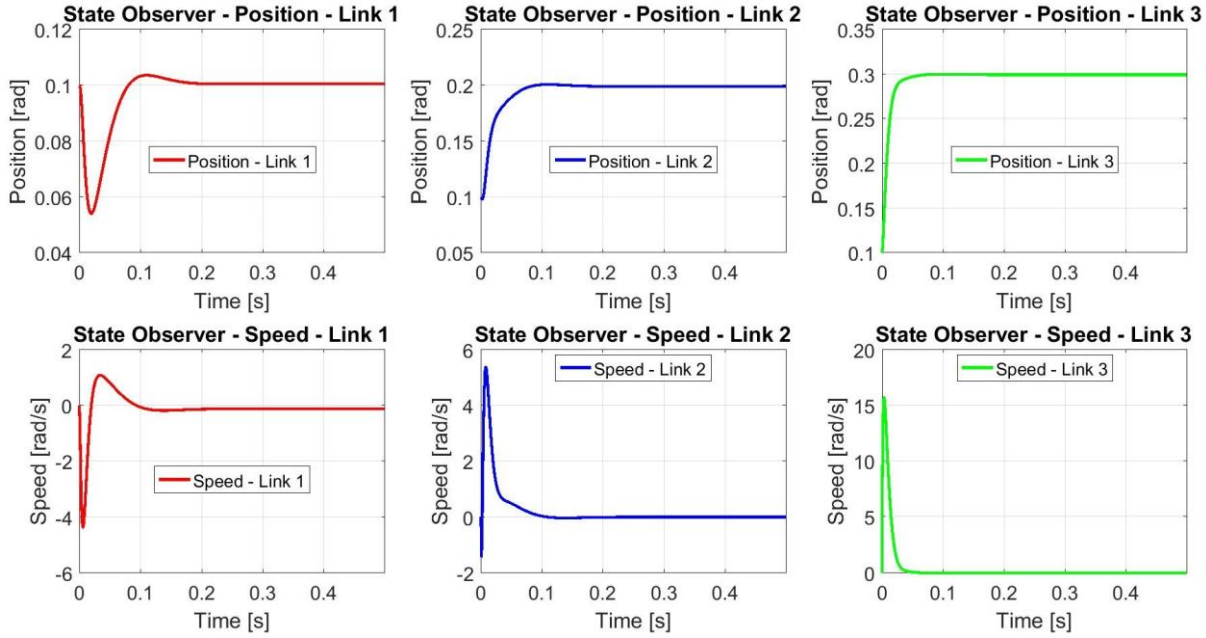

Source: Self Authorship.

6.3.2 State Observer in the second link speed, $\dot{\theta}_2$

To use the state observer in $\dot{\theta}_2$ the matrix $C(x)$, $R_{L\,Ob}$ and $Q_{L\,Ob}$ assumed the following values and the figures 27 and 28 show the simulation answer.

$$C(x) = \begin{bmatrix} 1 & 0 & 0 & 0 & 0 & 0 \\ 0 & 1 & 0 & 0 & 0 & 0 \\ 0 & 0 & 1 & 0 & 0 & 0 \\ 0 & 0 & 0 & 0 & 0 & 0 \\ 0 & 0 & 0 & 0 & 1 & 0 \\ 0 & 0 & 0 & 0 & 0 & 1 \end{bmatrix} \tag{6.37}$$

$$Q = \begin{bmatrix} 55 \times 10^3 & 0 & 0 & 0 & 0 & 0 \\ 0 & 1 & 0 & 0 & 0 & 0 \\ 0 & 0 & 55 \times 10^3 & 0 & 0 & 0 \\ 0 & 0 & 0 & 1 & 0 & 0 \\ 0 & 0 & 0 & 0 & 55 \times 10^3 & 0 \\ 0 & 0 & 0 & 0 & 0 & 1 \end{bmatrix} \tag{6.38}$$

$$R = \begin{bmatrix} 5 \times 10^{-5} & 0 & 0 \\ 0 & 5 \times 10^{-5} & 0 \\ 0 & 0 & 5 \times 10^{-5} \end{bmatrix} \tag{6.39}$$

$$Q_{Ob} = \begin{bmatrix} 10 \times 10^1 & 0 & 0 & 0 & 0 & 0 \\ 0 & 1 & 0 & 0 & 0 & 0 \\ 0 & 0 & 10 \times 10^1 & 0 & 0 & 0 \\ 0 & 0 & 0 & 1 & 0 & 0 \\ 0 & 0 & 0 & 0 & 10 \times 10^1 & 0 \\ 0 & 0 & 0 & 0 & 0 & 1 \end{bmatrix} \tag{6.40}$$

$$R_{Ob} = \begin{bmatrix} 1 \times 10^{-2} & 0 & 0 \\ 0 & 1 \times 10^{-2} & 0 \\ 0 & 0 & 1 \times 10^{-2} \end{bmatrix} \tag{6.41}$$

Figure 27 - Position and speed of the system and state observer on $\dot{\theta}_4$ with fixed point without concern about the path to this point.

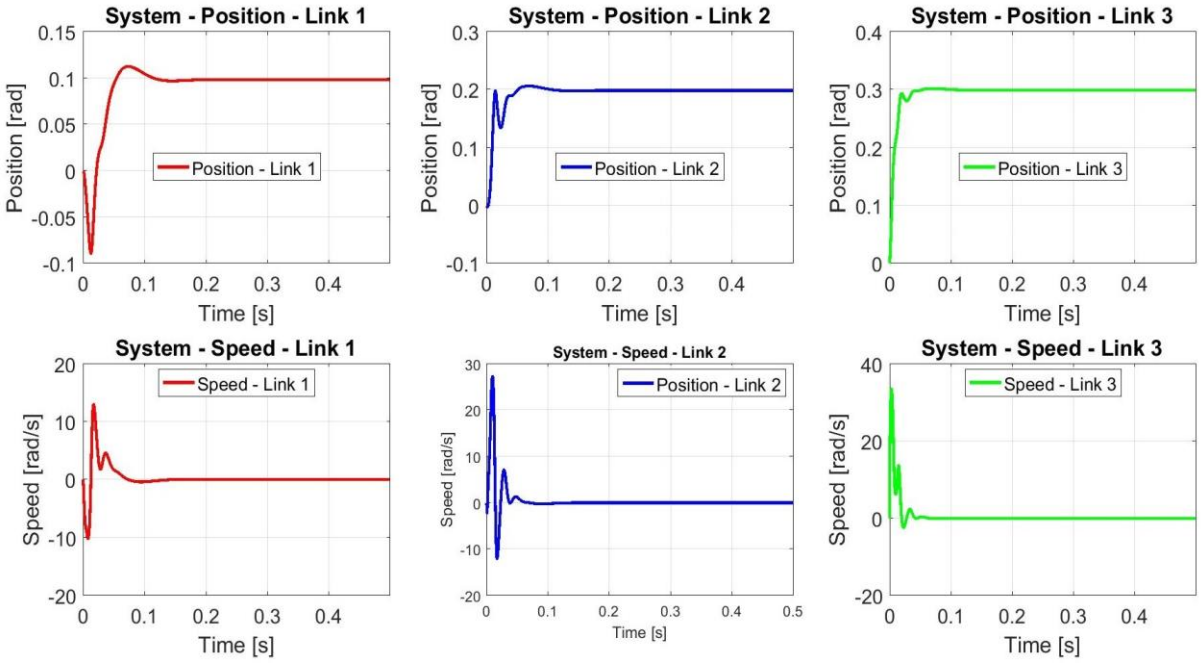

Source: Self Authorship.

Figure 28 - Position and speed of the State Observer

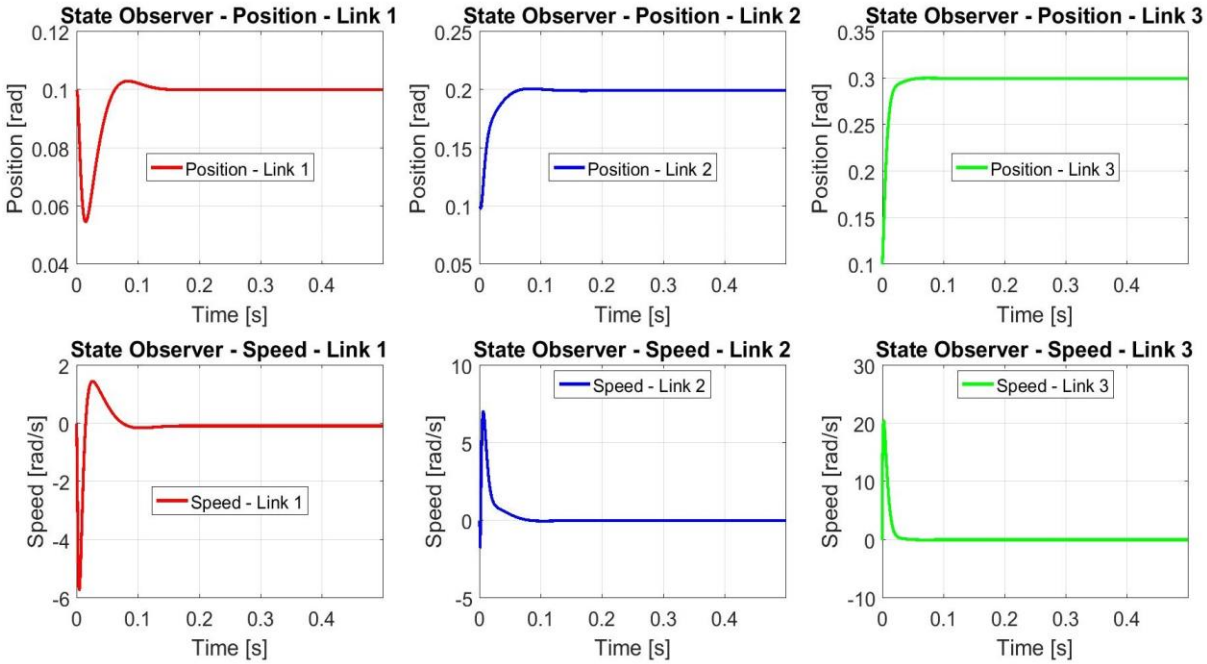

Source: Self Authorship.

6.3.3 State Observer in the first and second links speed, $\dot{\theta}_1$ and $\dot{\theta}_2$

To use the state observer in $x(2)$ and $x(4)$ at the same time the matrix $C(x)$, $R_{L\,Ob}$ and $Q_{L\,Ob}$ assumed the following values and the figures 29 and 30 show the simulation answer.

$$C(x) = \begin{bmatrix} 1 & 0 & 0 & 0 & 0 & 0 \\ 0 & 0 & 0 & 0 & 0 & 0 \\ 0 & 0 & 1 & 0 & 0 & 0 \\ 0 & 0 & 0 & 0 & 0 & 0 \\ 0 & 0 & 0 & 0 & 1 & 0 \\ 0 & 0 & 0 & 0 & 0 & 1 \end{bmatrix} \tag{6.42}$$

$$Q = \begin{bmatrix} 55 \times 10^3 & 0 & 0 & 0 & 0 & 0 \\ 0 & 1 & 0 & 0 & 0 & 0 \\ 0 & 0 & 55 \times 10^3 & 0 & 0 & 0 \\ 0 & 0 & 0 & 1 & 0 & 0 \\ 0 & 0 & 0 & 0 & 100 & 0 \\ 0 & 0 & 0 & 0 & 0 & 1 \end{bmatrix} \tag{6.43}$$

$$R = \begin{bmatrix} 1 \times 10^{-5} & 0 & 0 \\ 0 & 1 \times 10^{-5} & 0 \\ 0 & 0 & 1 \times 10^{-5} \end{bmatrix} \tag{6.44}$$

$$Q_{Ob} = \begin{bmatrix} 10 \times 10^1 & 0 & 0 & 0 & 0 & 0 \\ 0 & 1 & 0 & 0 & 0 & 0 \\ 0 & 0 & 10 \times 10^1 & 0 & 0 & 0 \\ 0 & 0 & 0 & 1 & 0 & 0 \\ 0 & 0 & 0 & 0 & 10 \times 10^1 & 0 \\ 0 & 0 & 0 & 0 & 0 & 1 \end{bmatrix} \tag{6.45}$$

$$R_{Ob} = \begin{bmatrix} 1 \times 10^{-2} & 0 & 0 \\ 0 & 1 \times 10^{-2} & 0 \\ 0 & 0 & 1 \times 10^{-2} \end{bmatrix} \tag{6.46}$$

Figure 29 - Position and speed of the system and state observer on $\dot{\theta}_1$ and $\dot{\theta}_2$ with fixed point without concern about the path to this point.

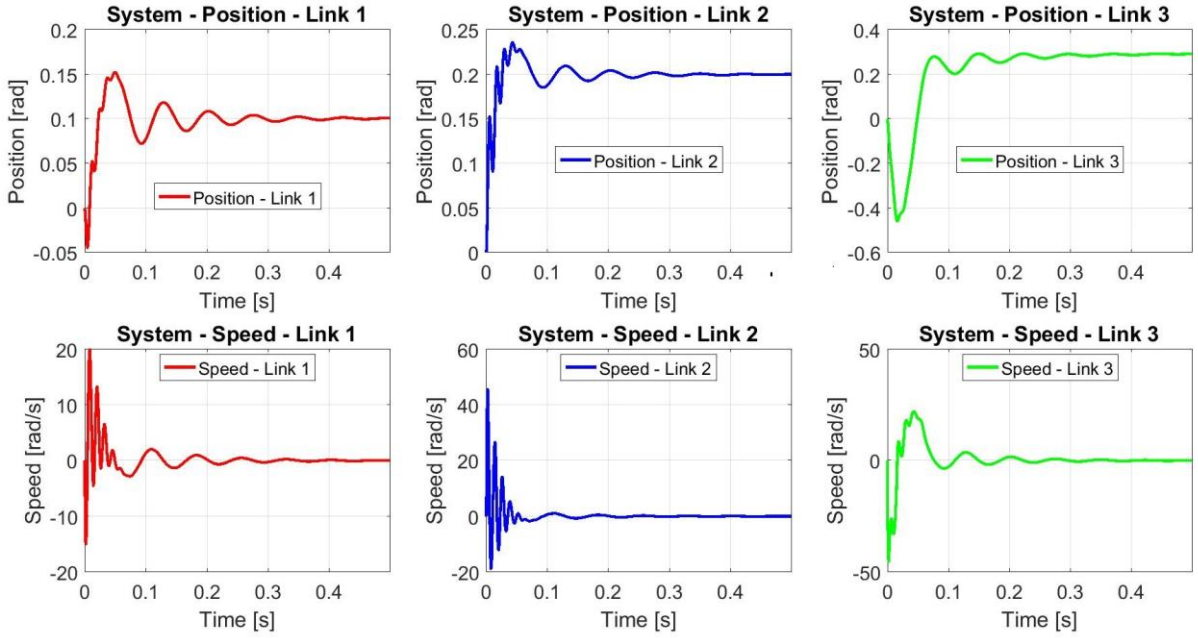

Source: Self Authorship.

Figure 30 - Position and speed of the State Observer.

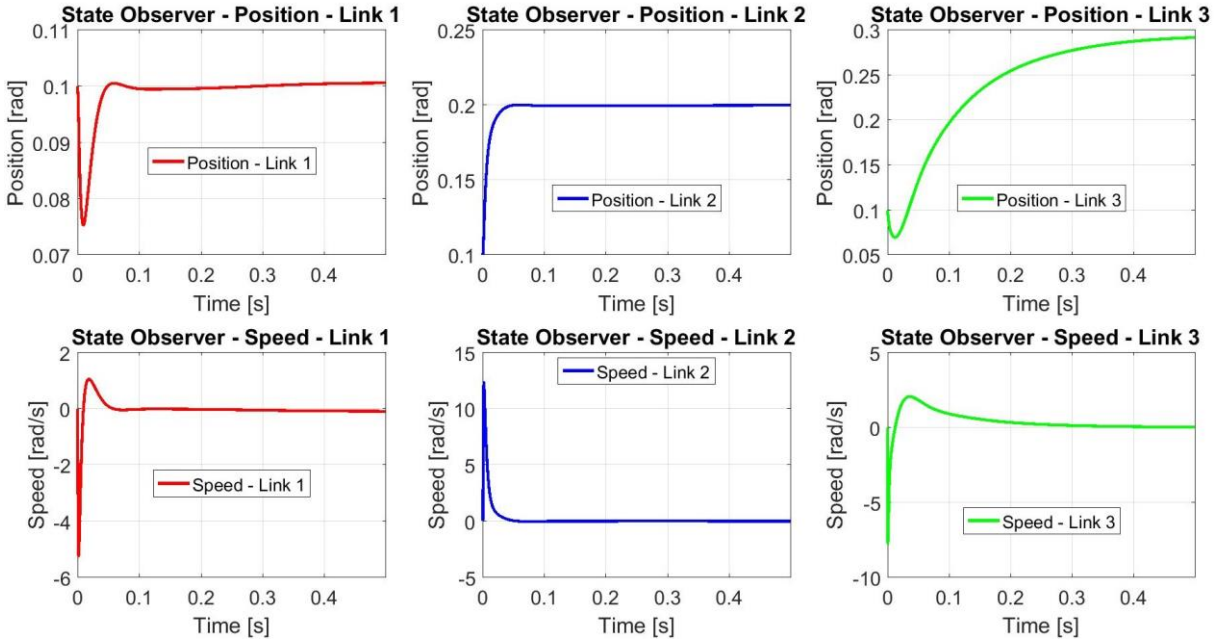

Source: Self Authorship.

6.4 TRAJECTORY PLANNING

The equations 5.1 to 5.3 were used to beget three vectors for position, speed and acceleration with i intermediates points between $\theta_{path\ i}$ and $\theta_{path\ f}$ for all the three joints. The vector with the trajectory point-to-point was express as θ_d, $\dot{\theta}_d$ and $\ddot{\theta}_d$ for position, speed and acceleration, respectively.

Tests and simulations made in the model indicated that to use the path setting for the acceleration, $\ddot{\theta}_d$, a new approach would be necessary to express the dynamical system and some modification would be necessary on the algorithm and simulation logic. As controlling the acceleration is not one of the interests of this work, this trajectory control was not considered on the analysis.

The path planning was based on two major values, the number of values on the Path Planning for θ_d and $\dot{\theta}_d$ and the number of interactions made to solve the complete path. All the other variables were dependents on those two major values, as the time interval, initial and final position and speed. The basis used to define the strategy for the path planning was define the vector for θ_d and $\dot{\theta}_d$, the total of interactions and the number of divisions of the complete path.

$$Total\ Number\ of\ interactions = n_1$$

$$\theta_d = 1 \times j = [\theta_{di\ j} \quad \theta_{di\ j+1} \quad \theta_{di\ j+2} \quad \dots \quad \theta_{df}]$$

$$\dot{\theta}_d = 1 \times j = [\dot{\theta}_{di\ j} \quad \dot{\theta}_{di\ j+1} \quad \dot{\theta}_{di\ j+2} \quad \dots \quad \dot{\theta}_{df}]$$

The solution used on this work was with n_1 as 100. This means that the path planning for the position is compose by 100 points as presented on the figure 31. The Path Planning solution was provided by controlling the system from the point $\theta_{d\ j}$ to the point $\theta_{d\ j+1}$, that means controlling the system from $n_1 = 1$ to $n_1 = 100$.

Figure 31 - Path Planning based on X internal points.

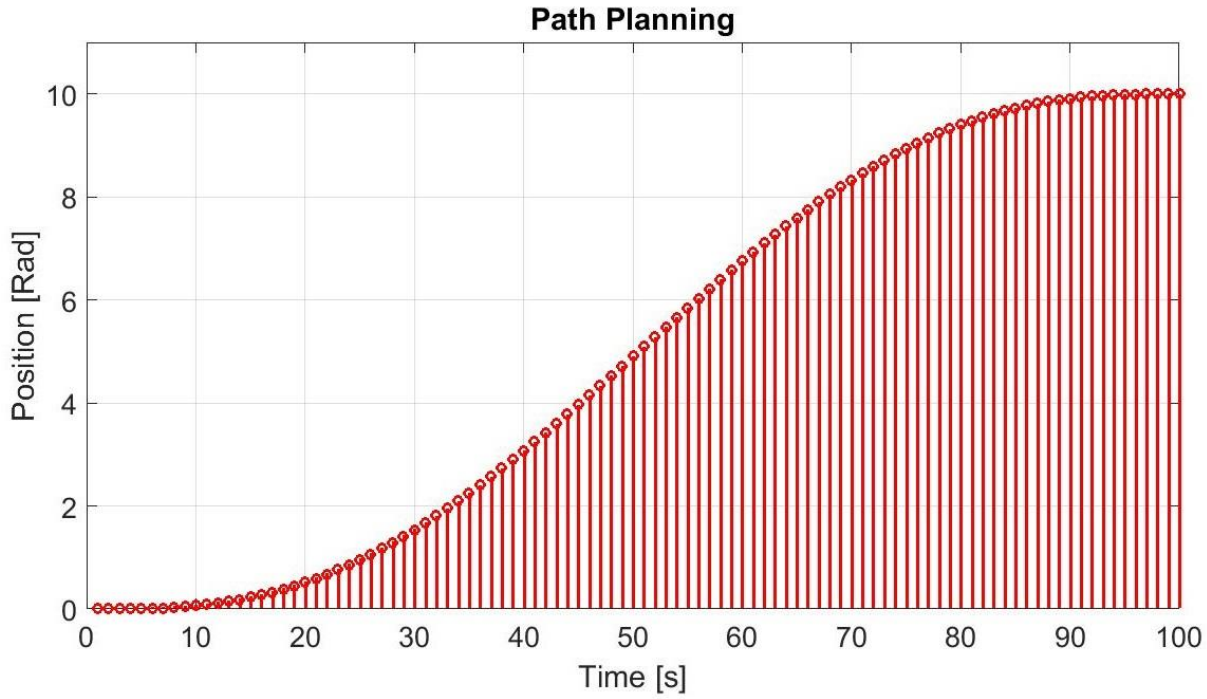

Source: Self Authorship.

The simplest approach is use the control to drive the system from $\theta_{d\,j}$ to $\theta_{d\,j+1}$ solving only one time between this position interval. This provide one matrix $k_{c\,j}$ corresponding to control the system for this interval. To improve the strategy and ensure that there was control over position and speed the solution chosen use this principle but solving the control five times between $\theta_{d\,j}$ and $\theta_{d\,j+1}$. The variable corresponding to this number of solutions was named n_2:

$$Total\ of\ interactions\ for\ each\ n_1\ point = n_2$$

The figure 32 shown this subdivision for the SDRE control on the Path Planning. The dots on red represent the desired position provided from the Path Planning and the blue dots represent the internal solutions for the control from $\theta_{d\,j}$ to $\theta_{d\,j+1}$.

Figure 32 - Division on the Path Planning for the SDRE solution.

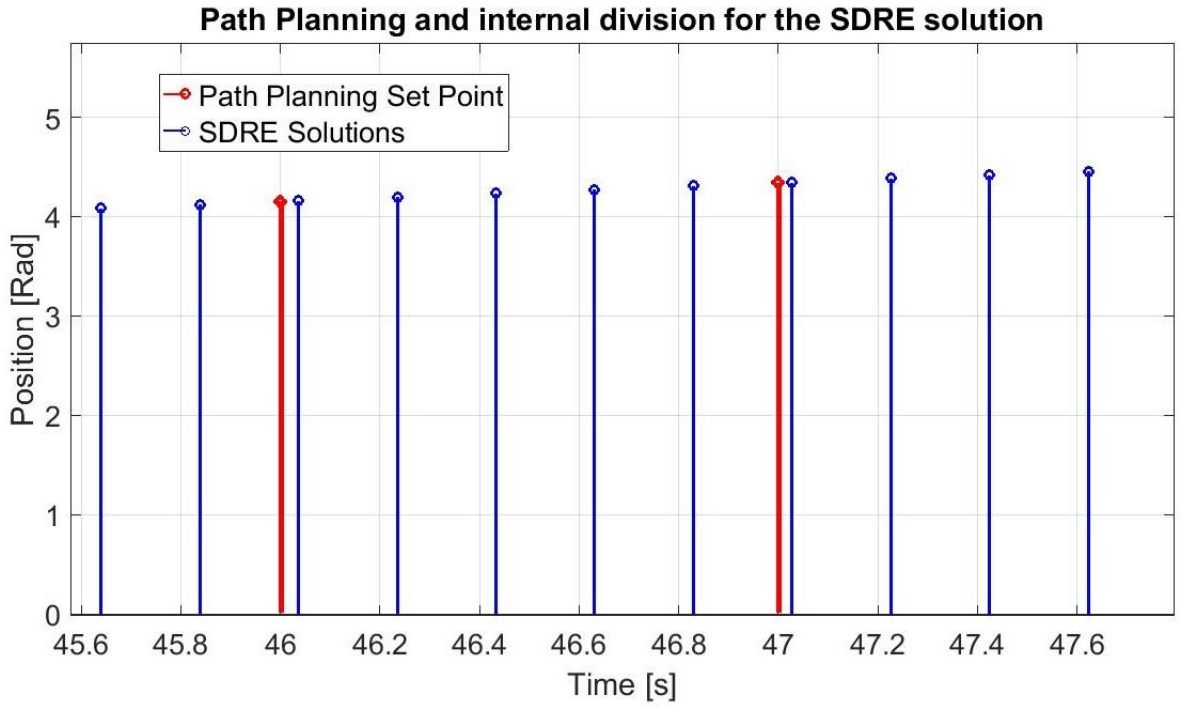

Source: Self Authorship.

The variable n_1, number total of interactions for the Path Planning, and the Total of interactions for each n_1 point, n_2, where used as the basis for define the final solution:

$$Total\ SDRE\ solution\ for\ the\ Path\ Planning = n_1 \times n_2 = 500$$

So, the final solution for the SDRE control for the Path Planning were provided from 500 interactions from $\theta_{d\ initial}$ to $\theta_{d\ final}$. This leads to the following vectors and matrices for the solution, where the columns where the system states, elements 1 to 6, and the state observers, elements 7 to 12, and the rows are the solutions found:

- SDRE solution from $\theta_{d\ j}$ to $\theta_{d\ j+1}$: matrix 12×5;
- System with Path Planning: matrix 12×500;
- Position Planning: vector 1×100;
- Speed Planning: vector 1×100.

After define the desired point for the SDRE control, the initial condition was defined using the last row of the matrix 12×5 provided from the SDRE solution from $\theta_{d\ j}$ to $\theta_{d\ j+1}$. The figure 33 shown an example of this relation.

Figure 33 - Initial and final values for the SDRE Control and Path Planning.

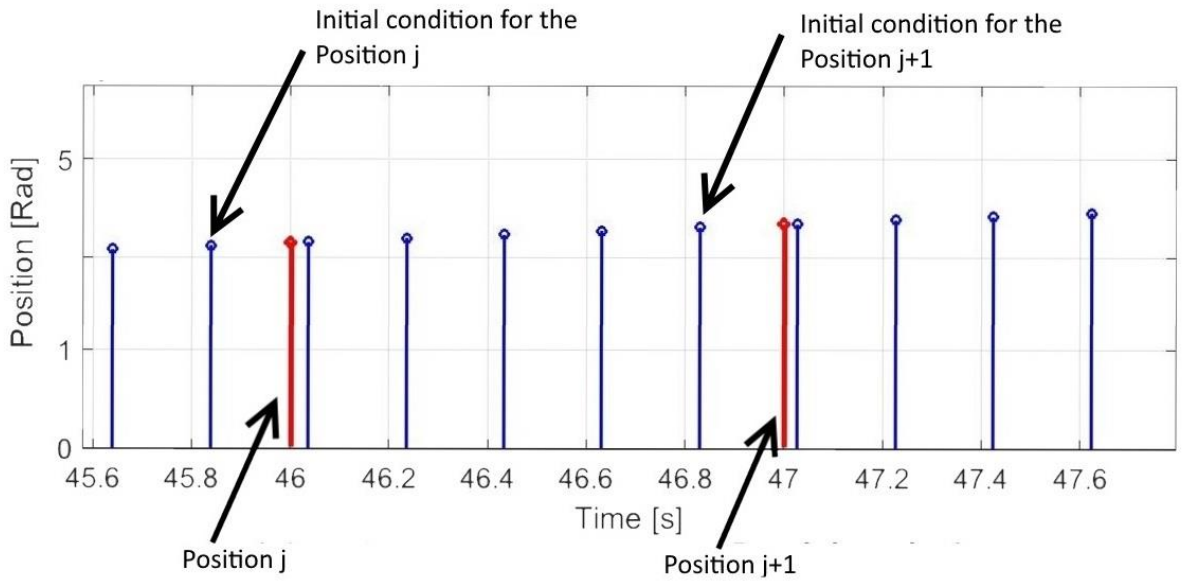

Source: Self Authorship.

The Path Planning were tested using the following combinations

- Control 1: Path Planning for the positions θ_1, θ_2 and θ_3 individually;
- Control 2: Path Planning for the positions θ_1, θ_2 and θ_3 at the same time;
- Control 3: Path Planning for the positions θ_1, θ_2 and θ_3 and the speeds $\dot{\theta}_1$, $\dot{\theta}_2$ and $\dot{\theta}_3$ at the same time;
- Control 4: Path Planning for the positions θ_1, θ_2 and θ_3 individually using the State Observer on $\dot{\theta}_1$;
- Control 5: Path Planning for the positions θ_1, θ_2 and θ_3 individually using the State Observer on $\dot{\theta}_2$;
- Control 6: Path Planning for the positions θ_1, θ_2 and θ_3 individually using the State Observer on $\dot{\theta}_1$ and $\dot{\theta}_2$ at the same time.

The table 5 show the data and parameters used on for the solution of the Control 1 to 3. Four sets of parameters were simulated, using the trajectory planning

on each joint individually, sets 1, 2 and 3 corresponding to the Control 1, and all three at the same time, set 4 corresponding to the Control 2. The equation 6.47 and 6.48 shown the matrices R and Qused for this for simulations.

Table 5 - Data for the trajectory planning and Control 1 and 2

Data	Simble	Unit	Values Set 1	Values Set 2	Values Set 3	Value Set 4
Time - Initial	t_0	s	0	0	0	0
Time - Final	t_f	s	2	2	2	2
Position Initial - Joint 1	θ_{01}	rad	0	0	0	0
Position Final - Joint 1	θ_{f1}	rad	$\pi/6$	0	0	$\pi/6$
Position Initial - Joint 2	θ_{02}	rad	0	0	0	0
Position Final - Joint 2	θ_{f2}	rad	0	$\pi/6$	0	$\pi/6$
Position Initial - Joint 3	θ_{03}	rad	0	0	0	0
Position Final - Joint 3	θ_{f3}	rad	0	0	$\pi/6$	$\pi/6$
Speed Initial - Joints 1, 2 e 3	ω_0	rad/s	0	0	0	0
Speed Final - Joints 1, 2 e 3	ω_f	rad/s	0	0	0	0
Acceleration Initial - Joints 1, 2 e 3	$\dot{\omega}_0$	rad/s^2	0	0	0	0
Acceleration Final - Joints 1, 2 e 3	$\dot{\omega}_f$	rad/s^2	0	0	0	0

Source: Self Authorship.

Figure 34 - Positions θ_1, θ_2 and θ_3 with θ_1 following the trajectory planning.

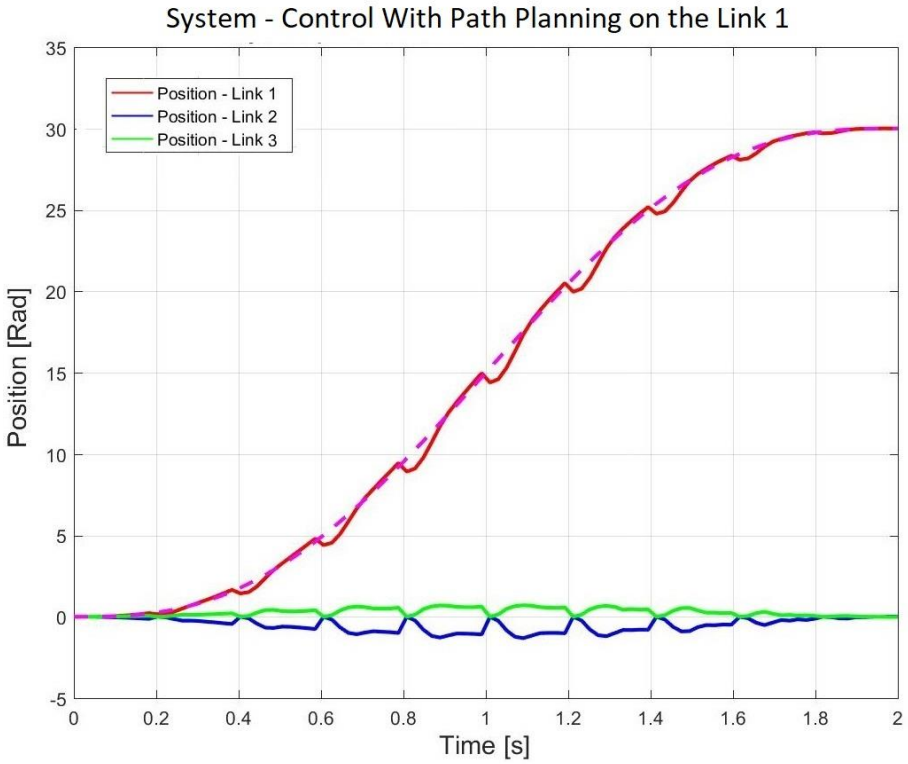

Source: Self Authorship.

Figure 35 - Positions θ_1, θ_2 and θ_3 with θ_2 following the trajectory planning.

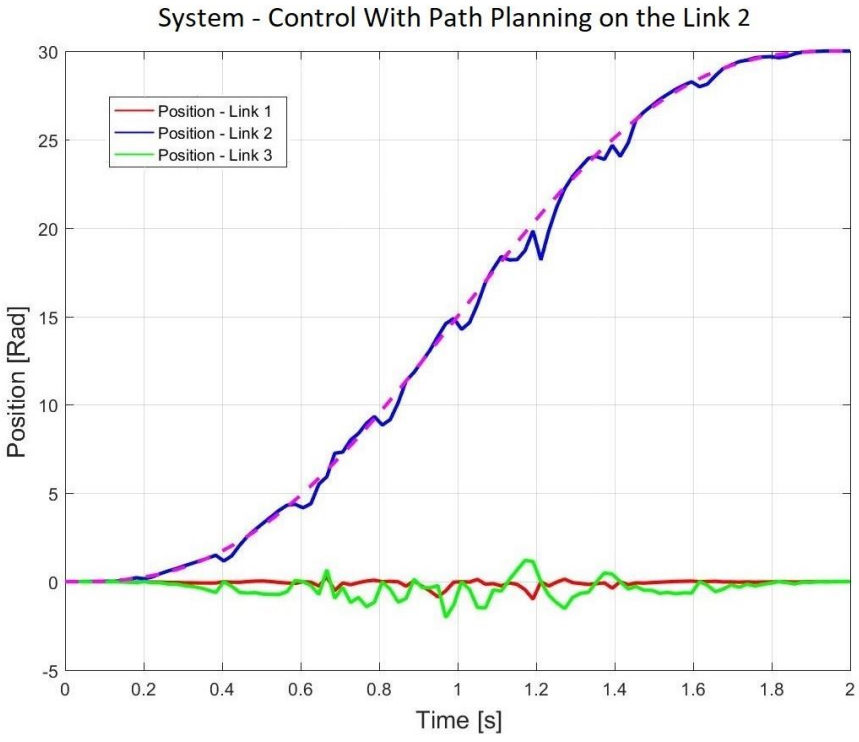

Source: Self Authorship.

Figure 36 - Positions θ_1, θ_2 and θ_3 with θ_3 following the trajectory planning.

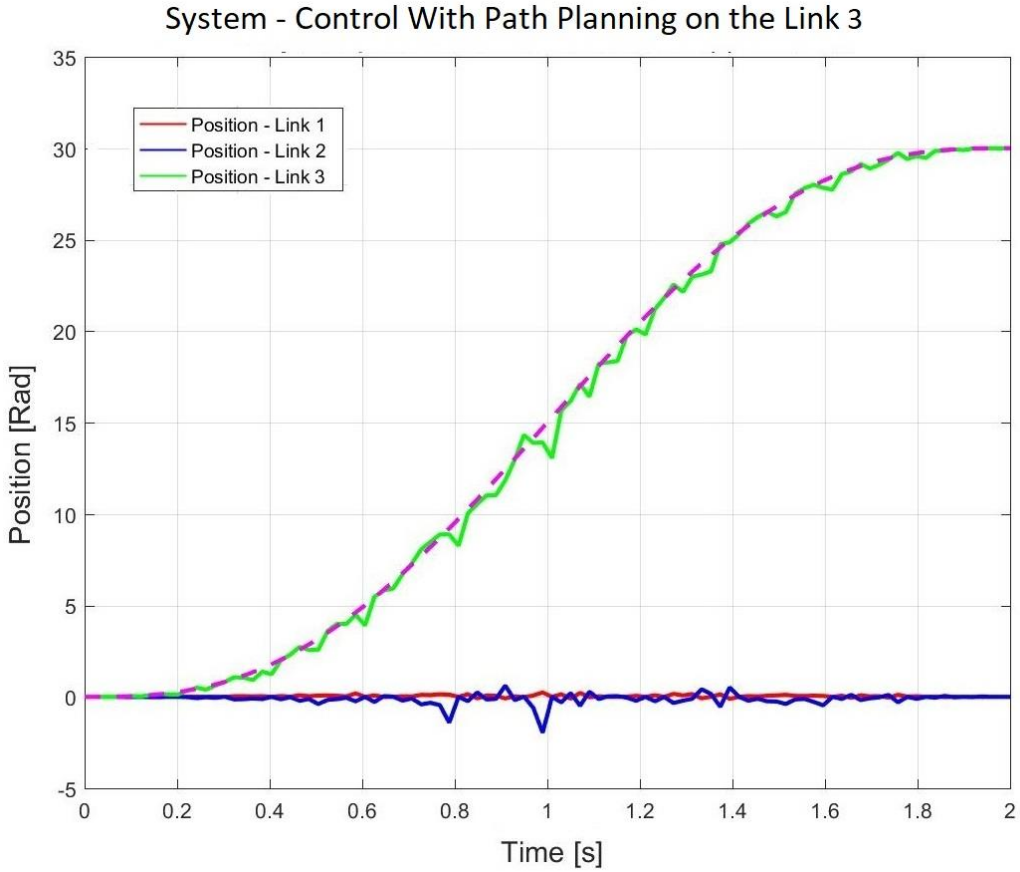

Source: Self Authorship.

$$Q = \begin{bmatrix} 2000 & 0 & 0 & 0 & 0 & 0 \\ 0 & 1 & 0 & 0 & 0 & 0 \\ 0 & 0 & 315 & 0 & 0 & 0 \\ 0 & 0 & 0 & 1 & 0 & 0 \\ 0 & 0 & 0 & 0 & 215 & 0 \\ 0 & 0 & 0 & 0 & 0 & 1 \end{bmatrix} \tag{6.47}$$

$$R = \begin{bmatrix} 50 \times 10^{-3} & 0 & 0 \\ 0 & 50 \times 10^{-3} & 0 \\ 0 & 0 & 50 \times 10^{-3} \end{bmatrix} \tag{6.48}$$

The configuration Control 3 was found using the same matrices $R$and Q presented on 6.48 and 6.49 and the behavior parameters presented on the table 6. The figure 37 shown the position control and the figure 38 the speed control for the dynamic system using the configuration Control 3.

Table 6 - Data for the trajectory planning and Control 3			
Data	Simble	Unit	Values
Time - Initial	t_0	s	0
Time - Final	t_f	s	2
Position Initial - Joint 1, 2 and 3	θ_{01}	rad	0
Position Final - Joint 1, 2 and 3	θ_{f1}	rad	$\pi/6$
Speed Initial - Joints 1, 2 e 3	ω_0	rad/s	0
Speed Final - Joints 1, 2 e 3	ω_f	rad/s	0
Acceleration Initial - Joints 1, 2 e 3	$\dot{\omega}_0$	rad/s^2	0
Acceleration Final - Joints 1, 2 e 3	$\dot{\omega}_f$	rad/s^2	0

Source: Self Authorship.

Figure 37 - Positions θ_1, θ_2 and θ_3 following the trajectory planning.

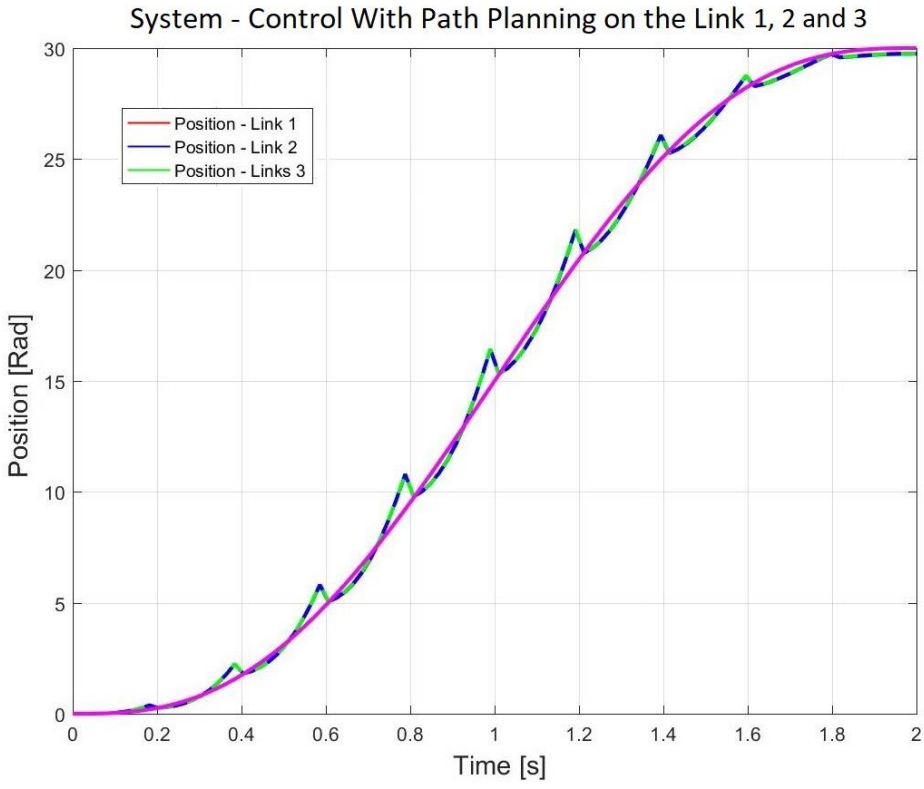

Source: Self Authorship.

Figure 38 - Speeds $\dot{\theta}_1$, $\dot{\theta}_2$ and $\dot{\theta}_3$ following the trajectory planning.

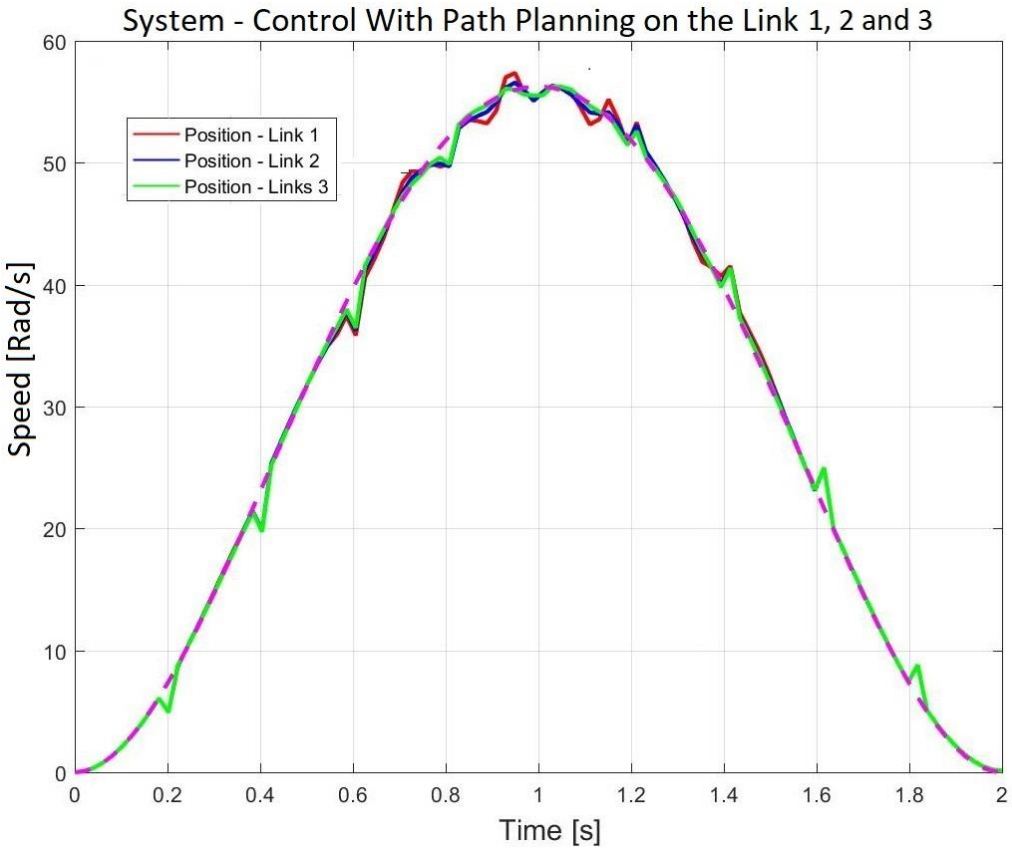

Source: Self Authorship.

The configuration Control 4 and 5 were tested using the data presented on the table 7. The same matrices $R_{L\,Ob}$ and $Q_{L\,Ob}$ were used to the three configurations, Control 4 to 6, and were composed by an identity matrix for $Q_{L\,Ob}$ and a diagonal matrix $R_{L\,Ob}$ as presented on 6.49 and 6.50. As those matrices were responsible to control the control over the error between the system states, $x(1)$ to $x(6)$, and the sate observer, $x(7)$ to $x(12)$, the solution found for one configuration can be extended for all the three configurations with similar characteristics.

$$Q_{L\,Ob} = \begin{bmatrix} 1 & 0 & 0 & 0 & 0 & 0 \\ 0 & 1 & 0 & 0 & 0 & 0 \\ 0 & 0 & 1 & 0 & 0 & 0 \\ 0 & 0 & 0 & 1 & 0 & 0 \\ 0 & 0 & 0 & 0 & 1 & 0 \\ 0 & 0 & 0 & 0 & 0 & 1 \end{bmatrix} \tag{6.49}$$

$$R_{L\,Ob} = \begin{bmatrix} 50 \times 10^{+4} & 0 & 0 \\ 0 & 50 \times 10^{+4} & 0 \\ 0 & 0 & 50 \times 10^{+4} \end{bmatrix} \quad (6.50)$$

Table 7 - Data for the trajectory planning and Control 4, 5 and 6

Data	Simble	Unit	Values
Time - Initial	t_0	s	0
Time - Final	t_f	s	2
Position Initial - Joint 1, 2 and 3	θ_{01}	rad	0
Position Final - Joint 1, 2 and 3	θ_{f1}	rad	10°
Speed Initial - Joints 1, 2 e 3	ω_0	rad/s	0
Speed Final - Joints 1, 2 e 3	ω_f	rad/s	0
Acceleration Initial - Joints 1, 2 e 3	$\dot{\omega}_0$	rad/s^2	0
Acceleration Final - Joints 1, 2 e 3	$\dot{\omega}_f$	rad/s^2	0

Source: Self Authorship.

The configuration Control 4, Path Planning on all the position with state observer on $\dot{\theta}_1$, was found using the matrices R, Q, R_{Ob} and Q_{Ob} presented on 6.51 to 6.54. The figure 39 shown the system and state observer answers.

$$Q = \begin{bmatrix} 2 \times 10^3 & 0 & 0 & 0 & 0 & 0 \\ 0 & 1 \times 10^3 & 0 & 0 & 0 & 0 \\ 0 & 0 & 3{,}15 \times 10^2 & 0 & 0 & 0 \\ 0 & 0 & 0 & 1 & 0 & 0 \\ 0 & 0 & 0 & 0 & 2{,}15 \times 10^2 & 0 \\ 0 & 0 & 0 & 0 & 0 & 1 \end{bmatrix} \quad (6.51)$$

$$R = \begin{bmatrix} 50 \times 10^{-2} & 0 & 0 \\ 0 & 50 \times 10^{-2} & 0 \\ 0 & 0 & 50 \times 10^{-2} \end{bmatrix} \quad (6.52)$$

$$Q_{Ob} = \begin{bmatrix} 5 \times 10^3 & 0 & 0 & 0 & 0 & 0 \\ 0 & 1 \times 10^3 & 0 & 0 & 0 & 0 \\ 0 & 0 & 1{,}015 \times 10^2 & 0 & 0 & 0 \\ 0 & 0 & 0 & 1 & 0 & 0 \\ 0 & 0 & 0 & 0 & 1{,}15 \times 10^2 & 0 \\ 0 & 0 & 0 & 0 & 0 & 1 \end{bmatrix} \quad (6.53)$$

$$R_{Ob} = \begin{bmatrix} 1 \times 10^{-2} & 0 & 0 \\ 0 & 1 \times 10^{-2} & 0 \\ 0 & 0 & 1 \times 10^{-2} \end{bmatrix} \quad (6.54)$$

To the configuration Control 5, Path Planning on all the position with state observer on $\dot{\theta}_2$, was found using the matrices R, Q, R_{Ob} and Q_{Ob} presented on 6.55 to 6.58. The figure 41 shown the system and state observer answers.

$$Q = \begin{bmatrix} 1 \times 10^3 & 0 & 0 & 0 & 0 & 0 \\ 0 & 1 & 0 & 0 & 0 & 0 \\ 0 & 0 & 5{,}15 \times 10^2 & 0 & 0 & 0 \\ 0 & 0 & 0 & 1 & 0 & 0 \\ 0 & 0 & 0 & 0 & 2{,}55 \times 10^2 & 0 \\ 0 & 0 & 0 & 0 & 0 & 1 \end{bmatrix} \quad (6.55)$$

$$R = \begin{bmatrix} 50 \times 10^{-3} & 0 & 0 \\ 0 & 50 \times 10^{-3} & 0 \\ 0 & 0 & 50 \times 10^{-3} \end{bmatrix} \quad (6.56)$$

$$Q_{Ob} = \begin{bmatrix} 3{,}5 \times 10^3 & 0 & 0 & 0 & 0 & 0 \\ 0 & 1 & 0 & 0 & 0 & 0 \\ 0 & 0 & 5{,}15 \times 10^2 & 0 & 0 & 0 \\ 0 & 0 & 0 & 1 & 0 & 0 \\ 0 & 0 & 0 & 0 & 2{,}55 \times 10^2 & 0 \\ 0 & 0 & 0 & 0 & 0 & 1 \end{bmatrix} \quad (6.57)$$

$$R_{Ob} = \begin{bmatrix} 50 \times 10^{-2} & 0 & 0 \\ 0 & 50 \times 10^{-2} & 0 \\ 0 & 0 & 50 \times 10^{-2} \end{bmatrix} \quad (6.58)$$

The configuration Control 6, control all the position with state observer on $\dot{\theta}_1$ and $\dot{\theta}_2$, was found using the matrices R, Q, R_{Ob} and Q_{Ob} presented on 6.59 to 6.62. The figure 41 shown the system and state observer answers.

$$Q = \begin{bmatrix} 2{,}5 \times 10^{3} & 0 & 0 & 0 & 0 & 0 \\ 0 & 0.1 & 0 & 0 & 0 & 0 \\ 0 & 0 & 2 \times 10^{2} & 0 & 0 & 0 \\ 0 & 0 & 0 & 0.1 & 0 & 0 \\ 0 & 0 & 0 & 0 & 2 \times 10^{2} & 0 \\ 0 & 0 & 0 & 0 & 0 & 1 \end{bmatrix} \tag{6.59}$$

$$R = \begin{bmatrix} 1 \times 10^{-2} & 0 & 0 \\ 0 & 1 \times 10^{-2} & 0 \\ 0 & 0 & 1 \times 10^{-2} \end{bmatrix} \tag{6.60}$$

$$Q_{Ob} = \begin{bmatrix} 0{,}75 \times 10^{3} & 0 & 0 & 0 & 0 & 0 \\ 0 & 50 & 0 & 0 & 0 & 0 \\ 0 & 0 & 1 \times 10^{2} & 0 & 0 & 0 \\ 0 & 0 & 0 & 10 & 0 & 0 \\ 0 & 0 & 0 & 0 & 1 \times 10^{2} & 0 \\ 0 & 0 & 0 & 0 & 0 & 1 \end{bmatrix} \tag{6.61}$$

$$R_{Ob} = \begin{bmatrix} 1 \times 10^{-2} & 0 & 0 \\ 0 & 1 \times 10^{-2} & 0 \\ 0 & 0 & 1 \times 10^{-2} \end{bmatrix} \tag{6.62}$$

The results presented in the figures 39 to 42 shown that the control was effective for the position Path Planning but for speed the analysis is not so simple as stating that it was not an effective control.

The response changes with different strategy used to control the robotic manipulator with Path Planning, as can be seen in the position control on the figures 34 and 39, for example. In this analysis, strategy means the process used to apply the Path Planning and the SDRE control, as discussed on the chapter 6.4 beginning and on the figures 31 to 33.

Comparing the figures 34 and 39, the strategy used on the second figure was much more effective to follow the Path Planning for position, presenting almost null error on position both for the system and the State Observer.

An analogous analysis can be made over the results shown in the figures 34 to 38. Comparing the speed control over the Path Planning in the figures 38 and 39 to 41 is another example of difference in responses when there is changes on the strategy used. The response in the figure 38 shown less error on controlling the speed compared to any one of the controls presented on 39 to 41.

The main conclusion over those results is that the control strategy used have a major influence and even with results on speed that isn’t the exactly the desired trajectory, change the controlled state variables or the strategy itself (as already discussed and shown in the figures 31 to 33) can improve the results.

Figure 39 - Control for all position using state observer on the speed of the first link, $\dot{\theta}_1$.

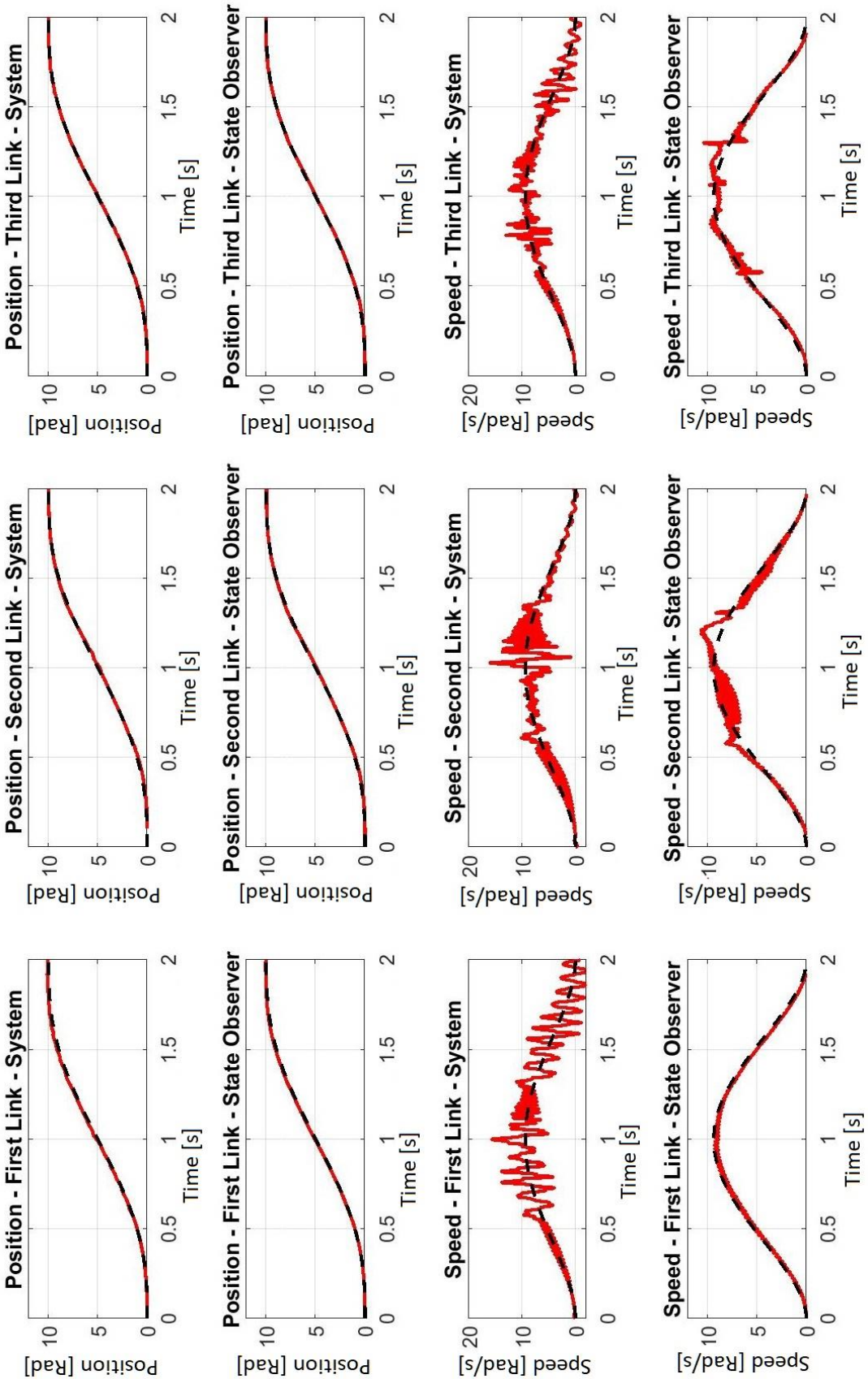

Source: Self Authorship.

Figure 40 - Control for all position using state observer on the speed of the first link, $\dot{\theta}_1$.

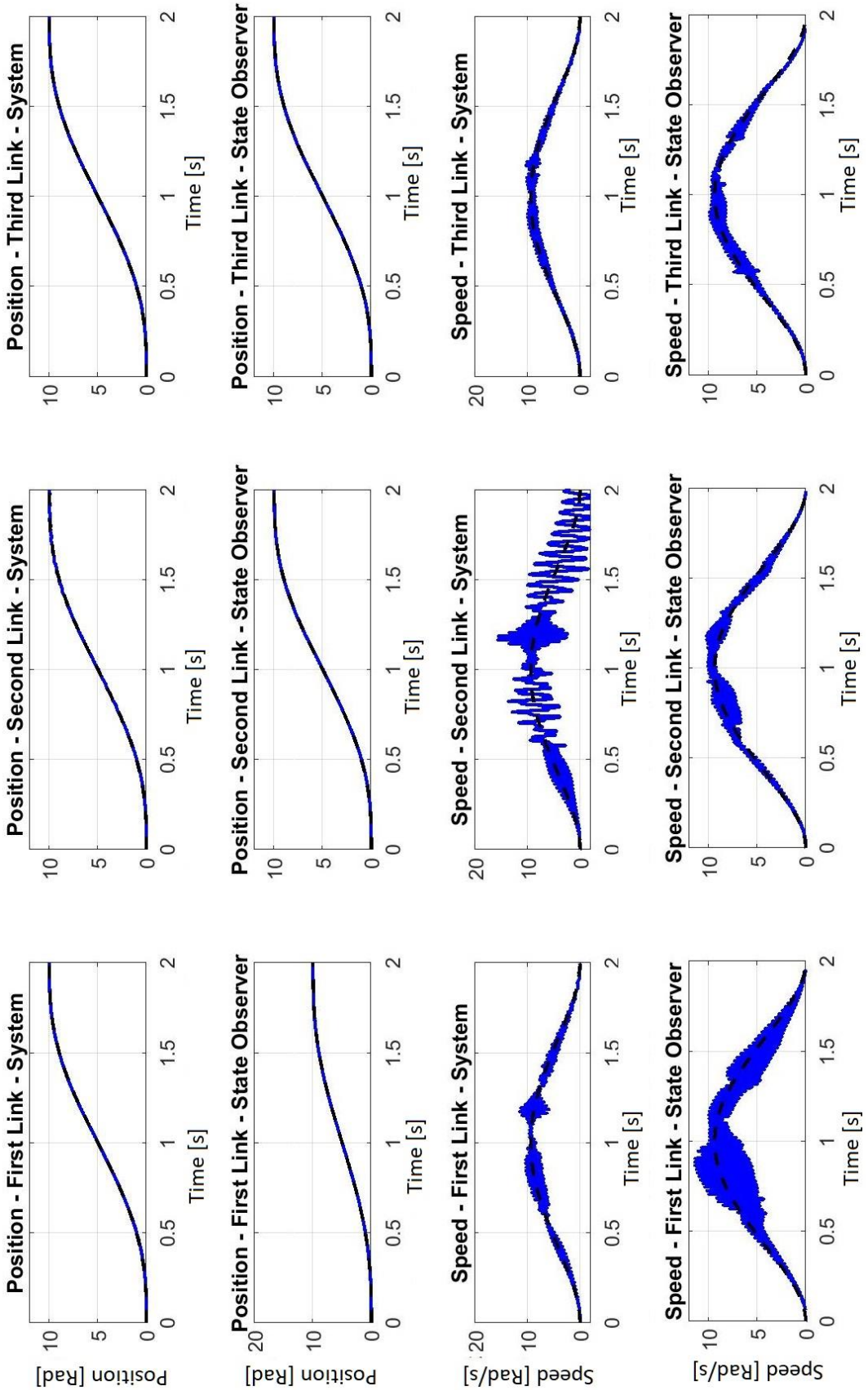

Source: Self Authorship.

Figure 41 - Control for all position using state observer on the speed of the first link, $\dot{\theta}_1$.

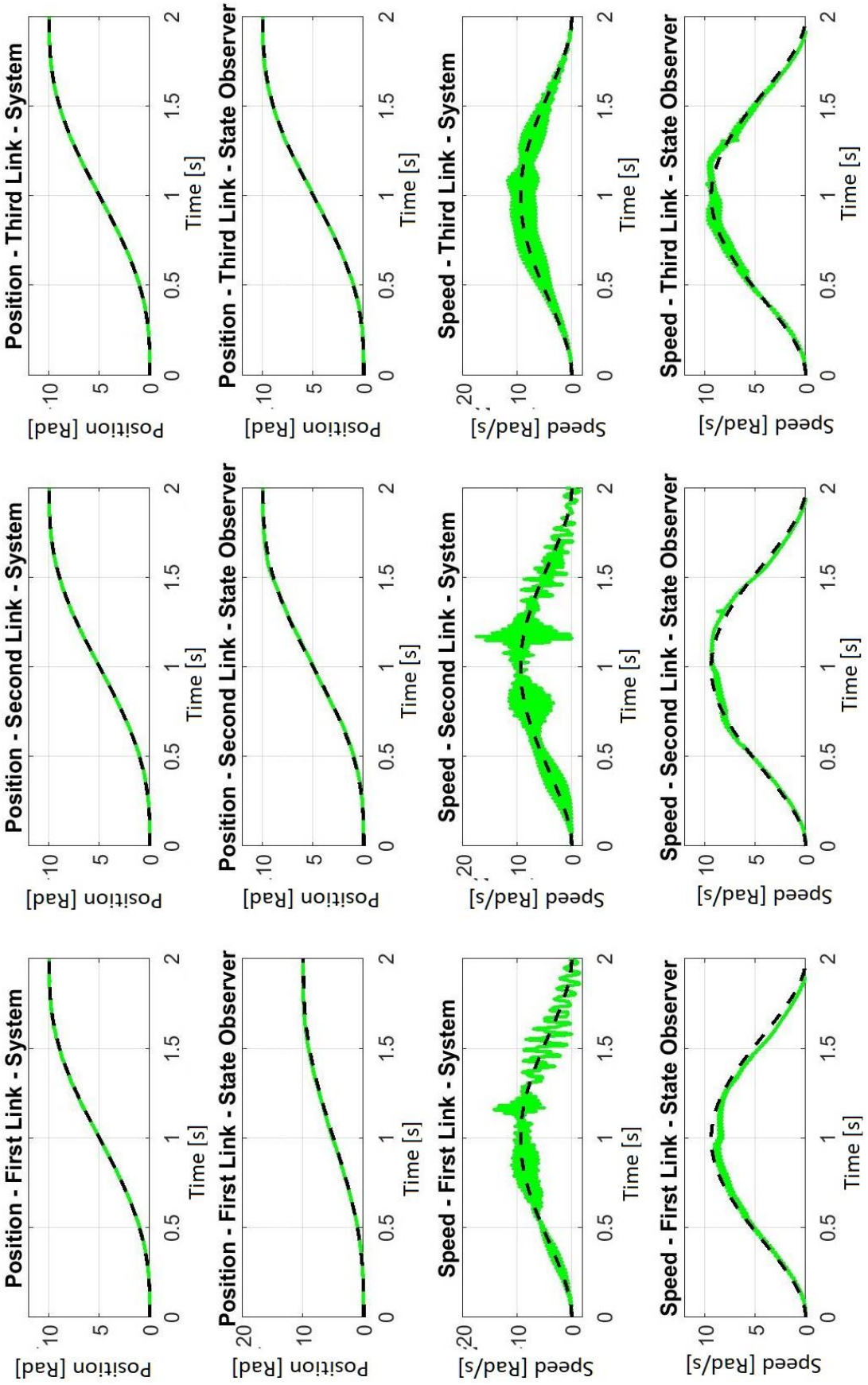

Source: Self Authorship.

6.5 CONTROL OVER PARAMETRIC ERROR AND MEASUREMENT NOISE

The parametric variation was found creating a vector with 100 elements and one of those elements was selected randomly on each 2000 interactions. Defining the values previously was the solution used to decrease in 20 times the simulation duration compares to calculate the parametric error in every one of the 2000 interactions. To test the control law were used fixed points to the desired final position. The figures 42 to 44 show the system position using the parametric variation presented on the figure 45.

$$\theta_{d\,1\,f} = \left(\pi/_{31,4}\right) = 0.1\,rad$$

$$\theta_{d\,2\,f} = \left(\pi/_{15,7}\right) = 0.2\,rad$$

$$\theta_{d\,3\,f} = \left(\pi/_{10,5}\right) = 0.3\,rad$$

Figure 42 - System position θ_1, θ_2 and θ_3 using the state observer on $\dot{\theta}_1$and parametric variations on the physical variables of the manipulator.

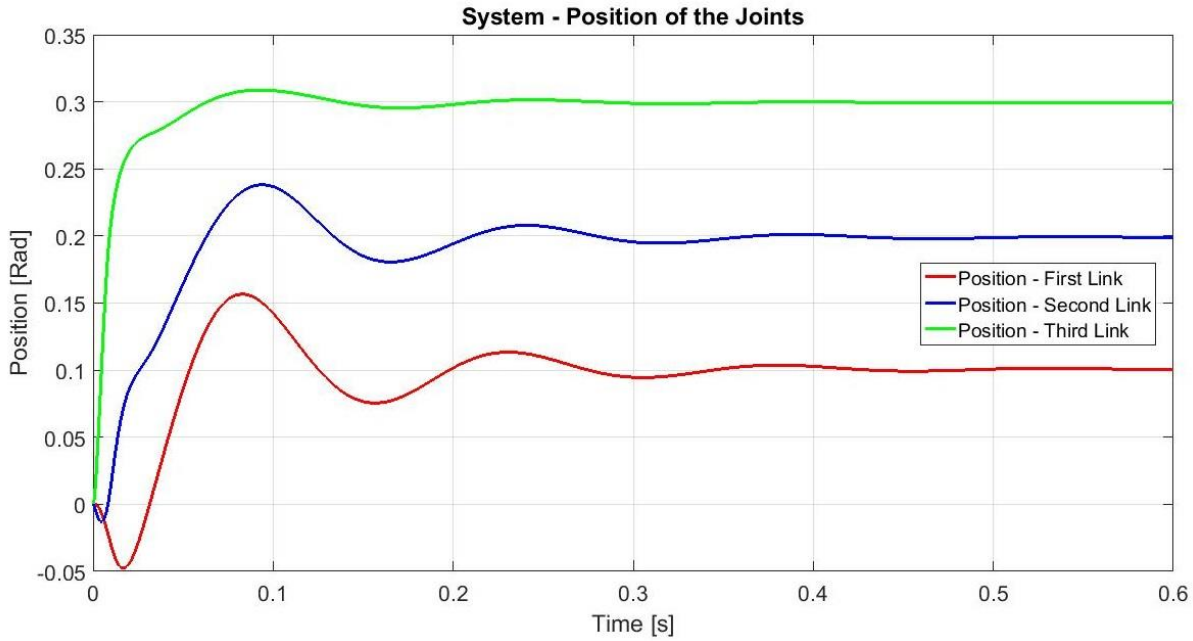

Source: Self Authorship.

Figure 43 - System position θ_1, θ_2 and θ_3 using the state observer on $\dot{\theta}_2$and parametric variations on the physical variables of the manipulator.

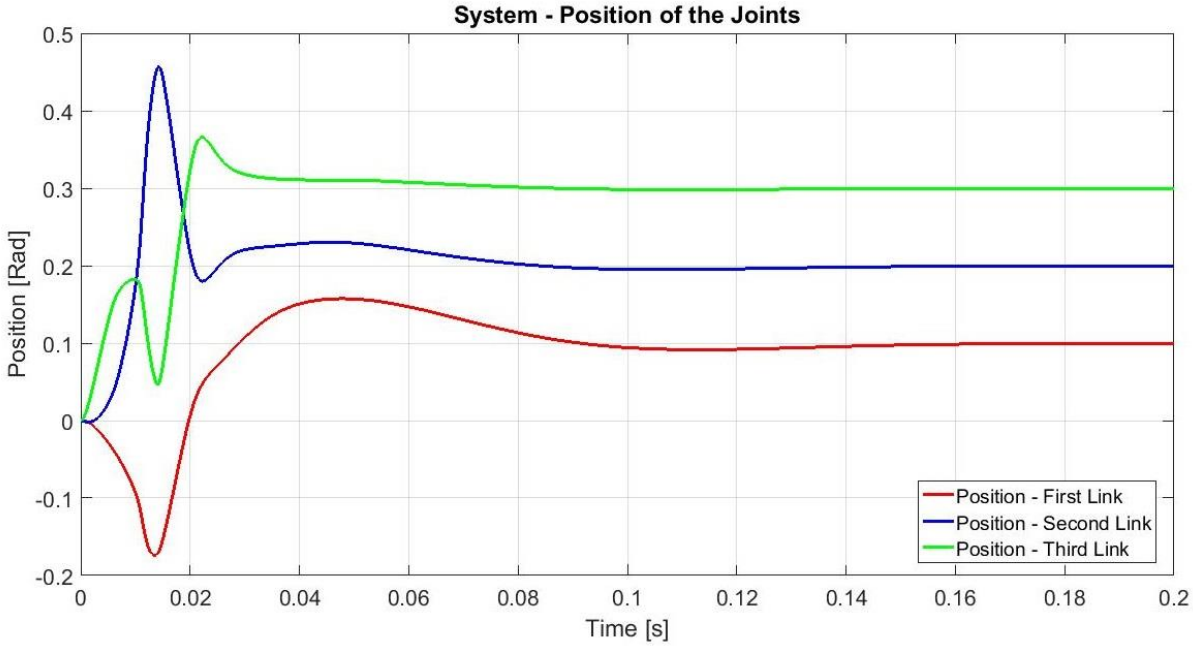

Source: Self Authorship.

Figure 44 - System position θ_1, θ_2 and θ_3 using the state observer on $\dot{\theta}_1$ and $\dot{\theta}_2$ at the same time and parametric variations on the physical variables of the manipulator.

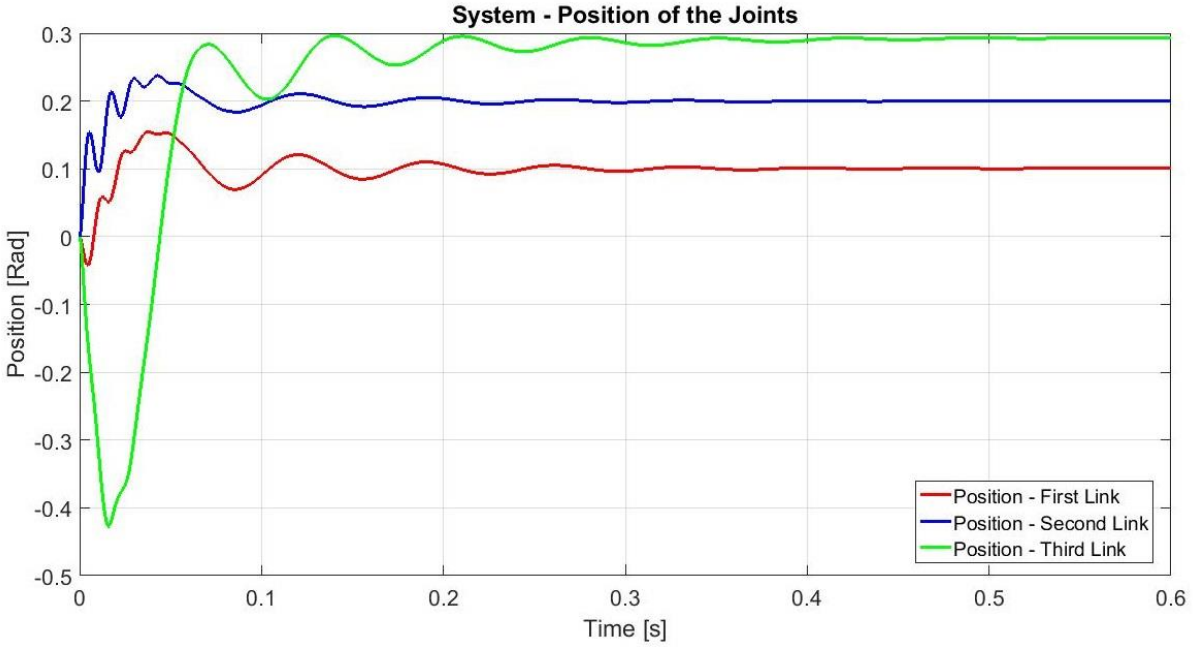

Source: Self Authorship.

6.6 DC ATUATORS

When the analysis is based on the actuators capacity one of the main interests on the manipulator side is the velocity behavior and the actuator side is the physical variable, as current and torque.

The figures 18 and 19, which shows the speeds resulting from the best response, without considering the physical limitation of the actuators and analyzing their values, the peak values cannot be satisfied by any DC actuator. The objective of this simulations was found a control configuration that can present more realistic values for the DC actuators. The weight matrices $Q_{L\,Ob}$, $R_{L\,Ob}$, Q_{Ob}, R_{Ob}, Q and $R$are tuned to prove an optimal result on control and within the physical limits of the DC actuators.

6.6.1 State Observer in $\dot{\theta}_1$ and DC Actuators limits analysis

To use the state observer in $\dot{\theta}_1$, state $x(2)$, and the DC actuators following their physical limitations the matrix $C(x)$, $R$and Q assumed the following values and the figures 46 to 47 show the simulation answer.

$$Q = \begin{bmatrix} 2000 & 0 & 0 & 0 & 0 & 0 \\ 0 & 1 & 0 & 0 & 0 & 0 \\ 0 & 0 & 315 & 0 & 0 & 0 \\ 0 & 0 & 0 & 1 & 0 & 0 \\ 0 & 0 & 0 & 0 & 215 & 0 \\ 0 & 0 & 0 & 0 & 0 & 1 \end{bmatrix} \tag{6.63}$$

$$R = \begin{bmatrix} 50 \times 10^{-3} & 0 & 0 \\ 0 & 50 \times 10^{-3} & 0 \\ 0 & 0 & 50 \times 10^{-3} \end{bmatrix} \tag{6.64}$$

Figure 45 - Parametric variations on the physical variables of the manipulators.

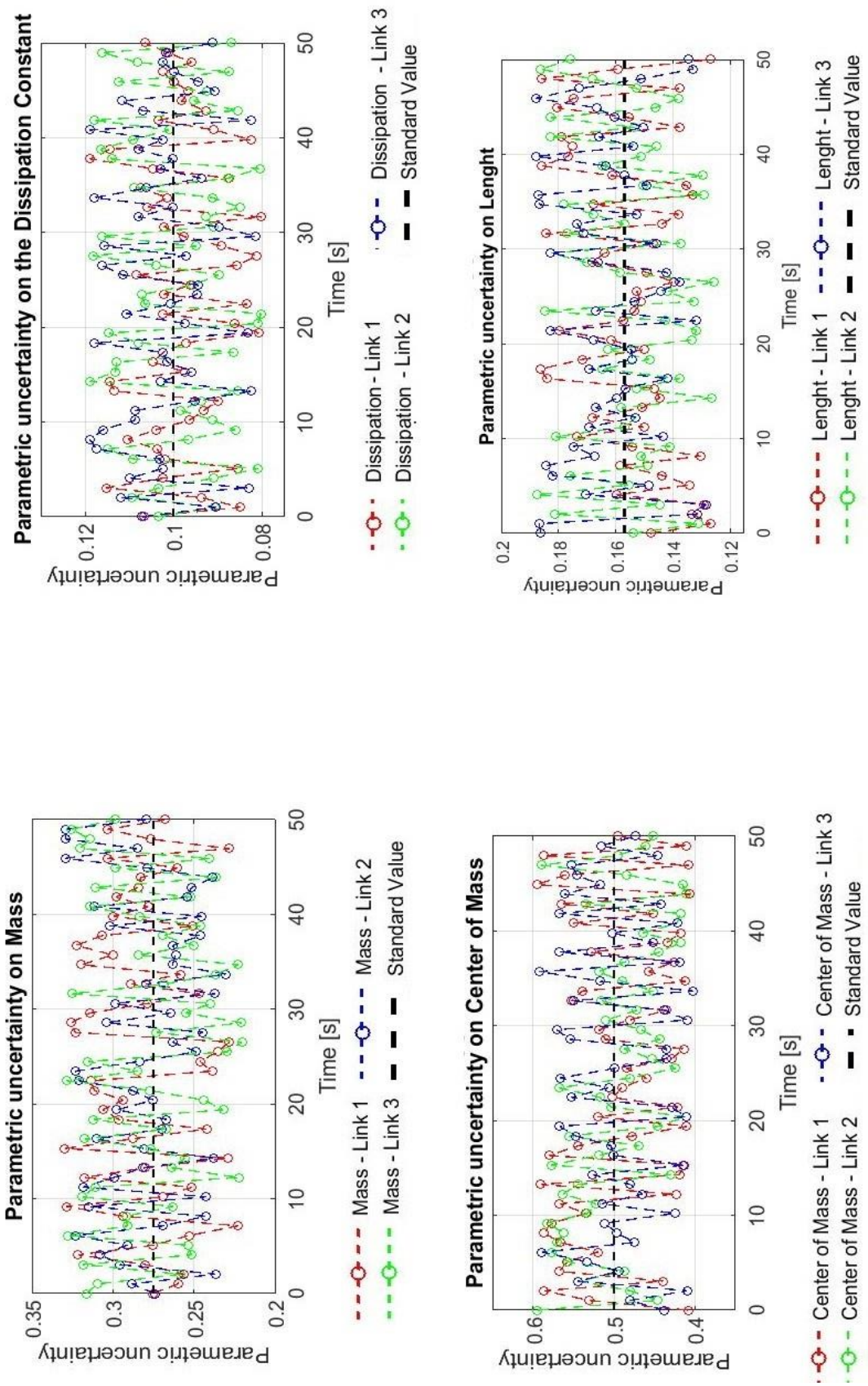

Source: Self Authorship.

Figure 46 - Positions of the system and state observer on $\dot{\theta}_1$ with fixed point following the physical limitations of the DC actuators.

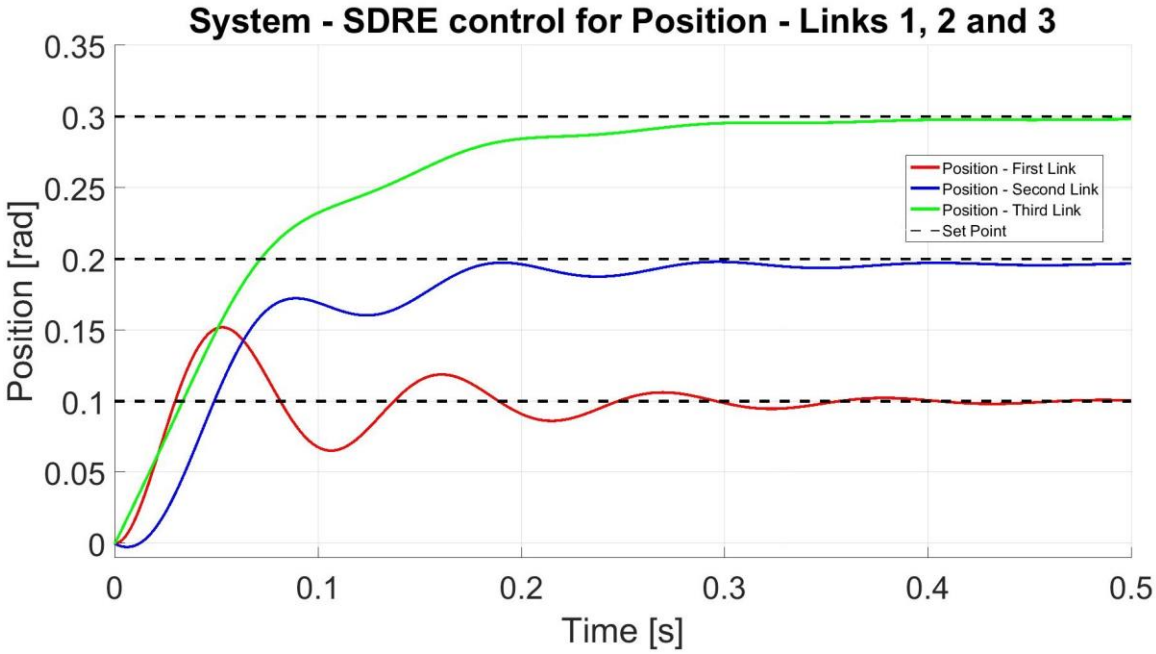

Source: Self Authorship.

Figure 47 - Speeds of the system and state observer on$\dot{\theta}_1$ with fixed point following the physical limitations of the DC actuators.

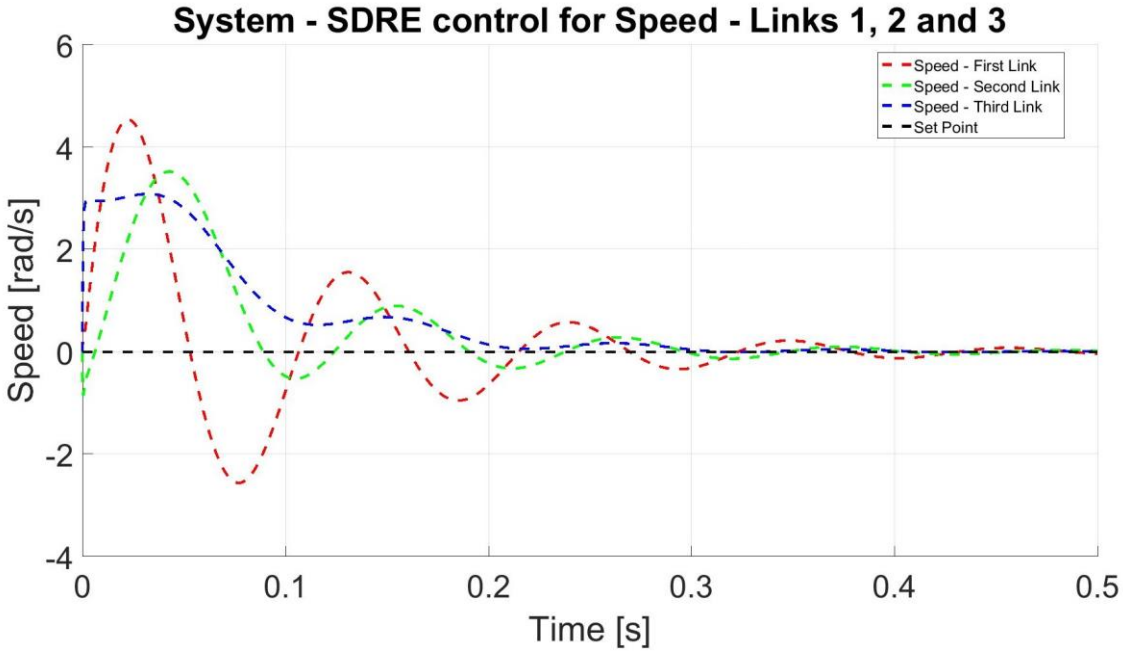

Source: Self Authorship.

6.6.2 State Observer in $\dot{\theta}_2$ and DC Actuators limits analysis

To use the state observer in $x(4)$ and the DC actuators following their physical limitations the matrix $C(x)$, R and Q assumed the following values and the figures 48 to 49 show the simulation answer.

$$Q = \begin{bmatrix} 1000 & 0 & 0 & 0 & 0 & 0 \\ 0 & 1 & 0 & 0 & 0 & 0 \\ 0 & 0 & 515 & 0 & 0 & 0 \\ 0 & 0 & 0 & 1 & 0 & 0 \\ 0 & 0 & 0 & 0 & 255 & 0 \\ 0 & 0 & 0 & 0 & 0 & 1 \end{bmatrix} \tag{6.65}$$

$$R = \begin{bmatrix} 50 \times 10^{-3} & 0 & 0 \\ 0 & 50 \times 10^{-3} & 0 \\ 0 & 0 & 50 \times 10^{-3} \end{bmatrix} \tag{6.66}$$

Figure 48 - Position of the system and state observer on $\dot{\theta}_2$ with fixed point following the physical limitations of the DC actuators.

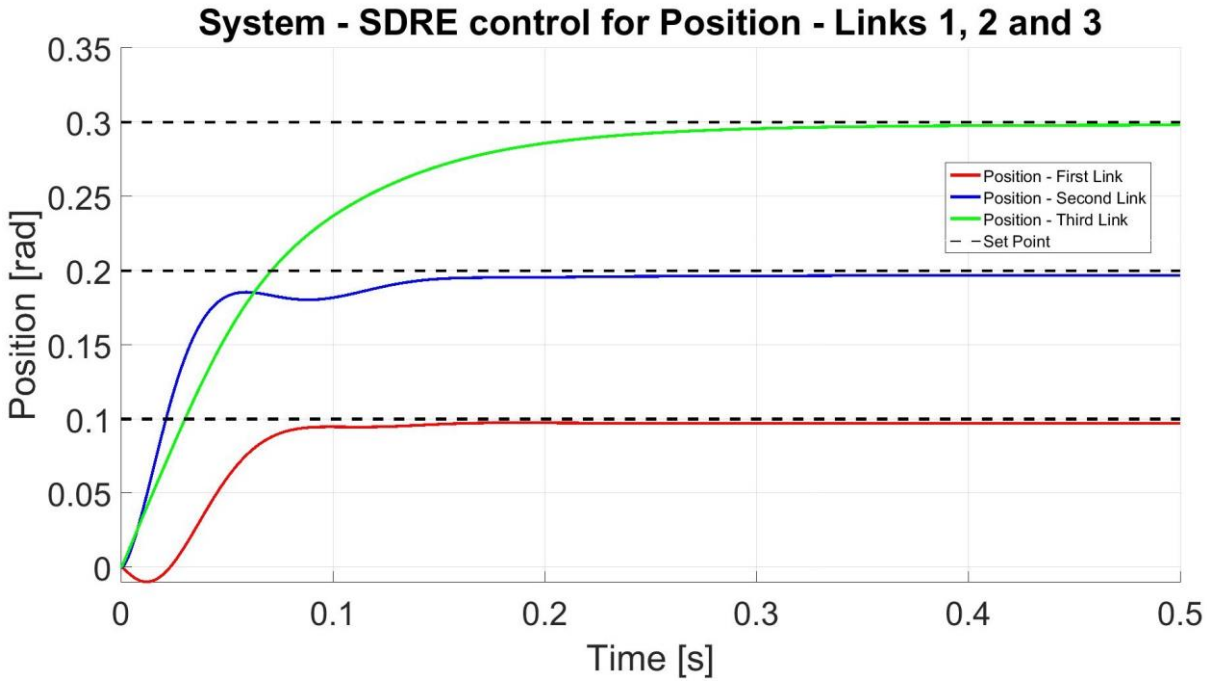

Source: Self Authorship.

Figure 49 - Speeds of the system and state observer on $\dot{\theta}_2$ with fixed point following the physical limitations of the DC actuators.

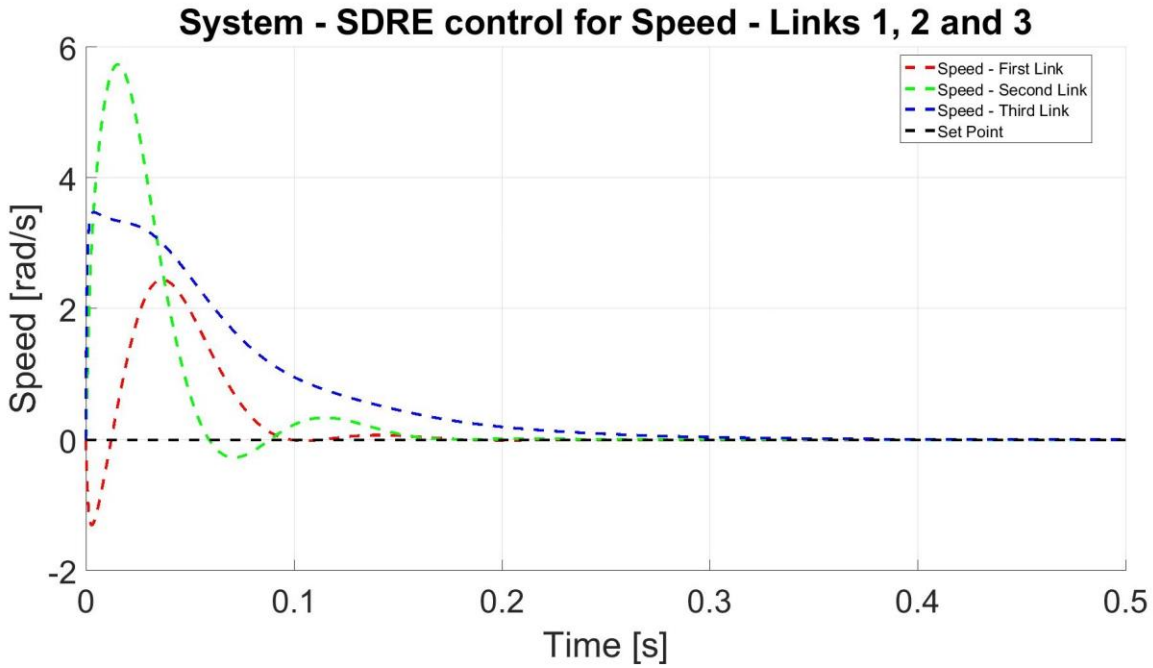

Source: Self Authorship.

6.6.3 State Observer in $\dot{\theta}_1$ and $\dot{\theta}_2$ with DC Actuators limits analysis

To use the state observer in $x(2)$ and $x(4)$ at the same time and the DC actuators following their physical limitations the matrix $C(x)$, R and Qassumed the following values and the figures 50 to 51 show the simulation answer.

$$Q = \begin{bmatrix} 55000 & 0 & 0 & 0 & 0 & 0 \\ 0 & 1 & 0 & 0 & 0 & 0 \\ 0 & 0 & 55000 & 0 & 0 & 0 \\ 0 & 0 & 0 & 1 & 0 & 0 \\ 0 & 0 & 0 & 0 & 100 & 0 \\ 0 & 0 & 0 & 0 & 0 & 1 \end{bmatrix} \tag{6.67}$$

$$R = \begin{bmatrix} 57{,}5 \times 10^{-3} & 0 & 0 \\ 0 & 57{,}5 \times 10^{-3} & 0 \\ 0 & 0 & 57{,}5 \times 10^{-3} \end{bmatrix} \tag{6.68}$$

$$x(t)_0 = [0 \quad 0 \quad 0 \quad 0 \quad 0 \quad 0.1] \tag{6.69}$$

Figure 50 - Position of the system and state observer on $\dot{\theta}_1$ and $\dot{\theta}_2$ with fixed point following the physical limitations of the DC actuators.

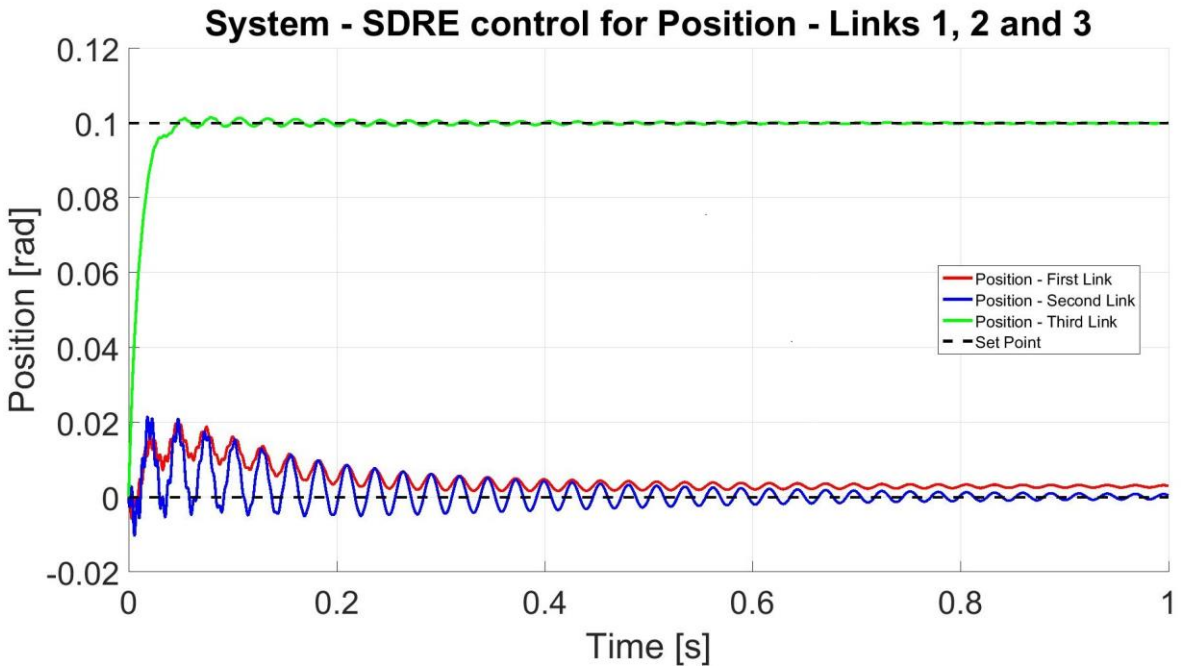

Source: Self Authorship.

Figure 51 - Speeds of the system and state observer on $\dot{\theta}_1$ and $\dot{\theta}_2$ with fixed point following the physical limitations of the DC actuators.

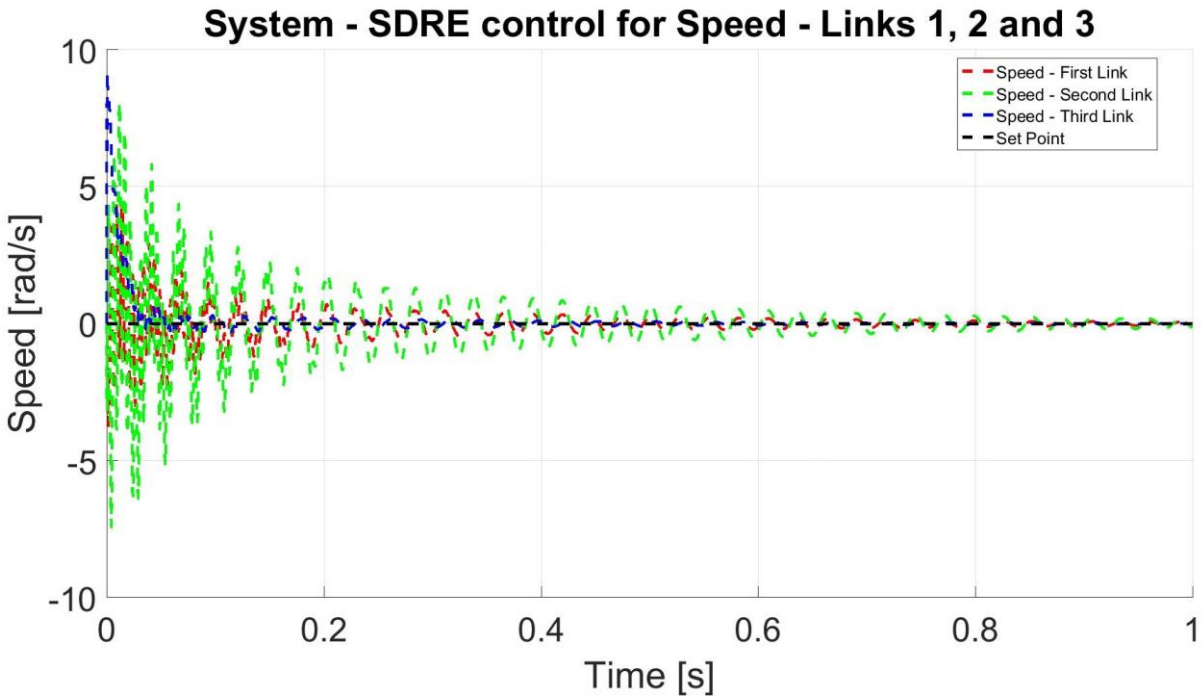

Source: Self Authorship.

The simulation and analysis made on the State Observer were used in $\dot{\theta}_1$ and $\dot{\theta}_2$, states $x(2)$ and $x(4)$, shown that the system can't provide control under the limitation of the DC actuators when a desired position were set to more than one link.

As the dynamical system was deduced using the links with initial condition presented on the figure 4, that position is analogous to use initial condition null to all the states. So, to control the system using the State Observer in $\dot{\theta}_1$ and $\dot{\theta}_2$ the final condition to the control must be different than zero to only one position and can be larger than $0{,}15$ radians, approximately 10º. The results presented in the figure 50 and 51 were obtained using the final condition presented on the equation 6.69.

CONCLUSION

The dynamical representation of the system was tested in several conditions and all the results prove that the system can be used to new projects and on the upcoming tests on some work. Some deductions using another methodology, as Newton-Euler and Denavit-Hartenberg, can provide some additional data for analysis to define if those new approaches can give some advantages on simplicity to the control or the computational needs to calculation.

The LQR/SDRE control was used as the basis for control the system and the State Observer error minimization with good results for each one. The results presented and discussed on the chapter 6 provide a lot of information proving the effectivity of the control strategy.

The main problem with the control analysis was to find the optimal vales for the weight matrices Q and R, both for the system, the State Observer and the State Observer gain. The lack of a tested and consolidated method for define those matrices from the desired behavior for the system.

One of the most important consideration is that the Path Planning have a major part on controlling the speed of the actuators. As already discussed, control the desired behavior, especially from the matrices Q and R isn't a very develop area from the theoretical point of view, so use the Path Planning for to mark the limits for the speed is a highly recommended and proven approach in this work.

The State Observer present a great result on supplying the need of sensing some system states or provide data to the control when some variables are not able to monitoring. The main goal of this part of the project was find the State Observer for the largest number of system states combination but finding the deduction for three combinations shown a great result using the estimated state on controlling the system. The figures 22 to 27 prove the efficiency on the State Observer on estimate the system variables, so this lead to the conclusion that to improve the control efficiency is necessary look at the system control applied on the dynamical system and not to the State Observer since its results are good in all simulations.

When tested over parametric variations using a maximum of 20% of variations, the system control was capable to provide great results, as presented on the figures 33 to 35. Those results prove that the system can work with noise on the sensing system or some rounding assumptions on the solving process.

With the presented results, the project can be improved with some additional analysis. Found new possibilities for the State Dependent Constants, SDC, and define If those representation can provide new combination for the State Observer. Tests new combinations for Q and R that not only identity matrices and search for optimization over the speed and torque application on the control. Analysis over the physical component, as the links and joints, to define if variations on the mass m_n and length l_n can provide control improvement without limitation on the work volume of the manipulator.

REFERENCES

ANDERSON, B. D. O; MOORE, J. B. **Optimal Control -** Linear Quadratic Methods. Rio de Janeiro: Prentice Hall, 1989.

ANGELES, J. **Fundamentals of Robotic Mechaical Systems**: Theory, Methods and Algorithms. 2nd Ed. New York: Springer, 2013.

BOTTEGA, V; PERGHER, R. **Dynamic Model and Control of Human Posture**. 20th International Congress of Mechanical Engineering. Gramado: November, 2009. ISBN 978-3-642-40063-6.

BRYSON, A. E.; HO, Y. C. **Applied Optimal Control**: Optimization, Estimation, and Control. Taylor & Francis, 1975. doi: 10.1109/TSMC.1979.4310229

CATHPOLE, K et al. **Safety, efficiency and learning curve in robotic surgery:** a human factory analysis. Surgical Endoscopy. Volume 30, Issue 9, pp 3749-376. September, 2016.

CHANG, P. H. **A Closed-Form Solution for the Control of Manipulators with Kinematic Redundancy**. Proceedings. 1986 IEEE International Conference on Robotics and Automation, 1986, pp. 9-14. DOI 10.1109/JRA.1987.1087073.

CRAIG, J. J. **Introduction to Robotics** - Mechanics and Control. 2. Ed. Addison Wesley. Ontario: 1989.

DORF, R. C.; BISHOP, R. H. **Modern Control Systems**. 12° ed. Pearson. New Jersey: 2010

DUKA, A. **AFINS based Solution to the Inverse Kinematics of a 3DOF Planar Manipulator**. 8th International Conference Interdisciplinarity in Engineering. Tirgu-Murse, Romania: October 2014.

FAHIMI, F. **Autonomous Robots** - Modeling, Path Planning and Control. Springer. Edmonton: 2009.

FROM, P. J; GRAVDAHL, J. T. **General Solutions to functional and kinematic Redundancy**. 2007 46th IEEE Conference on Decision and Control. New Orleans: LA. 2007. pp. 5779-5786.

FU, K. S; GONZALEZ, R. C; LEE, C. S. G. **Robotics**: Control, Sensing, Vision and Intelligence. McGraw-Hill. New York: 1987.

GROETSCH, C. W. **Inverse Problems in the Mathematical Sciences**. Vieweg. 1nd Ed. Ohio: 1993.

GLUCK, T; EDER, A; KUGI, A. **Swing-up Control of a triple pendulum on a cart with experimental validation**. Automatica, Vol. 49. Nº 3, p. 801-808, Gusshausstr: 2013.

GUO, Y; CHEN, L. **Adaptive Neural Network Control of Coordinated Motion of Dual-Arm Space Robot System with Uncertain Parameters**. 7th World Congress on Intelligent Control and Automation. Chongqing, China: June, 2008.

HIBBELER, R. C. **Engineering Mechanics -** Dynamics. 11ª Ed. Prentice Hall. Rio de Janeiro: 2006.

ITIK, M; SALAMCI, M. U; BANKS, S. P. **SDRE optimal control of drug administration in cancer treatment**. Turk J Elec Eng & Comp Sic. Vol. 18, Nº 5. 2010. DOI: 10.3906/elk-1001-411

KASTEV, S. **Streamlining of the state-dependent Riccati equation controller algorithm for an embedded implementation**. Thesis. Rochester Institute of Technology. Rochester, New York. 2006.

KACZMAR, J. M et al. **HPV-related oropharyngeal cancer: Risk factors for treatment failure in patients managed with primary transoral robotic surgery**. Head & Neck. January, 2016.

KIRK, D.E. **Optimal Control Theory**: An Introduction. Dover: 2004.

KORAYEM, M. H. **Dynamic of Flexible Manipulators and Applications to Determine Load Carrying Capacity**. Thesis. Department of Mechanical Engineering. Wollongong: March, 1994.

LEWIS, F. L; DAWSON, D. M; ABDALLAH, C. T. **Robot Manipulator Control** - Theory and Practice. 2nd Ed. Marcel Dekker. New York: 2004.

LIMA, J. J. **Controle não linear de posição e vibração de manipuladores robóticos com juntas e elos flexíveis utilizando materiais Inteligentes**. 2015. 104 p. Thesis (Master's on Eletrical Engineering) - UTFPR, Paraná, Ponta Grossa 2015.

MOORMAN H. G; GOWDA, S; CARMENA, J. M., **Control of Redundant Kinematic Degrees of Freedom in a Closed-Loop Brain-Machine Interface**. IEEE Transactions on Neural Systems and Rehabilitation Engineering, vol. 25, no. 6, pp. 750-760, June 2017.

MOHAMMED, A. M; LI, S. **Dynamic Neural Networks for Kinematic Redundancy Resolution of Parallel Stewart Platforms**. IEEE Transactions on Cybernetics. Vol. 46. Nº 7. July 2016.

MURRAY, R; SASTRY, S. S; ZEXIANG, L. **A Mathematical Introduction to Robotic Manipulation**. 1. Ed. CRC Press. 1994.

NAIDU, D.S. **Optimal Control Systems**. CRC press. NewYork: 2003. ISBN 9780849308925

NEUMAN, C. P; TOURASSIS, V. D. **Discrete Dynamic Robot Models**. IEEE Transactions on Systems, Man and Cibernectics. Vol. SMC-15. Nº 2. March, 1985.

NIKU, S. B. **Introduction to Robotics:** analysis, control and applications. Hoboken. 2nd Ed. New Jersey: 2011.

OGATA, K. **System Dynamics**. 4th Ed. Prentice Hall. New Jersey: 2004.

OGATA, K**. Modern Control Engineering**. 5th Edition. New Jersey. Person. 2010.

OGAWA, T. KANADA, H. **Solution for I11-Posed Inverse Kinematic of Robot Arm by Network Inversion**. Hindawi Publishing Corporation. Journal of Robotics. Vol. 2010.

ONG, C. **Dynamic Simulation of Electric Machinery**. Patrice Hall. 1nd Ed. New York: 1998.

PORAWAGAMA, C. D; MUNASINGH E, S. R. **Reduced Jerk Joint Space Trajetory Planning Method Using 5-3-3 Spline for Robot Manipulators**. 7th International Conference on Information and Automation for Sustainability, Colombo, 2014, pp. 1-6.

SPONG, M. W; HUTCHINSON, S; VIDYSAGAR, M. **Robot Modeling and Control**. John Wiley & Sons. Ed. 1. 2005. ISBN: 978-0-471-64990-8.

TELLEZ-ORNELAS, F; JESUS RICO, J. RUIZ-CRUZ, R. **Optimal Tracking for State-Dependent Coefficient Factorized Nonlinear Systems. Asian Journal of Control**, Vol. 16, p. 890-903. May: 2014. DOI 10.1002/asjc.761.

TUSSET, A. M; BUENO, A. M; NASCIMENTO, C. B; DOS SANTOS KASTER, M; BALTHAZAR, J. M. **Nonlinear state estimation and control for chaos suppression in MEMS resonator.** Shock and Vibration, vol. 20, no. 4, pp. 749-761, 2013. ISSN 1070-9622/13/$27.50.

YOU, S. S. **Dynamics and Controls for robot manipulators with open and closed kinematic chain mechanisms**. Dissertation. Ames, Iowa: 1994.

WINDER, J. S et al. **Implementing a robotics curriculum at an academic general surgery training program: our initial experience**. J Robotic Surg. London: September, 2016. DOI 10.1007/s11701-016-0569-9.

ZARGAR, H et al. **Trifecta and optimal perioperative outcomes of robotic and laparoscopic partial nephrectomy in surgical treatment of small renal masses**. BJUI International - Robotics and Laparoscopy. September, 2014. DOI 10.1111/bju.12933.

APPENDIX A - PRECEDENT CURRICULUM

PRECEDENT CURRICULUM

With the accomplishment of this work it was possible to generate two publications approved by specialized reviewers:

- Jose Adenilson Gonçalves Luz Junior; Angelo Marcelo Tusset; Frederic Conrad Janzen; Rodrigo Tumolin Rocha; Jose Manoel Balthazar; Airton Nabarrete. **Optimal control for robot manipulators with three degrees of freedom**. Paper In: 14th INTERNATIONAL CONFERENCE Dynamical Systems - Theory and Applications December 11-14, 2017. Lodz, POLAND., 2017, Lodz, Poland. Proceedings of DSTA 2017. Lodz, Poland: Technical University of Lodz, 2017. v. 2017. p. 1-10.

- Jose Adenilson Gonçalves Luz Junior; Angelo Marcelo Tusset; Frederic Conrad Janzen; Rodrigo Tumolin Rocha; Jose Manoel Balthazar; Airton Nabarrete. **Optimal control for robot manipulators with three degrees of freedom**. Chapter of the Book: Dynamical Systems. Editor: Jan Awrejcewicz, Springer, p. 1-10.